CHARACTERIZING THE IMPACT OF LAND USE AND LAND COVER CHANGE ON FRESHWATER INFLOWS

A Thesis

by

TEUKU FERIJAL

Submitted to the Office of Graduate Studies of
Texas A&M University
in partial fulfillment of the requirements for the degree of

MASTER OF SCIENCE

August 2008

Major Subject: Biological and Agricultural Engineering

CHARACTERIZING THE IMPACT OF LAND USE AND LAND COVER CHANGE ON FRESHWATER INFLOWS

A Thesis

by

TEUKU FERIJAL

Submitted to the Office of Graduate Studies of
Texas A&M University
in partial fulfillment of the requirements for the degree of

MASTER OF SCIENCE

Approved by:

Chair of Committee,	Patricia K. Smith
Committee Members,	Raghavan Srinivasan
	Yongheng Huang
Head of Department,	Gerald L. Riskowski

August 2008

Major Subject: Biological and Agricultural Engineering

ABSTRACT

Characterizing the Impact of Land Use and Land Cover Change on Freshwater Inflows.

(August 2008)

Teuku Ferijal, B.S., Brawijaya University, Indonesia

Chair of Advisory Committee: Dr. Patricia K. Smith

Freshwater inflows are a crucial component for maintaining estuarine health, function and productivity. Streamflows, the primary source of freshwater inflows, have been modified and altered from their natural flow by population growth and anthropogenic impacts on the contributing watersheds. The Guadalupe Estuary is a primary habitat for many endangered species. The Guadalupe River Watershed, which supplies 70% of freshwater inflows, experiences rapid urbanization and agricultural development. This study proposed to characterize the impact of land use/cover change in the Guadalupe River Watershed on freshwater inflows to the Guadalupe Estuary.

Pre-whitening, Mann-Kendall and bootstrap techniques were used to test for significant trends on streamflow and precipitation. Analyses suggested more trends in annual and seasonal minimum and mean streamflow than would be expected to occur by chance in the periods of 1930-2005 and 1950-2005. No significant trends were found in the period of 1970-2005. Significant trends were more prominent in the upper watershed and decreased as analysis moved downstream in the period of 1950-2005. Trend tests on

precipitation data in the period of 1950-2005 revealed more significant trends than would be expected by chance in mean annual and winter precipitation.

Analyses of Landsat images of the watershed using an unsupervised classification method showed an increase in forest, urban and irrigated land by 13, 42 and 7%, respectively, from 1987 to 2002. Urbanized areas were mostly found in the middle part of watershed surrounding the I-35 corridor. More than 80% of irrigated lands are distributed over the San Marcos and Middle Guadalupe River Watersheds.

Soil and Water Assessment Tool (SWAT) model was applied for the Guadalupe River Watershed. Calibration and validation using data recorded at USGS 08176500 indicated the model performed well to simulate streamflow. The coefficient of Nash-Sutcliffe, determination and percent bias were 0.83, 0.96 and 3.81, respectively, for calibration and 0.68, 0.75 and 29.38 for validation period. SWAT predicted a 2% decrease in annual freshwater inflow rates from the effect of land use/cover change from 1987 to 2002. Reservoirs increased freshwater inflows during low flow months and decreased the inflows during high flow months. Precipitation variability changed characteristics of monthly freshwater inflows.

ACKNOWLEDGEMENTS

My great gratefulness is to the chair of my committee, Dr. Patricia Smith, who gave me abundant support and guidance during my study at Texas A&M University and my research course as well. I highly appreciate her time, energy, and patience in helping me to complete my degree. I would also like to thank to my committee members, Dr. Raghavan Srinivasan and Dr. Yongheng Huang for their advice.

I also wish to thank my friends and colleagues, and the department faculty and staff for their help, support and shared experiences. My gratitude also goes to the Fulbright Foundation which provided me a full scholarship.

Special thanks to my wife, Syarifah Ayu Raihan, and my son, Teuku Rafie, for their endless love and support throughout this research.

TABLE OF CONTENTS

CHAPTER Page

LIST OF FIGURES

FIGURE Page

LIST OF TABLES

TABLE Page

CHAPTER I

INTRODUCTION

Freshwater is a critical component for human life and most of the World's ecosystems. It is a valuable natural resource for many purposes including drinking water, industrial use, waste disposal, irrigation, hydropower, transportation and recreation. Most ecosystems rely on a continuous freshwater supply to maintain their optimum condition. Freshwater not only provides water as a critical component for organisms but also carries important dissolved nutrients along with the flow to ecosystems. Reduction in freshwater supply due to increasing demand for freshwater upstream has caused degradation of many ecosystems.

Although freshwater is a renewable resource, the availability of freshwater in many places has been showing a decreasing trend over time. The main factor in decreasing availability of freshwater is the rapid growth of human populations. Population growth has put more pressure on freshwater availability by increasing upstream freshwater demands. The rate of population growth is faster than the freshwater renewal process and has reduced global freshwater availability. Today, freshwater scarcity affects more than a billion people and the integrity of many world ecosystems (UNEP, 2006).

This thesis follows the style of *Transaction of ASABE*.

Freshwater flows are part of the hydrologic cycle. The ultimate source of freshwater is precipitation in the form of rainfall and snow. On the surface, freshwater will form water bodies such as rivers, lakes and ponds which mainly flow toward the oceans. Freshwater availability is highly influenced by its interaction with other hydrologic components, for instance, infiltration, percolation, evaporation and transpiration.

Population growth and anthropogenic change have been recognized as primary factors in altering the hydrologic cycle. The result is urbanization, deforestation, industrial development and agricultural expansion. Those activities have dramatically modified freshwater availability and flow regimes. Globally freshwater withdrawals mainly go to irrigated agricultural (70%) followed by industry (21%) and domestic use (10%) (UNEP, 2006). Water diversion has changed natural flow regimes by altering the amount of water released seasonally. For example, the flows released from reservoirs are generally lower during wet seasons than in dry seasons. Higher input during wet seasons is used for restoration purposes and released when it is required. Altering the natural flow regime has changed the characteristics of freshwater input to many ecosystems, particularly downstream ecosystems such as wetlands and estuaries.

Estuaries, partially enclosed water bodies where upland freshwater meets the ocean's saltwater, are some of the most diverse, productive and active ecosystems. The combination of freshwater and saltwater creates unique ecosystem characteristics. Estuaries are active ecosystems because they are influenced by tidal movement and salinity level fluctuation. Estuaries are also considered very productive ecosystems with

some of the most diverse wildlife, because they have large populations of phytoplankton and zooplankton. In addition, estuaries are a source of income to local economies since they provide benefits such as a place for recreation, biological study, and fish and shellfish harvesting. Lastly, the geological function of estuaries as a filter for freshwater before it enters the ocean is also crucial.

Concerns about the availability of freshwater inflows have been increasing as many of the World's estuaries are experiencing a decrease in freshwater input. The rate of freshwater inflows is highly influenced by land use and land cover (LULC) change, upstream water diversion for human uses, and the effects of climate change (Russell et al., 2006). These changes affect estuarine chemical and physical properties (Xu and Wu, 2006). Salinity is used as an indicator of estuary condition because it strongly affects estuaries' productivity. Upstream water diversions and extractions may impact the natural salinity of estuaries both on an annual and seasonal basis. For example, increasing salinity and decreasing *Mulinia coloradoensis* population in the Colorado River Delta of Baja California, Mexico, were the result of extensive upstream diversion on the Colorado River (Rodriguez et al., 2001). In addition, reducing freshwater influx to the Colorado River Estuary has accelerated the growth of two main bivalve mollusk species in the northern Gulf of California by 6 to 28% (Schone et al., 2003).

The Texas Water Development Board (TWDB) and Texas Parks & Wildlife Department (TPWD) have conducted long term data collection and analytical studies for Texas bays and estuaries (Longley, 1994). The purpose of study was to establish the quantity of freshwater inflows needed by seven Texas estuaries, including Nueces,

Mission-Aransas, Guadalupe, Lavaca-Colorado, Trinity-San Jacinto, and Sabine-Neches estuaries, to maintain a sound and healthy environment. The final recommendations were obtained from model simulation. The model relied on computer optimization and hydrodynamic modeling to estimate minimum freshwater inflows (termed MinQ flow) to maintain healthy estuary condition and freshwater flows required to maximize the fisheries harvest (termed MaxH flow) based on historical data.

The Guadalupe Estuary is part of the San Antonio Bay system with an area of approximately 356 km^2. This estuary is the primary habitat for many endangered and threatened species including brown pelican, reddish egret, white-faced ibis, wood stork, bald eagle, white-tailed hawk, peregrine falcon, and whooping crane (TPWD, 2008). The Whooping Crane coordinator of Aransas National Wildlife Refuge, Tom Stehn, reported that fluctuation of freshwater inflow to the Guadalupe Estuary may significantly influence the health and survival of whooping crane (Stehn, 2001). Another study of the impact of freshwater inflow to the Guadalupe Estuary on the blue crab population (Hamlin, 2005), showed a significant relationship between freshwater inflows, salinity, and blue crab population which is one of the most important species in the food network of the estuary.

The Guadalupe Estuary receives freshwater flows from the Guadalupe and the San Antonio River Watersheds. Increase in urbanization and agricultural development in both of these contributing watersheds places more pressure on freshwater inflows to the Guadalupe Estuary. Figure 1 illustrates the final recommendation for monthly freshwater inflows to the Guadalupe Estuary and its median historical flows. The total freshwater

inflows to the Guadalupe Estuary were calculated using following equation (TWDB, 2007):

$$Q_{FWI} = Q_{Gaged} + Q_{Modeled} + Q_{Returned} - Q_{Used} \quad (1)$$

Where:

Q_{FWI} = Total freshwater inflows reaching the estuary

Q_{Gaged} = Total gauged flows obtained from USGS

$Q_{Modeled}$ = Total ungauged runoff calculated by the simulation model

$Q_{Returned}$ = Total returned flows or unconsumed flows

Q_{Used} = Total consumed flows for municipal, industrial, agricultural, and other users.

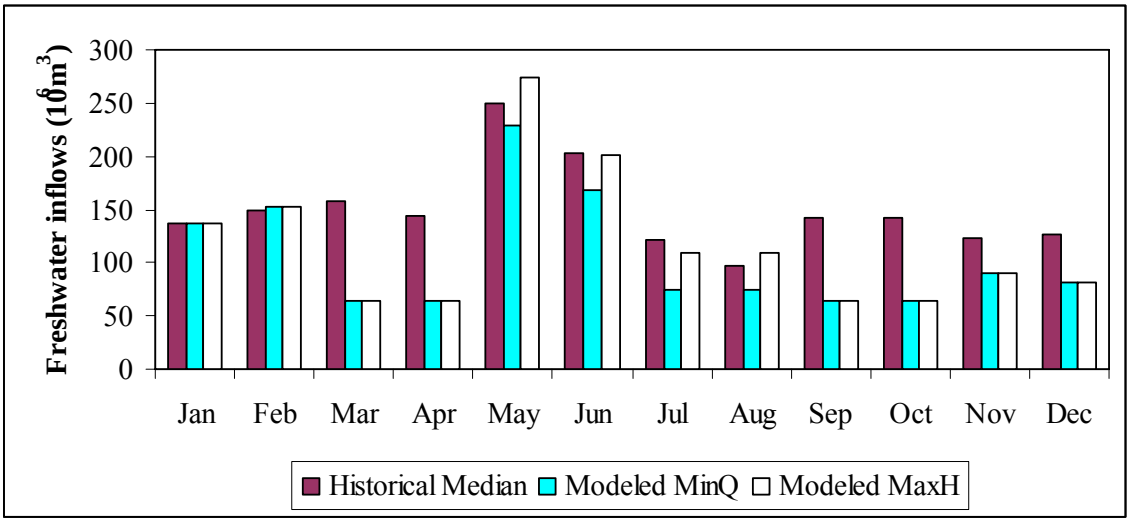

Figure 1. Historical (1941-1999) and modeled freshwater inflows to the Guadalupe Estuary.
Source: TPWD, 2007 and TWDB, 2007

Although Figure 1 clearly shows that the freshwater inflows to the Guadalupe Estuary are good enough to maintain productivity in the estuary, there are some months particularly in the summer that flows are less than those required for maximum fisheries harvest and in February historical flows are less than the minimum required flow. The modeled freshwater inflows suggested that the Guadalupe Estuary needs at least 1,269 x 10^6 m^3 annually to maintain its normal condition and additional 146 x 10^6 m^3 to optimize the productivity. Those needs generally can be fulfilled by more than 30% during May and June. The historical median flows are subject to change and depend on the numbers of available data. Moreover, the possibility of existing trends due to watershed development within the seasonal flows and characteristics of freshwater inflows contributed by the Guadalupe River Watershed alone are not clearly presented.

Generally, most studies conducted previously have focused on the change in freshwater flow regime as a response to LULC changes. The studies involve analysis of hydrographs and time series from recoded flow and application of a hydrologic model to simulate and predict the freshwater flow. Various parameters of the hydrograph have been used to study the relationship between LULC and streamflow regime including daily flow (Costa et al., 2003; Konrad et al., 2005; Potter, 1991), peak flow (Iroume et al., 2005; Pizarro et al., 2006; Potter, 1991; Rose and Peters, 2001), low flow (Rose and Peters, 2001), runoff (Iroume et al., 2005; Rose and Peters, 2001), and baseflow (Dow, 2007; Rose and Peters, 2001). Application of hydrologic modeling provides more reliable results in simulating the watershed response because of LULC changes compare

to conventional paired catchment methods particularly on larger areas and for longer periods of time.

On the other hand, estuarine studies generally place emphasis on estuarine ecosystems response to the variability of freshwater inflows. Besides the previous mentioned studies by Rodriguez et al. (2001) and Schone et al. (2003), various investigations on variability in freshwater inflows and their associated impact on estuaries were done using field experiment or modeling approaches. For example, a descriptive study on variability of freshwater inflows to the Northern Gulf of Mexico contributed by three rivers located on northwest Lake Pontchartrain, Louisiana, was done by Xu and Wu (2006). They found the highest and lowest freshwater contribution to the lake came from the Amite River and Tickfaw River, respectively. They also found that population and climate variability affected freshwater inflows by 20 years of low flow (1954-1973) and 24 years of high flow (1975-1998). Freshwater inflows were also documented to have significant impact on habitat (Hamlin, 2005; Rozas et al., 2005), water quality (Granskog et al., 2005; Russell et al., 2006) and siltation (Pontee et al., 2004) of estuaries.

Hence, it is essential to link the LULC changes on a watershed scale to freshwater inflows to estuaries. On the Guadalupe Estuary, it is essential to analyze the characteristics of historical freshwater inflows and the possibility to connect changes in these flows with urbanization and agricultural development occurring in the contributing watershed. Both the Guadalupe and San Antonio River Watersheds are contributing crucial freshwater inflows to the Guadalupe Estuary. Previously, Sahoo (2008) studied

the effect of LULC change and climate variability from the San Antonio River Watershed on freshwater inflows to the Guadalupe Estuary. Since the Guadalupe River Watershed contributes more freshwater inflows than the San Antonio Watershed, it is important to focus on contributed flows from the Guadalupe River Watershed. It is also important to analyze the effect that human activities on the Guadalupe River Watershed have on freshwater inflows.

The primary objective of this study is to characterize the annual and seasonal freshwater inflows to the Guadalupe Estuary in response to LULC changes on the Guadalupe River Watershed. This overall objective will be accomplished by the following specific objectives:

1. Identify the presence of monotonic trends within the historical hydrologic and meteorologic data record.
2. Identify the possibility that detected trends in hydrologic variables can be attributed to trends in meteorological variables.
3. Extract historical LULC information from remotely sensed data captured within last the 30 years.
4. Calibrate and validate the Soil and Water Assessment Tool (SWAT) model to simulate the freshwater flows on the Guadalupe River Watershed by comparing the simulated flow with Guadalupe River flows measured at a USGS gauging station near Victoria, Texas (USGS 08176500).

5. Describe the characteristics of annual and seasonal freshwater inflows to the Guadalupe Estuary in response to historical LULC changes from 1987 to 2002 and to the impact of water regulation from reservoirs.

This study consists of three components to address all specific objectives. The first component focused on statistical analysis of hydrological and meteorological variables. The second component involves an image classification process to extract historical information of LULC within the study area. The last component focuses on application of a hydrologic model to simulate and to characterize the impacts of LULC on freshwater inflows.

The results of this study are expected to explain the general characteristics of historical freshwater flows of the study area and characterize the freshwater flows to the Guadalupe Estuary as they are impacted by LULC changes. Since this study uses a hydrologic model, the results are expected to verify the effectiveness of the selected model to simulate freshwater inflows. It is also expected that the model will be able to predict availability of freshwater inflows with various scenarios of watershed development. Finally, the results, hopefully, will provide a recommendation to local agencies in implementing sustainable water policies.

CHAPTER II

STUDY AREA

The Guadalupe River Watershed is situated in the central part of Texas between latitude 30°15’47.66” N and 28°30’8.66” N and longitude 99°41’48.11”W and 96°53’19.31”W. It is neighbored by the San Antonio River Watershed on the west side, the Colorado River Watershed on the north side and the Lavaca and Lavaca-Guadalupe River Watersheds on the east side. The watershed encompasses 10 counties including Kerr, Kendall, Comal, Hays, Caldwell, Guadalupe, Gonzales, De Witt, Goliad and Victoria. The major cities in this area are Kerrville, San Marcos, New Braunfels, Seguin and Victoria. The climate in this area is classified as humid subtropical characterized by hot and humid summers and cool to mild winters.

The Guadalupe River is 370 km in length and covers 15,721 km^2. The river rises from Kerr County and is joined by the San Antonio River before emptying into the Guadalupe Estuary. Two main tributaries, the Comal and San Marcos Rivers, are the most important water resources contributing to the Guadalupe River flow (TWDB, 2008). At least four reservoirs have been built since 1928 mainly for hydropower and recreation. Canyon Lake which is built and managed under collaboration between the U.S. Army Corps of Engineers and the Guadalupe-Blanco River Authority (GBRA) is mainly intended for flood control and water supply (GBRA, 2008). On the lower part of the watershed, the Coleto Creek Dam is also intended for flood control and has been in operation since 1980.

The Watershed is divided into four subwatersheds, the Upper, Middle and Lower Guadalupe and San Marcos River Watersheds (Figure 2). The Upper Guadalupe subwatershed is underlain by the Edwards Plateau and is a part of the catchment area for the Edwards Aquifer. The total area of the Upper Guadalupe River Watershed is 3,745 km^2. The area is dominated by evergreen forest which occupies almost 50% of the total area, shrubland and grassland. The Middle Guadalupe River Watershed has an area of about 5,517 km^2 which covers Gonzales, Guadalupe and some parts of De Witt, Comal, and Caldwell Counties. The main land cover is pasture/hay, deciduous forest, grassland and shrubland. Sandies Creek is the main tributary conveying runoff from this area and emptying to the Guadalupe River in De Witt County. The San Marcos River Watershed is located on the eastern side of the Middle Guadalupe River Watershed which covers most of Caldwell and part of Hays and Blanco Counties. This subwatershed has a total area of 3,520 km^2 which is mainly covered by pasture/hay, deciduous forest, evergreen forest, grassland and shrubland. The Lower Guadalupe River Watershed has an area of about 2,704 km^2 covering parts of Victoria, De Witt and Goliad Counties. This area is underlain by the Western Gulf Coastal Plain which is mainly covered by grassland and shrubland on the upper side and wetland and row crops on the lower side (TWDB, 2008).

Urbanization is concentrated in the middle part of the Guadalupe River Watershed mainly in the Comal, Hays, Guadalupe and Caldwell Counties. This area is changing rapidly since it is crossed by the I-35 corridor, a major thoroughfare

connecting Duluth, Minnesota to Laredo, Texas. The total population of those counties increased approximately 57% from 1990 to 2000 and 21.4% from 2000 to 2005.

On the lower part of the watershed, agricultural development has changed the natural land cover to row crops. The lower part which is mainly underlain by Gulf prairies and marshes is fertile farmland. Irrigated lands have increased significantly. The irrigated lands within DeWitt and Victoria Counties increased 95% from 1997 to 2000 while in Gonzales and Guadalupe Counties there was an increase of 60% for the same period. Total irrigated land in the Guadalupe River Watershed increased 65% from 1997 to 2000 (USDA, 2007). This indicates that there is a trend of increasing agricultural activity as well as urbanization in this watershed.

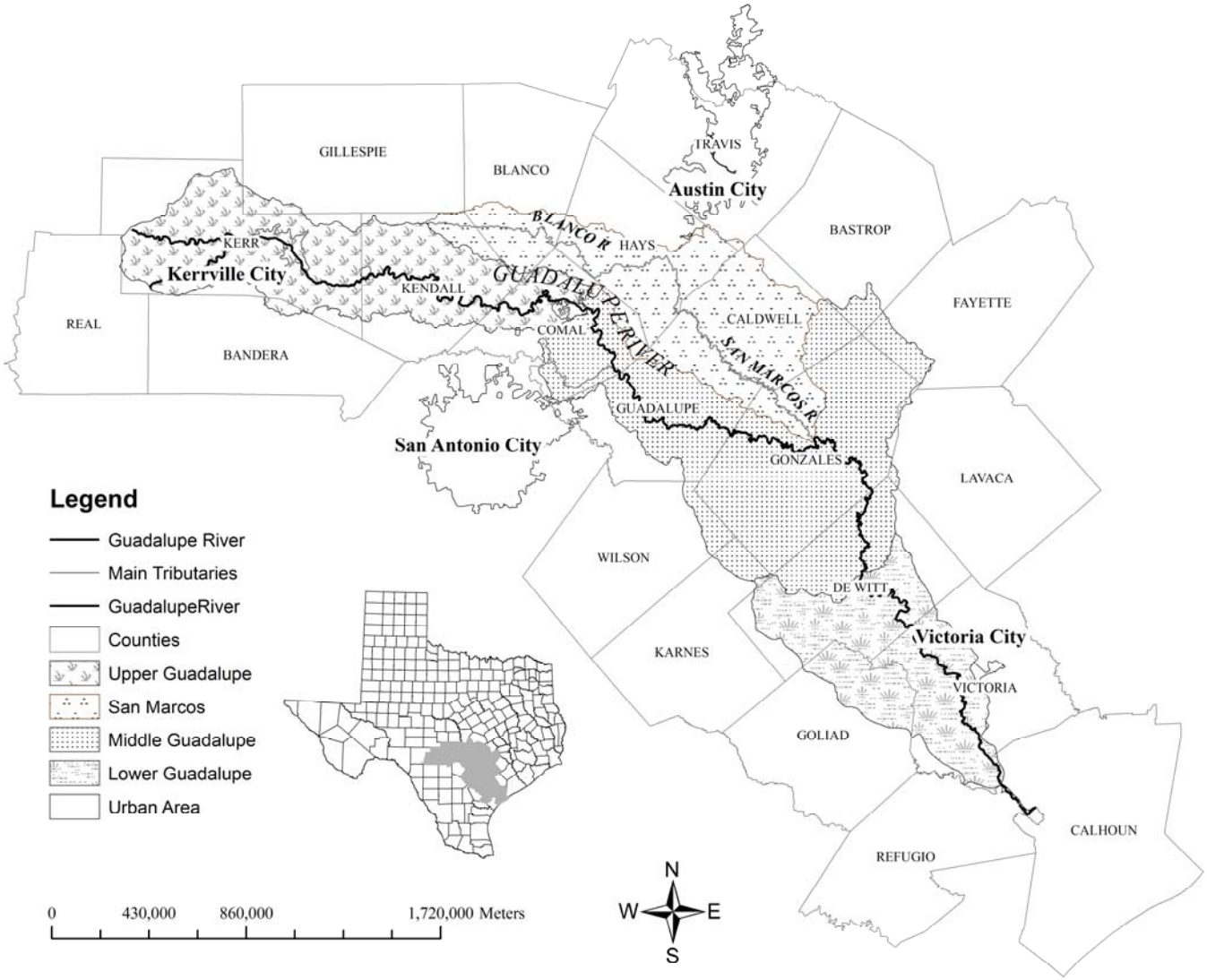

Figure 2. Guadalupe River Watershed, subwatersheds, rivers and tributaries.

CHAPTER III

HYDROLOGIC AND METEOROLOGIC TREND DETECTION

INTRODUCTION

Freshwater ecosystems are always linked to their contributing watersheds. As a part of the complex interactions between the land and hydrologic process components, freshwater ecosystems are highly influenced by land modifications. The timing and the amount of water received and conveyed are easily affected by changes in land use land cover (LULC). For example, urbanization in the Peachtree Creek Watershed, in Atlanta, Georgia has increased peak flows and storm recession rates as the result of efficiency of collection and transmission of water by impervious surfaces and artificial channels to the stream network (Rose and Peters, 2001). The conversion of perennial vegetation to seasonal row crops through deforestation over the last 60 years has increased the flows of the Mississippi River as the result of decreasing evapotranspiration and runoff, and decreasing groundwater recharge, baseflow, and thus streamflow (Zhang and Schilling, 2005). Increasing area under farmland and settlements in the Chemoga Watershed of northwestern Ethiopia has increased surface runoff (Bewket and Sterk, 2005). The runoff and peak flows in four catchments located in the Tenth Region of Chile found that effects of reduction of vegetative cover have increased summer runoff and peak discharge of streamflow (Iroume et al., 2005). The changes in land cover for agricultural purposes have affected the discharge of the Tocantins River, Central Brazil, at seasonal and long-term time scales (Costa et al., 2003).

Vegetation plays an important role mainly in terms of evapotranspiration and interception. Vegetation extracts water from the soil surface and releases it to the atmosphere, providing greater water storage capacity in the soil for the next precipitation event. Some part of precipitation will be intercepted by vegetation and evaporated to the atmosphere again while the other part will reach the ground. Since soil generally has high storage capacity, more precipitation will infiltrate and a small part of it becomes runoff. Part of infiltrated water, then, percolates and becomes potential groundwater recharge. Hence, the existence of vegetative cover is beneficial in reducing runoff and increasing interflow and groundwater flow. The conversion of vegetation to other land use will consequently change the infiltration rate, the volume of runoff and the amount of groundwater flow.

Urbanization and agricultural expansion are the most significant factors in LULC changes. They increase impervious surfaces, disturb natural land cover and soil properties and modify the natural flow regimes. Urbanization increases impervious land uses, reduces infiltration, and causes more runoff and higher peak discharges (Ward and Trimble, 2004). These effects are clearly seen during periods of high precipitation. Water diversion for irrigation purposes also has a significant impact on streamflow. In studying the impact of LULC on streamflow regime, irrigation diversion was found to have the most direct influence on the discharge magnitude of the flows of the Mae Chaem River, Thailand (Thanapakpawin et al., 2007).

Time series analyses have been widely used to describe existing patterns in streamflow variation. Compared to other hydrologic parameters, streamflow is the

easiest variable to be analyzed as an indicator of watershed response. Streamflow data is the most readily available and easiest to access. The US Geological Survey (USGS) has been collecting streamflow data since 1889 and has more than 7,000 continuous record stations (Phillips and Melcher, 2006).

One of the most widely used methods for time series analysis is trend detection. Trend detection is used to determine the existence of significant trends within a time series. The Mann-Kendall (MK) test is one of the most widely used trend detection techniques. It was presented by Mann (1945) as a non-parametric test for monotonic trend which involves application of Kendall's test for correlation. Non-parametric tests are more suitable for hydro-meteorological data (Yue et al., 2002) because they do not assume a distribution for the data. The MK test has been used successfully to evaluate the presence of monotonic trends within time series of data including water quality (Hirsch et al., 1991), streamflow (Burn and Elnur, 2002; Douglas et al., 2000; Novotny and Stefan, 2007; Paquini and Depetris, 2007; Zhang et al., 2006; Zhang et al., 2001a; Zhang et al., 2001b), runoff (Lindstrom and Bergstrom, 2004), temperature and precipitation (Zhang et al., 2000), and evaporation (Burn and Hesch, 2007).

If consecutive values within a time series have a strong correlation to each other then serial correlation exists in the data set. Serial correlation within a time series may increase the chance to reject the null hypothesis of no trend when it is actually true (type I error). Pre-whitening is a method to remove serial correlation within time series (Burn and Elnur, 2002; Douglas et al., 2000; Zhang et al., 2001a; Zhang et al., 2001b; Zhang et al., 2000). Yue et al. (2003) argued that the conventional technique of pre-whitening

removes a portion of trend where the slope of the trend after removing the serial correlation will not be the same as the original slope, hence they introduced a Mann-Kendall Trend Free Pre-Whitening (MK-TFPW) technique which can remove the serial correlation without removing the portion of the trend.

Trend analysis performed at multiple locations/stations within a region raises the question whether local significant trends are also considered significant at a regional scale. The bootstrap or resampling technique has been adopted to determine the critical value of percentage of stations expected to show significant trends by chance (Burn and Elnur, 2002). The bootstrap involves generation of N new time series datasets using a resampling technique from existing data and trend analysis for the N new time series.

Flow in the Guadalupe River is important because the river serves as the primary contributor of freshwater to the Guadalupe Estuary. The rapid changes in landscape characteristics of the Guadalupe River Watershed potentially impact the streamflow regime. Previous studies have not focused on long term trend analysis of streamflow in the Guadalupe River. Garg (2004) conducted long term analysis on historical, naturalized and regulated flows of the Guadalupe River Watershed. Naturalized and regulated flows were obtained from modeling using a combination of Water Availability Model (WAM) and the Water Right Analysis Package (WRAP). Although the study found an increasing linear trend in flow at Victoria, the results did not provide information on the significance of detected trends.

The objectives of this study are:

1. Identify the presence of monotonic trends within time series of hydrologic and meteorologic variables within the Guadalupe River Watershed. Streamflow was selected as the hydrologic variable and precipitation as the meteorologic variable of interest.
2. Identify the possibility of that detected trends in hydrologic variables can be attributed to trends in meteorologic variables.

METHODOLOGY

This study involved the analysis of trend test on recorded streamflow and precipitation time series for local and regional scale. The MK-TFPW technique proposed by Yue et al. (2003) was used to determine local significance while a bootstrap or resampling approach adopted by Burn and Elnur (2002) was used to determine regional significance. Briefly, the overall objectives are accomplished by the following steps:

1. Perform the MK test on all selected time series of both hydrologic and meteorologic variables.
2. Assess the serial correlation within the time series. The serial correlation will be removed using a trend free pre-whitening (TFPW) technique if it is significantly different from zero. The MK test is then only performed on the time series with the serial correlation removed if the serial correlation was positive and significant otherwise the MK trend test is conducted on the original time series.

3. Assess the field significance using a bootstrap/resampling method. This step is used to obtain the critical value for which each parameter is also considered significant at the regional scale.

Mann-Kendall Test

In this study, the MK test was selected for trend detection analysis within the time series data. The MK test statistic is defined as

$$S = \sum_{k=1}^{n-1} \sum_{k=i-1}^{n} \text{sign}(X_j - X_i) \tag{2}$$

Where X_i; X_j are the sequence of data, n is number of data pairs and

$$\text{sign}(X) = \begin{cases} +1 & \text{if} \quad X_j > X_i \\ 0 & \text{if} \quad X_j = X_i \\ -1 & \text{if} \quad X_j < X_i \end{cases} \tag{3}$$

Equation 2 yields a population of values -1, 0 and +1 of size n(n-1)/2. When the time series exhibits increasing monotonic trends, the number of positive values is dominant and the total summation is positive. When there is a decreasing trend, the S value will be negative. This method allows the small increasing or decreasing trends within datasets to be accounted for. Trends are statistically tested for significance at a predefined significance level. The test statistic is given by:

$$U_C = \begin{cases} \dfrac{S-1}{\sqrt{\text{Var}(S)}}, & \text{if} \quad S > 0 \\ 0 \quad , & \text{if} \quad S = 0 \\ \dfrac{S+1}{\sqrt{\text{Var}(S)}}, & \text{if} \quad S < 0 \end{cases} \tag{4}$$

and

$$\mathrm{Var}(S) = \frac{n(n-1)(2n+5)}{18} \tag{5}$$

Under the null hypothesis that there is no trend in the data, the hypothesis is rejected if $|U_C| > z_{1-\alpha/2}$, where Z is from standard normal distribution and α is the local significance level. To incorporate the uncertainty involved in hydrologic processes, this study used a 10% significance level. The slope magnitude can be predicted using a non-parametric slope estimation described as (Burn et al., 2004; Burn and Elnur, 2002; Hirsch et al., 1982):

$$\beta = \mathrm{median}\left[\frac{(x_j - x_i)}{(j-i)}\right] \quad \text{for all } i < j \tag{6}$$

A positive slope indicates an increasing trend and negative, decreasing.

Serial Correlation

The TFPW method was applied to remove serial correlation within time series data. It was accomplished by the following steps:

1) The estimated linear trend was removed using:

$$Y_t = X_t - \beta \cdot t \tag{7}$$

where β is slope calculated by equation (6), X_t is original time series data at time t, Y_t is the detrended series.

2) Serial correlation (lag-1) for the de-trended series, Y_t, was computed. Statistical Package for the Social Sciences (SPSS) was used to calculate the serial correlation. SPSS gives the value of serial correlation and its significance (p-value). In SPSS, the

significance value was computed using the Box-Ljung Q statistic using the following formula (Warner, 1998):

$$Q = N\sum_{k=1}^{m} r_k^2 \tag{8}$$

where N is number of observations and m is the number of lags (r-1). The Q follows a χ^2 distribution with m degree of freedom (df). Under a null hypothesis that the serial correlation equals zero, the null hypothesis is rejected if the p-value of positive serial correlation is less than the selected level of significance. A higher level of confidence, 5%, was selected in this process to minimize the type I error. Less confidence will increase the possibility of rejecting the null hypothesis when it is true. Rejecting a null hypothesis that serial correlation is equal to zero produces a conclusion that data is serially dependent. This conclusion will cause a modification in the original time series by removing its serial correlation.

3) If the positive serial correlation value was not significantly different from zero (p-value less than 0.95) or was negative, then the data was considered serially independent and the MK test result from the original time series was used. If the positive serial correlation was significantly different from zero, then the positive serial correlation was removed from time series using the following formula:

$$Y_t' = Y_t - r_1 \cdot Y_{t-1} \tag{9}$$

Where Y_t' is the serially independent detrended series at time t, and r_1 is lag 1 serial correlation.

4) The estimated trend then was added back to time series by:

$$Y_t'' = Y_t' + \beta \cdot t \quad (10)$$

The MK test is then used to test the pre-whitened (Y_t'') series. The significance level for this test was 10% and any values that exceed this value were considered significant at the local significance value.

Regional Significance and Cross-Correlation

Regionally significant values were assessed using the following steps:

(1) A year was randomly selected from the range of the selected study period. The data from each site for the selected year were entered to a new dataset. This step was repeated until the new dataset had the same number of station-years as the original dataset.

(2) The MK test was applied to each site in the new dataset. The percentage of sites which have a significant trend at the local significance (α_L) level were determined.

(3) Steps (1) and (2) were repeated 500 times and the population of the percentage of stations showing a significant trend was recorded. The critical value at the regional significance level was obtained by plotting the bootstrap empirical cumulative distribution (BECD) for the population using:

$$P(x) = \frac{r}{N+1} \quad (11)$$

where r is the bootstrap data ranked in ascending order and N is the number of repetitions (500). Based on the chosen regional significance level, the critical value for the percentage of significant trends within a network was determined.

To be consistent with the local significance level, a 10% of regional significance was chosen for this study. Based on that, the number of populations from each parameter that exceeded the regional significance level was selected as the critical value. Each parameter having a percentage of local significance greater than the critical value was considered to be regionally significant. This method will preserve the cross correlation within the region by entering all station-data values of the given year which is selected using the resampling technique.

Data

Study Periods

The study periods were selected based on the availability of mean daily streamflows recorded by USGS stations. For uniformity, the last recording date was December 31, 2005. The result was a high variation of record length varying from less than 1 year to more than 80 years leading to difficulty in choosing the most representative observation period. The selection of period of record should be long enough to increase the power of the statistical test in detecting a trend. A minimum of 35 years was selected and the study was focused on three periods: 1930-2005; 1950-2005 and 1970-2005. The reason for selecting 3 periods was to include more data from stations having more data and also to increase the possibility that stations which have a shorter record will be accounted for. The record length resulted in 4, 7 and 13 stations for the periods 1930-2005, 1950-2005 and 1970-2005, respectively. Table 1 lists the 13

selected stations. The locations of stations were distributed over all sub-basins as well as major rivers and tributaries within the Guadalupe River Watershed.

Hydrologic Variables

Twelve hydrologic time series were selected to be tested for trends including minimum, maximum and mean of annual and seasonal flows. Three seasonal flow periods were selected December-March; April-July and August-November corresponding to winter, spring/summer and autumn flows. The mean flows were calculated by summing the total flows and dividing by the number of days within a given period.

Meteorologic Variables

Meteorologic variables often have very strong correlations to hydrologic variables. Hence, it is important to determine whether any significant trends detected in hydrologic variables can be explained by correlation to trends in meteorologic variables. In this study, precipitation was selected as the meteorologic variable. Better Assessment in Science Integrating Point and Non-point Sources (BASINS) 4.0 available from United States Environmental Protection Agency (www.epa.gov) was used to select the meteorological stations that representatively explain the variability of precipitation within the Guadalupe River Watershed. The study periods were selected to coincide with the study period of hydrologic variables that exhibited the greatest number of significant trends.

The data from the selected stations were downloaded from the National Climatic Data Center (NCDC) of National Oceanic and Atmospheric Administration (NOAA). Any missing values were replaced by a corresponding value from the closest alternative station (a station located within 5 miles). If no corresponding station-data was available then the value was set to be a missing value. Since the minimum precipitation will always be zero, only maximum and mean precipitation were selected to be investigated for a monotonic trend using the MK test. The maximum precipitation is a maximum recorded value within the period of interest; annual or seasonal. The mean precipitation is the total recorded value divided by number of the days that have recorded data within the period of interest.

Table 1. USGS stations within the Guadalupe River Watershed used in trend analysis

USGS Station no.	Record from	Located at		Drainage Area (km^2)
		River	Sub-basin	
08165300	8/1/1967	Guadalupe River	Upper Guadalupe	438
08165500	4/23/1965	Guadalupe River	Upper Guadalupe	746
08167000	6/1/1939	Guadalupe River	Upper Guadalupe	2173
08167500	7/1/1922	Guadalupe River	Upper Guadalupe	3406
08168500	12/19/1927	Guadalupe River	Middle Guadalupe	3932
08169000	12/19/1927	Comal River	Middle Guadalupe	337
08171000	9/1/1924	Blanco River	San Marcos	919
08171300	6/1/1956	Blanco River	San Marcos	1067
08172000	5/1/1939	San Marcos River	San Marcos	2170
08172400	5/1/1959	Plum Creek	San Marcos	290
08175000	4/1/1930	Sandies Creek	Middle Guadalupe	1422
08175800	1/1/1964	Guadalupe River	Lower Guadalupe	12779
08176500	12/1/1934	Guadalupe River	Lower Guadalupe	13463

RESULTS

Appendices A and B compiled the MK results for annual and seasonal streamflows and precipitation respectively. The appendices show the MK test on the original time series as well as the detrended time series, the slope magnitude (slope) and serial correlation (lag-1). The final decision of significant trend (trend) or no-significant trend (no-trend) is presented in the last column. The trend or no-trend finding was made by comparing the significant value of the MK test (p-value) with the chosen significance level (5%). The significant value of the MK test of the original time series (p-value original) was used when the serial correlation was negative or positive and not significant (NS).

Appendices A and B also illustrate the bootstrap empirical cumulative distribution (BECD) for each variable that had at least one station showing a significant trend. Each graph was used to determine the critical value for the number of locally significant trends. The critical values for the 10% level of significance ranged from 1 to 2. For all tested variables, if the number of locally significant trends was greater than their critical value then those variables were regionally significant.

Removing positive serial correlation did not significantly change the result of MK test of trend or no-trend. The shifting from significant trend to insignificant was found on minimum annual and minimum Spring/Summer flows of station 08172000 within the period 1950-2005. However, applying the MK test on the detrended time series has changed the power of rejecting the null hypothesis of no-trend within the time series, but it does not have a clear tendency to increase or decrease the power.

Mann-Kendall Trend Test for Hydrologic Variables

Tables 2, 3 and 4 summarize the MK trend test on all hydrological variables for the periods of 1930-2005, 1950-2005 and 1970-2005, respectively. Apparent from the tables, increasing the length of the recording period decreased the density of the stations. During the period 1930-2005 the results showed that no significant trend was detected in maximum annual flows recorded by the four stations while 75% of the stations showed a significant increasing trend on minimum and mean annual flows. Similar results were found when analysis shifted to seasonal flows, particularly for winter and autumn. In spring/summer, the minimum flows showed a significant increasing trend indicated by significant trends found for three stations. Although, local trends were also found on maximum and mean flows in spring/summer and maximum flow in autumn, those trends were not significant at the regional level. Generally, with the exception of mean spring/summer flows, the significant increasing trends found on local minimum and mean flows were also significant at regional level.

An increase in minimum and mean flows is more evident from the MK tests for flows during 1950-2005. The percentage of station having a significant trend on minimum and mean flows range from 57% to 100% and 29% to 100%, respectively. All slope trends were positive indicating increased flow during this period. All detected trends were also significant at the regional level. Shifting the beginning of the period of record from 1930 to 1950 resulted in an increase in the power of the trend from insignificant to significant on minimum and mean flows recorded at USGS 08169000 both annually and seasonally. The percentage of locally significant trends in mean flow

increased for spring/summer and decreased for autumn when the study period was lengthened. During the period 1950-2005, locally and regionally significant trends of maximum seasonal flow for winter were found at three stations, including 08167000, 08167500 and 08169000.

No significant trends were found in flows recorded from 1970 to 2005. The number of observation (n) decreased, which reduces the variance of S, so the decrease in U_C was most likely caused by very little difference in the total positive (+1) and negative (-1) populations. In addition, the trends from 1970-2005 showed more negative slopes. This is evidence that there were more decreasing flows detected during this period, though not significantly decreasing.

Selected Meteorological Stations

BASINS was used to determine the meteorological stations that would represent precipitation variability within the watershed. Eight stations were selected for this study. Two stations were located within the watershed including COOPID 410832 (Blanco) and 413622 (Gonzales). The rest of the stations were located on surrounding watersheds including COOPID 410428 (Austin), 410639 (Beeville), 414254 (Hondo), 415650 (Mason), 417945 (San Antonio), and 419363 (Victoria). The highest percentage of missing data was 0.042% found at the Mason Station.

Table 2. The slope magnitude of USGS stations for the period 1930-2005

USGS Station	Annual			Season 1 (Dec-Mar)			Season 2 (Apr-Jul)			Season 3 (Aug-Nov)		
	Min	Max	Mean	Min	Max	Mean	Min	Max	Mean	Min	Max	Mean
08167500	0.64*	65.90	3.30*	1.51*	4.84	3.54*	1.02*	-10.72	2.56	0.86*	18.91*	3.51*
08168500	1.28*	-22.26	4.24*	1.67*	0.34	4.56*	2.00*	-26.80*	3.10	1.44*	0.23	5.09*
08169000	-0.83	5.70	0.30	0.40	0.55	0.73	-0.56	1.08	0.12	-0.37	1.15	0.14
08171000	0.27*	19.74	1.32*	0.51*	1.31	1.17	0.50*	0.81	1.38*	0.36*	0.92	0.87*
Percent**	**75%**	0%	**75%**	**75%**	0%	**50%**	**75%**	25%	25%	**75%**	25%	**75%**

Note: -* these values indicate locally significant at 90%
-** these bold values indicate regionally significant at 90%

Table 3. The slope magnitude of USGS stations for the period 1950-2005

USGS Station	Annual			Season 1 (Dec-Mar)			Season 2 (Apr-Jul)			Season 3 (Aug-Nov)		
	Min	Max	Mean	Min	Max	Mean	Min	Max	Mean	Min	Max	Mean
08167000	0.87*	27.38	3.71*	2.13*	5.96*	4.62*	1.34*	7.08	4.58*	1.35*	3.18	3.53*
08167500	1*	63.22	6.11*	2.67*	111.32*	6.88*	2.15*	15.53	8.15*	1.79*	25.36	4.17*
08168500	1.69*	-4.10	7.65*	2.80*	7.62	10.29*	3.21*	-0.70	10.23*	2.44*	5.18	5.18
08169000	1.75*	4.27	2.58*	2.46*	2.72*	3.38*	2.08*	4.83	3.37*	2.41*	2.56	3.38*
08171000	0.23	19.53	1.65	0.62*	4.05	2.05*	0.65*	3.96	2.39*	0.46*	0.43	0.68
08172000	0.77	16.79	3.93	1.56*	4.50	5.39*	1.33	-28.47	5.04	1.44*	-1.41	1.94
08176500	3.96	131.83	23.64*	9.57*	58.38	29.14*	9.75*	-22.50	24.39	7.70*	44.92	16.07
Percent**	**57%**	0%	**71%**	**100%**	**43%**	**100%**	**86%**	0%	**71%**	**100%**	0%	**43%**

Note: -* these values indicate locally significant at 90%
-** these bold values indicate regionally significant at 90%

Table 4. The slope magnitude of USGS stations for the period 1970-2005

USGS Station	Annual			Season 1 (Dec-Mar)			Season 2 (Apr-Jul)			Season 3 (Aug-Nov)		
	Min	Max	Mean	Min	Max	Mean	Min	Max	Mean	Min	Max	Mean
08165300	0.10	-7.20	-0.07	0.15	0.40	0.23	0.21	0.10	0.22	0.00	0.02	-0.12
08165500	0.20	-2.80	0.01	0.30	1.06	0.57	0.30	0.03	0.53	0.06	-0.46	0.02
08167000	-0.25	-25.66	0.59	0.80	9.05	2.78	0.00	-7.17	0.71	-0.13	1.70	0.27
08167500	-0.71	-83.93	0.77	0.64	18.39	4.16	0.09	-44.86	0.13	-0.03	27.90	-1.31
08168500	0.68	14.72	3.05	1.57	19.00	6.02	-0.87	-2.10	-0.60	0.88	-6.17	-1.95
08169000	-0.34	3.30	0.59	1.03	2.10	0.99	0.18	-15.21	-0.69	0.12	1.32	0.57
08171000	0.00	60.00	2.19	0.22	7.22	1.72	0.02	-21.94	-0.21	0.08	0.01	0.46
08171300	0.00	36.80	1.55	0.07	4.50	1.26	-0.23	-30.03	-0.52	-0.10	-4.77	-0.11
08172000	0.00	41.67	4.11	0.52	16.28	5.99	-0.37	-96.88	-2.14	0.16	0.64	0.77
08172400	0.00	7.22	0.08	0.00	0.00	0.20	0.00	-31.43	-1.49	0.00	0.00	0.00
08175000	-0.02	6.13	0.59	0.00	10.71	1.26	0.00	-20.97	-1.14	-0.03	3.30	0.15
08175800	-4.21	185.19	15.32	0.65	48.36	27.20	-3.90	-211.25	-18.00	-4.24	12.77	0.08
08176500	-5.65	246.67	14.26	2.28	55.81	25.83	-5.54	4.97	1.10	-3.07	-205.79	-20.94
Percent**	0%	0%	0%	0%	0%	0%	0%	0%	0%	0%	0%	0%

Note: -* these values indicate locally significant at 90%
-** these bold values indicate regionally significant at 90%

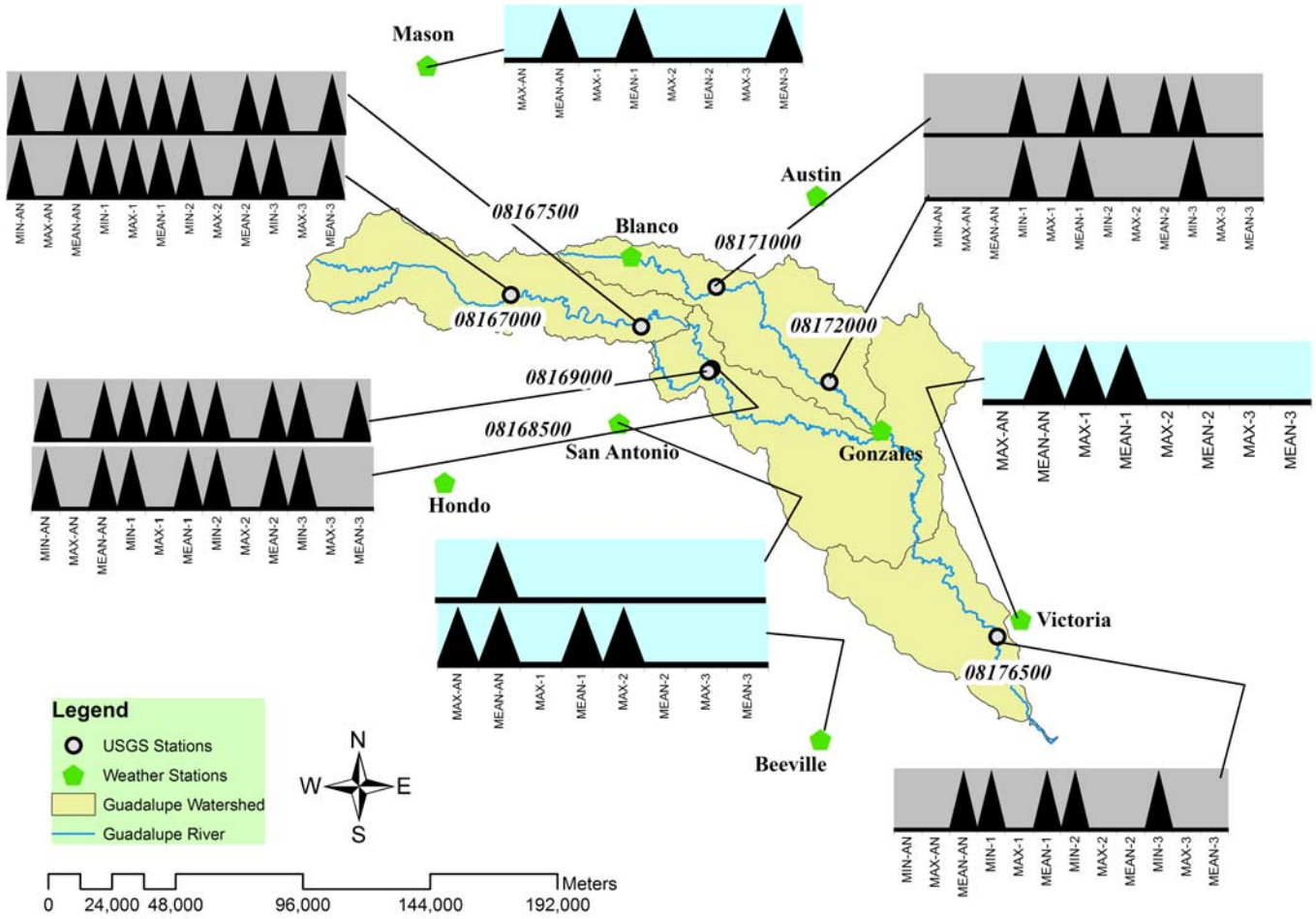

Figure 3. Locally significant trends on streamflow and precipitation (1950-2005). The abbreviation of AN, 1, 2, and 3 in the figure refer to annual, winter, spring/summer and autumn, respectively.

Table 5. The slope magnitude of precipitation stations for the period 1950-2005

Station Name	Annual		Season 1 (Dec-Mar)		Season 2 (Apr-Jul)		Season 3 (Aug-Nov)	
	Maximum	Mean	Maximum	Mean	Maximum	Mean	Maximum	Mean
Mason	0.00533	0.00053*	0.00518	0.00058*	-0.00431	0.00046	0.01000	0.00063*
Hondo	0.00833	0.00026	0.00647	0.00024	0.01188	0.00043	-0.00190	-0.00005
Beeville	0.02477*	0.00052*	0.01100	0.00048*	0.01905*	0.00058	0.00622	0.00025
San Antonio	0.01134	0.00054*	0.00370	0.00026	0.00196	0.00055	-0.00547	0.00043
Austin	0.01282	0.00040	0.00049	0.00034	-0.00161	0.00007	0.00434	0.00054
Gonzales	0.00434	0.00034	0.00672	0.00039	0.00236	0.00023	-0.00839	0.00024
Victoria	0.01430	0.00083*	0.01340*	0.0006*	0.01000	0.00089	-0.00852	0.00026
Blanco	0.00972	0.00020	0.00289	0.00018	-0.00443	-0.00009	0.00289	0.00001
Percentage**	12.50%	**50%**	12.50%	**37.50%**	12.50%	0%	0%	12.50%

Note: -* the values indicate local significant at 95%
-** the bold values indicate field significant at 90%

Mann-Kendall Trend Test for Meteorological Variables

The MK tests were done on precipitation data recorded from 1950-2005. This period was chosen because more hydrological variables with significant trends were detected in the previous analysis during this period. Table 5 summarizes the MK test results for precipitation. The two stations located within the watershed, Blanco and Gonzales, did not exhibit any significant trends at the local level. Precipitation recorded at Beeville was found to have the highest number of significant trends including trends in mean and maximum annual precipitation, mean winter precipitation, and maximum spring precipitation. The significant trends found at Mason were in mean annual precipitation, mean winter precipitation, and mean autumn precipitation. The Victoria station had significant increasing trends in mean annual precipitation, and maximum and mean winter precipitation.

Only local trends found in mean annual and mean winter precipitation were also significant at the regional level. Although some other precipitation variables showed significant trends, the trends were considered local phenomena and insignificant at the regional level. Those regionally significant variables all showed on increasing trend during the period of interest. The spatial analysis of precipitation showed that most of the significant trends were found at the Beeville, Victoria and Mason stations. With the exception of the San Antonio station which exhibited an increasing trend in mean annual precipitation, no trends were found in precipitation at stations located in the middle part of the watershed.

DISCUSSION

The Guadalupe River is an aquifer fed river characterized by constant baseflow generated from Comal and San Marcos Springs. Under normal conditions, those springs provide about 30 percent of the instreamflows for the Guadalupe River, while under drought condition they contribute roughly 70 percent of the river flows (McKinney et al., 2003). This implies that under normal conditions any change in the amount of surface flow will affect the total instreamflows of the river.

The Guadalupe River was characterized by an increase in minimum and mean annual and seasonal flows. This increase was detected during both the periods of 1930-2005 and 1950-2005. The increase in mean flow was primarily a result of a significant increase in minimum flows and an increase in mean annual precipitation. It is more likely that increasing minimum flows were a larger contributor to the increase mean flows. In spring/summer and autumn flows when precipitation changes were not significant the main contribution in increasing mean flows came from significantly increased minimum flows. However, both precipitation and minimum flows played an important role in increasing mean annual and some seasonal flows.

Increased minimum flows could be a result of an increase in agricultural activities and groundwater extraction. As mentioned earlier, the Guadalupe River Watershed is experiencing an increase in irrigated land by 65% from 1997 to 2000. Unused irrigation water flows back to the nearest stream network contributing to baseflow. During April to November, when irrigation is most in use, the significant increase in minimum flows may have been the result of increased return flows from

irrigation. Increasing minimum flows from April to November also suggested increasing groundwater extraction because 48% of water use in the watershed comes from groundwater.

An increase in maximum flows was only detected in winter flow. Since maximum flows are typically correlated to maximum precipitation, it was expected that maximum precipitation would also exhibit more trends during this period. All stations did indeed have a positive slope which means that maximum precipitation tended to increase during 1950-2005. These results have led to several conclusions.

First, most of the significant trends in maximum streamflow were found to be on the upper part of watershed where trends in maximum precipitation were not significant (Figure 3). On the other hand, the Victoria weather station showed a significant increase in maximum precipitation while the nearest USGS station, 08176500, did not exhibit a significant trend in maximum flow. Those results implied that not all of variability in streamflow can be explained by variability in precipitation. However, because the positive slopes were found on both variables, a small increase in maximum winter precipitation has contributed to a significant increasing trend in maximum winter streamflow.

Second, the significant increasing trends in mean annual and winter precipitation contributed to the increase in minimum and mean annual and winter flows. However, the increase in precipitation was less than the increase in streamflow. The results suggested that increased minimum flows during period 1950-2005 were mainly introduced by changing responses of the watershed to precipitation.

Results obtained during the period of 1970-2005 when compared with the other two periods indicated a significant change in streamflow trends. All trends found during both periods 1930-2005 and 1950-2005, disappear in this period. The basic characteristic of the MK test, which does not consider the magnitude of the differences between the values, suggested more variations existed in 1970-2005 flows. The variations could be attributed to some factors that directly affect the flows such as variability in precipitation and changes in watershed characteristic.

In summary, the significant trends that were present on minimum and mean flows were not fully explained by the significant trends in precipitation. Lack of relationship between hydrologic and meteorologic variables suggested the presence of other significant factors influencing the increase in streamflow. It is important to examine the possibility of changes in climate and LULC within the watershed because those factors have been acknowledged to have significant impact on the changes in streamflow.

CHAPTER IV

LAND USE AND LAND COVER CHANGE ANALYSIS

INTRODUCTION

Land use and land cover (LULC) changes are the product of human activities that have significant impact on environment. The impact has been a big concern and efforts have been to monitor, study and minimize it. The changes in LULC mainly involve the conversion of natural vegetation to crops or urban areas. Previous studies showed that LULC change significantly altered the hydrologic cycle in terms of runoff, baseflow and evapotranspiration (Bewket and Sterk, 2005; Costa et al., 2003; Iroume et al., 2005; Zhang and Schilling, 2005). Although it is poorly understood because of its complexity, long term impact of LULC change has been documented to change precipitation patterns by changing the global climate (Gero and Pitman, 2006; Notaro et al., 2005; Taylor et al., 2002).

The most significant development in LULC study has been achieved within the last two decades by launching and utilizing satellites as platforms for Earth's observation. The improvement in both spectral and temporal resolutions of satellite images allows more observations on larger areas. The developments also increased the ability and effectiveness of studying land use/cover change. Changes can now be easily detected by comparing images from different acquisition dates.

Remote Sensing for Land Use and Land Cover Change Studies

Remotely sensed data has been widely used to extract LULC information. The availability of remote sensing techniques to capture varying resolutions of the Earth's objects enables study at scales ranging from local to global. The spatial resolution refers to the area of the Earth's surface covered by a pixel in an image. The higher the resolution, the less the area covered by a pixel, which means more detail is discernable in the objects of interest.

Remote sensing in this case is the application of sensors to extract information of reflected or emitted electromagnetic energy from an object or area of interest at a remote point. The energy is divided into many spectra and stored based on their spectral bands. The number of bands used to restore an image is known as the spectral resolution. Multispectral remote sensing uses many bands to store the collected information while hyperspectral applies hundreds of bands.

The Landsat program is the United States' oldest land-surface observation satellite system (Jensen, 2005) managed by the National Aeronautics and Space Administration (NASA). Seven satellites have been launched as platforms since 1972 (Table 6). The Landsat program has used four different type of sensors; Multi-Spectral Scanner (MSS), Thematic Mapper (TM), Enhanced Thematic Mapper (ETM) and Enhanced Thematic Mapper Plus (ETM+). MSS was the only recording instrument on Landsat 1 to 3, recording 4 spectral bands from 0.5 – 1.1 μm (Table 7). Landsat 4 and 5 used both MSS and TM sensors. The TM sensor has a higher spectral, spatial, temporal and radiometric resolution than MSS (Jensen, 2005). Landsat 6 was trying to carry the

ETM sensor but, unfortunately, it failed to reach orbit. The ETM+ sensor carried by Landsat 7 has the capability to record 15 m panchromatic band and a higher spatial resolution of band 6 than TM.

A scanner measures the reflected electromagnetic radiation and stores it in bands based on their wavelength. The information is recorded in analog format and transformed to a discrete digital number before it is sent to an Earth-based station. The digital number (DN) represents the brightness value (BV) of an object or an area on the Earth's surface and has a range dependent on the data format being used. For example, the ranges are from 0-128 and 0-255 for 7 bit and 8 bit data format, respectively. A higher resolution allows more information to be stored in the image, but then more capacity is needed to store that information. Generally, the brightness value of an image can be expressed by (Peschel, 2004):

$$BV_{ijk} = \begin{Bmatrix} x_{1,1,k} & x_{1,2,k} & \cdots & x_{1,m,k} \\ x_{2,1,k} & x_{2,2,k} & \cdots & x_{2,m,k} \\ \vdots & \vdots & \ddots & \vdots \\ x_{n,1,k} & x_{n,2,k} & \cdots & x_{n,m,k} \end{Bmatrix} \tag{12}$$

where *i* is number of rows, *j* is number of columns and *k* is number of spectral bands. Image analysis such as classification, transformation, and segmentation are performed on these unique values.

Table 6. The platforms, durations recorded and sensors of the Landsat program *

Satellite	Period of recording	Sensor
Landsat 1	July 23, 1972 to January 6, 1978	MSS
Landsat 2	January 22, 1975 to July 27, 1983	MSS
Landsat 3	March 5, 1978 to September 7, 1983	MSS
Landsat 4	July 16, 1982 to present	MSS, TM
Landsat 5	March 1, 1984 to present	MSS, TM
Landsat 6	October 5, 1993 (did not reach orbit)	ETM
Landsat 7	April 15, 1999 to present	ETM+

* Source: Jensen, 2005

Table 7. Multi-Spectral Scanner (MSS), Thematic Mapper sensor (TM) and Enhanced Thematic Mapper Plus (ETM+) Bands*

Bands	MSS		TM		ETM +	
	Spectral Resolution (μm)	Spatial Resolution (m)	Spectral Resolution (μm)	Spatial Resolution (m)	Spectral Resolution (μm)	Spatial Resolution (m)
1			0.45 – 0.52	30 x 30	0.450 – 0.515	30 x 30
2			0.52 – 0.60	30 x 30	0.525 – 0.605	30 x 30
3			0.63 – 0.69	30 x 30	0.630 – 0.690	30 x 30
4	0.5 – 0.6	79 x 79	0.76 – 0.90	30 x 30	0.750 – 0.900	30 x 30
5	0.6 – 0.7	79 x 79	1.55 – 1.75	30 x 30	1.550 – 1.750	30 x 30
6	0.7 – 0.8	79 x 79	10.40 – 12.50	120 x 120	10.4 – 12.5	60 x 60
7	0.8 – 1.1	79 x 79	2.08 – 2.35	30 x 30	2.08 – 2.35	30 x 30
Panchromatic					0.52 - 0.90	15 x 15

* Source: Jensen, 2005

The sensors do not perfectly reproduce the images. Reflected energies are often time experiencing distortions or errors while traveling through the air to the sensor. Generally, there are two types of errors; internal and external errors (Jensen, 2005). Internal errors are mainly introduced by sensor or platform errors which is generally systematic. External errors are usually caused by atmosphere condition, elevation, slope and aspect. Error corrections are typically done before the classification process which involves radiometric and geometric corrections. Radiometric distortion is caused by several factors generally grouped into atmospheric attenuation, caused by scattering and absorption in the atmosphere, and topographic attenuation. Atmospheric correction is not necessarily performed before classification if the spectral signatures characterizating the desired classes are derived from the image to be classified (Song et al., 2001). Geometric correction processes attempt to remove internal errors and errors associated with the curve of the Earth's surface. Geometric corrections are typically performed using two methods: image to map registration or image to image rectification. The latter uses a corrected image while the former uses a map. The selected correspondence points of two images will be used to correct the errors. DN values of the new geometrically corrected image are generated using resampling methods.

Image Classification

Image classification is a primary component of LULC mapping. The main purpose is to assign each pixel to a group of pixels that have identical spectral characteristics or classes that have been previously determined. The classes are commonly based on the image resolution and the availability of classification systems.

Today, there are many classification schemes providing defined classes for classification. The 30 x 30 m spatial resolution of Landsat images commonly use a level 1 USGS classification scheme consisting of 9 classes: water, developed, barren, forested upland, shrubland, non-natural woody, herbaceous upland natural/seminatural vegetation, herbaceous planted/cultivated and wetland (Jensen, 2005). The higher the spatial resolution the more information that can be extracted from the image and more classes can be created in the classification process. Principally, level 2 classification schemes are subdivisions of classes in level 1. For instance, forested upland can be categorized into deciduous, evergreen and mixed forest.

The two most widely used classification techniques are supervised and unsupervised classification. Supervised classification depends upon a sample of pixels selected by the user to represent various surface cover types called the training site. The training site should be as homogenous as possible. In many cases the pixel is a combination of more than one surface cover type and it is difficult to obtain a homogenous training site although the user may know the site very well. Based on the class characteristic, a computer algorithm then defines the spectral signature of each class and assigns all pixels to their class according to spectral information from those pixels. Porter-Bolland et al.(2007) applied supervised classification to classify the La Montaña region in Campeche-Mexico, during two periods, 1988 and 2005. Additional information such as ground control points, land uses, soil types and topography were used for discriminating forest type in the region. In the final classification the image from 2005 was 87% accurate. A maximum likelihood supervised classification was used

for land use mapping of irrigated agricultural area, below the Chardara Reservoir in southern Kazakhstan, using Landsat 7 ETM+ images (El-Magd and Tanton, 2003). A multistage classification process was employed and regional information about 11 LULC types were used to extract LULC spectral signatures. Using 44 training samples, resulted in an 85% overall accuracy.

Instead of relying upon training sites, the unsupervised classification method clusters the pixels into a number of classes previously defined by the user. User inputs such as the number of classes and statistical parameters are needed prior to the classification process. In most applications, the numbers of class inputs are more than the number of classes of interest, and the user combines classes to come up with the final number of classes. The Iterative Self-Organizing Data Analysis Technique (ISODATA) is the most well known and widely used unsupervised algorithm. Musaoglu et al. (2005) used an ISODATA unsupervised classification procedure to classify Landsat 5 TM images of Beykoz Province, Istanbul, Turkey, for the years the 1984, 1992 and the 2001. The classification accuracies were 84% for 1984 and 1992 images and 80% for 2001 image. The accuracies were assessed by generating 100 random points and comparing to corresponding points at the same coordinates on higher resolution images (SPOT PAN Indian Remote Sensing, Orthophoto and Thematic maps). The ISODATA method was also used to classify Landsat 7 ETM+ images of eight ecoregions covering 25 million hectares across portions of Washington, Oregon and California (Jiang et al., 2004). In this study, digital orthophoto quadrangle (DOQQ) data, aerial photos and field investigations were used for assigning clusters to a specific class. A cluster that did not

match any class would be rerun until assigned to a class. The overall accuracy was 90% which is higher than previous studies in that region.

Previous studies have tried to document LULC information of the Guadalupe River Watershed. Most of them focused on the upper part of watershed including the Upper Guadalupe River and parts of San Marcos and Middle Guadalupe River Watersheds. These areas are of interest because they are underlain by the Edwards Aquifer, the primary source of water for the City of San Antonio. Peschel (2004) classified this area into five land cover classes including water, grassland, woodland, irrigated land and impervious surface, using Landsat Thematic Mapper (TM) and Enhanced Thematic Mapper plus (ETM+) satellite data captured in 1986, 1993 and 2001. The overall accuracies were 76.6%, 77.2% and 76.0% for 1986, 1993 and 2001, respectively. Afinowicz et al. (2005) classified the Upper Guadalupe River Watershed into eight classes to discriminate wooded area. The overall accuracies were 74.4% when comparing against manually interpreted aerial photographs and 90% when using ground surveys.

The USGS National Land Cover Dataset (USGS-NLCD) provides a 1:250,000 scale digital land cover dataset available for the entire US. The dataset adopted level II of the Anderson classification system. USGS-NLCD has produced digital land cover datasets for the years 1992 and 2001. Wickham et al. (2004) performed an accuracy assessment for the 1992 dataset for the western United States which includes the State of Texas. The overall accuracies were 74% for level II and 44% for level I.

Limited historical LULC information is the primary reason for classifying LULC in the Guadalupe River Watershed. This chapter focuses on the extraction of historic LULC within the Guadalupe River Watershed using image classification techniques and Landsat satellite images. The specific objectives were to: (1) classify Landsat satellite images captured in years 1987, 1999 and 2002 into six land cover classes: water, forest, grassland, irrigated land, urban and wetland, using an ISODATA unsupervised classification method; and (2) assess the accuracy of the classification results using higher resolution DOQQ images. The desired result of this study was a land cover dataset for the Guadalupe River Watershed with accuracies of 70% or greater. The land cover classes in this chapter were used as input for the SWAT model detailed in the next chapter.

METHODOLOGY

This study involved the classification process of Landsat satellite images and the accuracy assessment on the classification results. An ISODATA unsupervised algorithm was selected to classify the Landsat satellite data into six land use/cover classes including water, forest, grassland, irrigated land, urban and wetland. Because of the difficulty in discriminating between grass, pasture and other cultivated plants, those land covers were all assigned to grassland. Wooded areas such as forest or brushland were classified into forested area. Additional images derived from elevation data and transformed original Landsat data were employed to improve the inherent variation between the pixels. The accuracies were determined by comparing ground truth points

acquired from the higher resolution image to points from the classified image and presented using an error matrix.

Image Classification

Data Acquisition and Pre-Processing

Three different periods, 1987; 1999 and 2002, were selected to assess LULC changes on the Guadalupe River Watershed. Four scenes from each period were overlain to cover the entire watershed including: path 27 row 39, path 27 row 40, path 26 row 40 and path 28 row 39. The images of year 1986 were collected using Landsat 5 (TM) while most of the images for years 1999 and 2002 were from Landsat 7 (ETM+). All images of 1987 and 1999 were obtained from USGS while 2002 images were downloaded from the Texasview website (www.texasview.org). Cloud free images are essential for the classification process to avoid misclassification. Clouds in images are represented by high DN values which are frequently misclassified to bare soil or urban area. Area falling within cloud shadows will have low DN values and can be misclassified as water bodies.

Table 8 presents a description of the images used in this study. In the 1980's, most cloud free images of the watershed area were captured in September to December. The best combination of cloud-free images for all scenes was taken in September. Two sets of images in 1987, path/row 26/40 and 28/39 were excluded because they were not cloud-free images. Those images were replaced by images captured in 1985 and 1986 during the same time of year. The selection of images representing the LULC in the

1990's was based on availability of ETM+/Landsat 7 images. The 1999 Landsat 7 image of path/row 26/40 was replaced by a Landsat 5 image recorded at the same time of the year because the 1999 image was covered with clouds. Because a cloud-free image for path/row 28/39 was unavailable both from Landsat 5 and 7, the image was replaced with one captured in December. The 2002 images were free images available on the Texasview website.

Most of the images have a Universal Transverse Mercator (UTM) Zone 14 coordinate system with the World Geographic System of 1984 (WGS84) datum. The path 28/ row 39 image was the only image that needed to be reprojected because it had a North American Datum of 1983. The projection process was performed using the Environment for Visualizing Images 4.3 (ENVI 4.3).

Table 8. Sensors, dates and locations of Landsat images used to classify land cover in the Guadalupe River Watershed

Path/Row	Acquisition Date	Sensor/satellite
26/40	October 17,1986	TM/Landsat 5
26/40	October 5, 1999	TM/Landsat 5
26/40	November 22, 2002	ETM+/Landsat 7
27/39	September 25, 1987	TM/Landsat 5
27/39	October 20, 1999	ETM+/Landsat 7
27/39	November 13, 2002	ETM+/Landsat 7
27/40	September 25, 1987	TM/Landsat 5
27/40	October 20, 1999	ETM+/Landsat 7
27/40	November 22, 2002	ETM+/Landsat 7
28/39	September 26, 1985	TM/Landsat 5
28/39	December 14, 1999	ETM+/Landsat 7
28/39	November 22, 2002	ETM+/Landsat 7

An image to image registration process was selected for geometric correction. At least 20 points were selected from the 1987 and 1999 images and their corresponding points on the georeferenced image from 2002. The registration processes were completed by maintaining a root mean square (RMS) error less than 0.5.

The USGS provides 8-digit hydrologic unit codes (HUC) over the entire United States. The Guadalupe River Watershed consists of four 8-digit HUC watersheds: the Upper Guadalupe (12100201), the Middle Guadalupe (12100202), the San Marcos (12100203) and the Lower Guadalupe (12100204). Information for watershed boundaries was extracted and reprojected to the remotely sensed data projection. The study area of each watershed was created using the edit feature utilities within ArcGIS 9.1. The study areas were slightly larger than the watershed boundaries and were converted to vector files prior to being used in the sub-setting process using the ENVI subset tool. The study area not only reduced the amount of data to be analyzed but also allowed pixels outside the watershed boundaries to be counted in the classification process. Simple radiometric correction using the dark subtraction approach was applied to all subsetted images. The user minimum value parameter was chosen in this process. To obtain full coverage of each subwatershed, subsetted images were merged together using the mosaic tool in ENVI. Color adjustments were applied in merging processes to minimize gap between subsetted images.

Image Classification Technique

The main inputs for the calibration process in this study are the Landsat image and the Digital Elevation Data (DEM). Figure 4 illustrates the classification process which is explained in the following paragraphs. In general, the classification process utilized the selected band from the original image, the transformed image bands and a slope band derived from the DEM.

Principal Component Analysis (PCA) and Normalized Difference Vegetation Index (NDVI) were used to transform the raw Landsat data. These transformation techniques have been widely used. PCA transforms the original remotely sensed dataset into a substantially smaller and easier to interpret set of variables that represent most of the information present in the original dataset (Jensen, 2005). The ability of PCA to present the information in a smaller number of bands increases the efficiency of the classification process. NDVI transformation is based on the differences of reflected energy from vegetation between the near-infrared band (NIR) and red band (RED). Chlorophyll, the leaf pigment, reflects more near-infrared and absorbs visible light. The more vegetation, the stronger near-infrared is reflected. The NDVI transformation uses the following equation:

$$\mathrm{NDVI} = \frac{(\mathrm{NIR} - \mathrm{RED})}{(\mathrm{NIR} + \mathrm{RED})} \tag{13}$$

DEM dataset presents surface elevation information in raster format. From the DEM, other information such as slope, contour or aspect can be easily extracted. DEM and its derivatives have been widely used in the classification process, prior to

classification or along with the process as an input band. Oetter et al.(2000) added the DEM dataset to several Tasseled Cap bands obtained from multi-dated Landsat TM images to classify the William River Basin of western Oregon using a supervised maximum likelihood technique. More complex inputs of DEM, slope, aspect and landform have been applied in classification of vegetation type on the Kaibab National Forest in northern Arizona using a decision tree (Joy et al., 2003).

In this study, DEM datasets were downloaded from the USGS website using the Seamless Data Distribution page (seamless.usgs.gov/website/seamless/viewer.htm). The spatial analysis extension tools within ArcGIS 9.1 were used to produce the percentage of slope information. The raster dataset was converted to geo-tiff format for further analysis using ENVI software.

ENVI was used to compile the input of slope, first PCA, NDVI band and selected original spectral bands into a new image dataset. The spectral band from the original dataset was selected as long as it had low correlation (<0.6) to both PCA and NDVI. 5000 points were randomly generated within the study area using Hawth's tool, an extension of ArcGIS created by Hawthorne Beyer (www.spatialecology.com). The digital numbers of each band corresponding to each random point were collected and calculated for their correlation. The process was conducted for each image 1987, 1999 and 2002, separately. Based on their correlation information images from 1987 and 1999 had 4 bands of input: PCA, NDVI, Band 4 of the original Landsat image and slope while the 2002 image had in addition Band 3 of the original Landsat image.

Urban and wetland areas were extracted from the main scene and independently classified. The shape files were used to create masks for urban and wetland areas in ENVI. Urban area shape files within the State of Texas were downloaded from the Texas General Land Office website (www.glo.state.tx.us). Data was manually corrected to minimize the possibility of excluding certain urban areas. The wetland shape file was downloaded from the National Wetland Inventory website (www.fws.gov/nwi), which manages and provides the newest information about wetlands.

An ISODATA unsupervised classification technique was chosen to extract LULC information within the watershed. The parameters were set to classify the images for up to 250 classes with a maximum number of iterations of 20 and a threshold change of 5%. These two numbers are very important for the classification process in that classification will terminate after 20 iterations or a 5% or less pixel change for each class. The minimum class distance and maximum class standard deviation were set at five and three, respectively. Only two classes were allowed to be merged. These parameters were applied over the entire image including urban and wetland area classification processes.

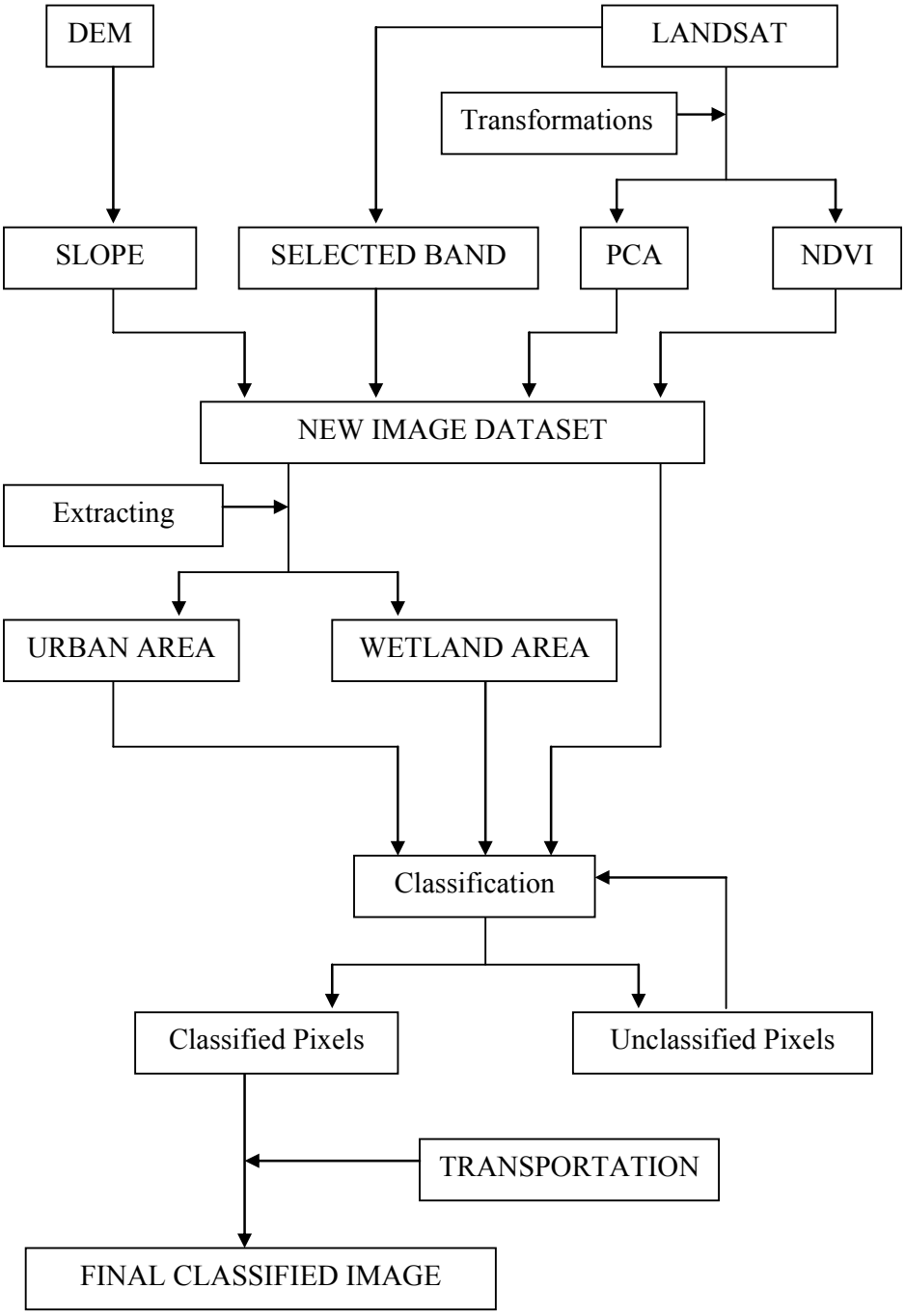

Figure 4. Schematic of classification process.

The original Landsat image and geo-referenced DOQQs downloaded from Texas Natural Resource Information Server (TNRIS) were used as a source for assigning each clustered pixel to one of the land cover classes. The scene was divided into three scenes: main, urban, and wetland scenes. The main scene covered the entire watershed area while the urban and wetland scenes covered only urban and wetland areas, respectively. The process was intended to classify the main scene into water, forest, grassland, and irrigated land. The urban scene was assigned into urban and non-urban. The wetland scene was classified into wetland and non-wetland. Clustered pixels resulting from the first classification of the main scene were assigned into five classes, water, forest, grassland, irrigated land, and unclassified. Each urban scene was grouped into urban, non-urban, and unclassified while each wetland scene was assigned to water, forest, grassland, irrigated land, wetland, and unclassified. Because there was no urban area in the main scene, the roads, bare lands and other urban features were classified into grassland. Classified images were saved in geo-tiff format.

The second classification process was used to classify the unclassified pixels into classes which were similar to the classes in first classification. Using the same parameters as the first classification, the second classification grouped all unclassified pixels into one of the defined classes. The spatial analyst extension tools of ArcGIS 9.1 were used to create the masks for the second classification.

Transportation files or Texas Department of Transportation (TxDOT), downloaded from TNRIS, were merged and clipped so only the portion within the Guadalupe River Watershed was used. Visual identification and manual correction were

performed to remove or add transportation elements for the 2002, 1999 and 1987 images. The shape files were then converted to a raster dataset having a 30 x 30 m resolution.

The final classified images were a combination of the first and second classification results of the main scene, the urban area, the wetland area and the transportation raster dataset. The process of combining the results was done using the raster calculator option of spatial analysis tools in ArcGIS 9.1.

Classification Accuracy Assessment

Accuracy assessment is essential to give information about how closely the image classifications reflect the LULC. The information attained is the overall and class errors caused by misclassification. The most common means of expressing classification accuracy is an error matrix (*confusion matrix* or a *contingency* table) (Lillesand and Kiefer, 1994). The error matrix compares information from a pixel in the remote sensing-derived classification map to ground test information (Jensen, 2005). Columns in the matrix represent the ground point data while rows are the points derived from the classified image. From here other descriptive measurement can be extracted such as producer, user and overall accuracies. The producer's accuracy indicates how well a particular land cover type can be classified and is obtained by dividing the number of pixels correctly classified by the total number of referenced data points for that land cover type. The user's accuracy describes the probability that a pixel's classification into a particular category on the map actually represents that category on the ground (Lillesand and Keifer, 1994). The user's accuracy is calculated as the number of pixels

correctly classified into a particular class divided by the total number of pixels that fall into that class. The overall accuracy is obtained by dividing the number of reference pixels that are correctly classified into their category by the total number of reference pixels.

In this study, the ground test information was derived from randomly selected points within the DOQQ images. At least 300 points per image were generated randomly and verified against DOQQ images. The 1 m resolution DOQQ images provide a better visual observation on objects or areas within the images than 30 x 30 m of Landsat images.

RESULTS AND DISCUSSION

Image Classification

Upper Guadalupe River Watershed

The Upper Guadalupe River Watershed has an area of 3,734 km^2 and was classified into five land cover classes. The Upper Guadalupe River Watershed drains part of Kerr, Kendall and Comal Counties. Table 9 and Figure 5 present the classification results for this subwatershed. Water area increased by 20.5% (7 km^2) from 1987-2002. The main existing water body is Canyon Lake which has an area of approximately 33 km^2. The trend increase and decrease in water areas during the period of study were most likely influenced by the amount of precipitation falling over this area. The nearest weather stations located within this area, Kerrville and Blanco Stations, showed the total accumulation of precipitation one month prior to when the images were

captured increased by 25 % from 1987 to 2002 (198 to 247 mm). The water level of Canyon Lake also increased from 276.7 to 277.2 m (USACE, 2008).

Although the results tend to overestimate the actual area, the increase in irrigated land from 1999 to 2002 agreed with U.S. census data. The recorded irrigated lands within Kerr, Kendall and Comal County were 11 km^2 and 14 km^2 for 1997 and 2000 (US Census). Urban area was mostly found at Kerrville and the area surrounding Canyon Lake Reservoir. This area increased approximately 67 km^2 from 1987 to 2002.

San Marcos River Watershed

The San Marcos River Watershed is named after the San Marcos River which is one of main tributaries to the Guadalupe River. The watershed area is approximately 3,535 km^2. Figure 6 shows the classified images for this watershed for 1987, 1999 and 2002. The changes in area covered by the five land use classes are summarized in Table 10. With the exception of a decrease in grassland area by 14.8% (322 km^2), all land cover types increased from 1987 to 2002. Water area increased by 96.7% (12 km^2), which was the greatest percentage change but one of the smallest by magnitude. No large reservoirs were found within the watershed, but a number of smaller reservoirs were distributed over the area. The increase in area covered by water was mainly contributed by the presence of new reservoirs or ponds. They were distributed over Caldwell and Guadalupe Counties where most irrigated land is found.

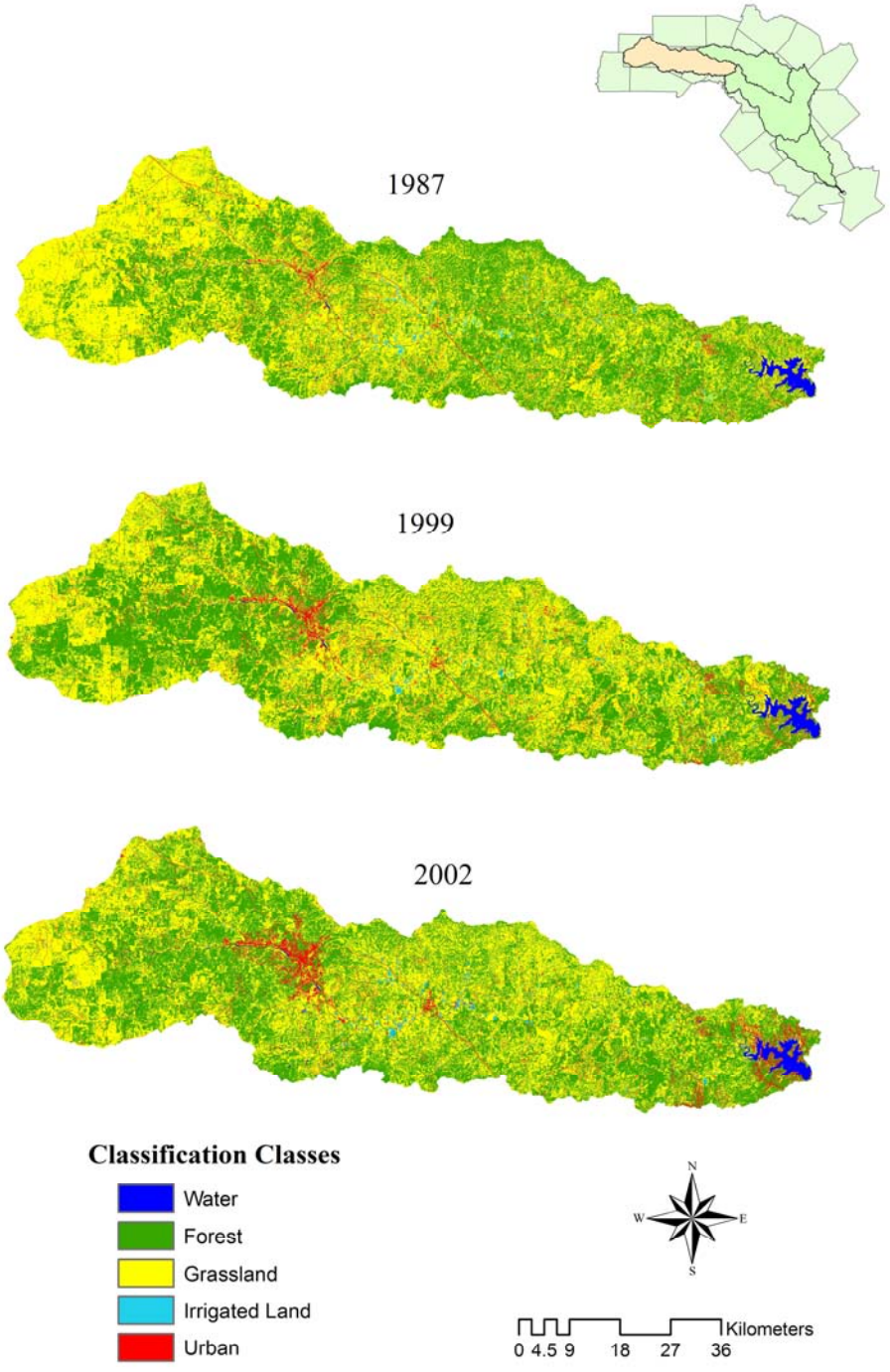

Figure 5. Land cover classification of the Upper Guadalupe River Watershed for 1987, 1999 and 2002.

Table 9. Classification results for the Upper Guadalupe River Watershed from 1987 to 2002

Land Cover Classification	1987 Area (km^2)	1999 Area (km^2)	2002 Area (km^2)	1987-2002 change (km^2)	1987-2002 change (%)
Water	33	37	40	7	20.5
Forest	1,613	1,719	1,774	161	10.0
Grassland	1,947	1,789	1,717	-230	-11.8
Irrigated Land	33	22	29	-4	-12.5
Urban	107	166	174	67	62.6

Table 10. Classification results for the San Marcos River Watershed from 1987 to 2002

Land Cover Classification	1987 Area (km^2)	1999 Area (km^2)	2002 Area (km^2)	1987-2002 change (km^2)	1987-2002 change (%)
Water	12	16	24	12	96.7
Forest	1,006	925	1,230	224	22.3
Grassland	2,171	2,223	1,849	-322	-14.8
Irrigated Land	242	244	250	8	3.2
Urban	104	127	183	79	75.3

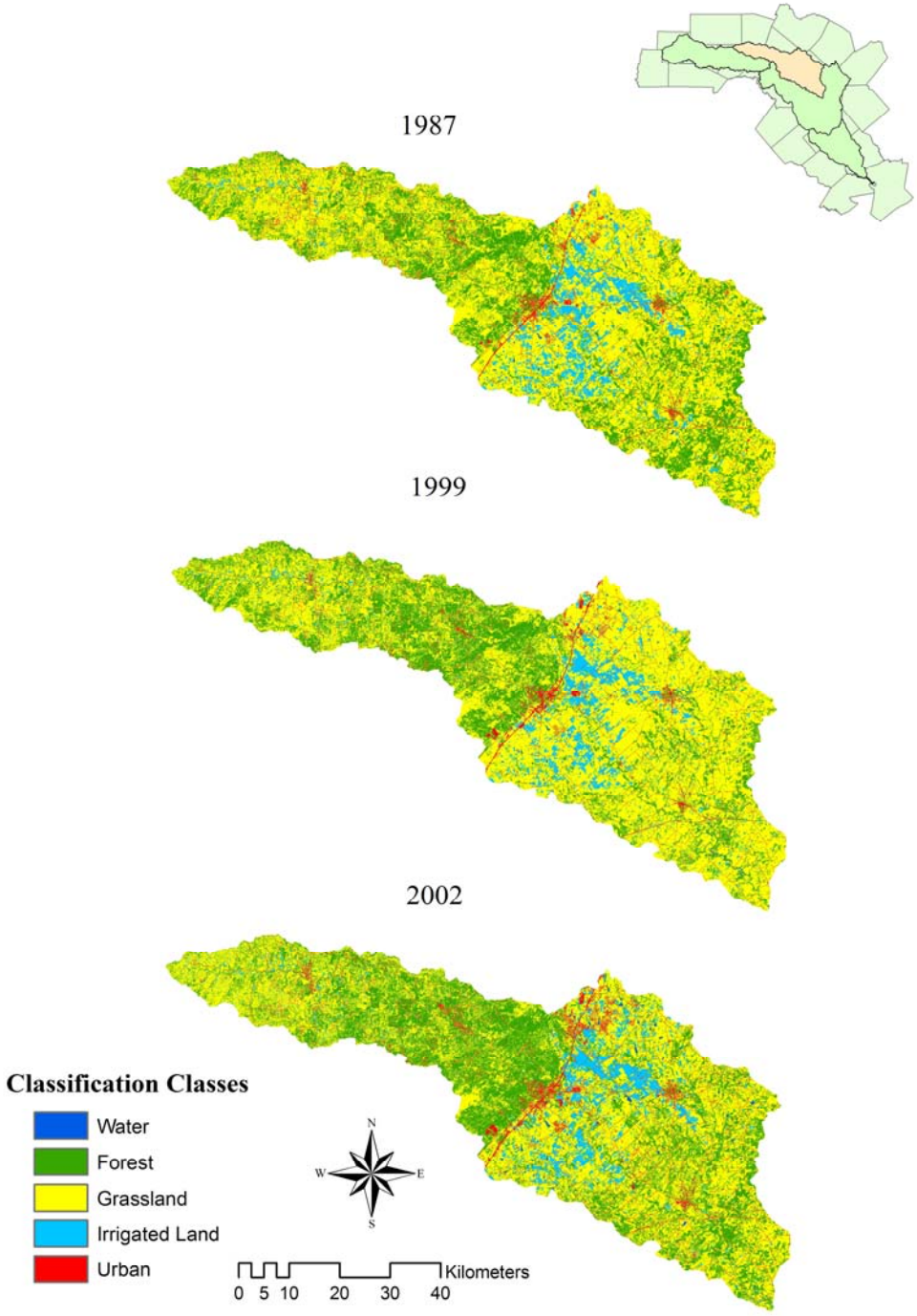

Figure 6. Land cover classification of the San Marcos River Watershed for 1987, 1999 and 2002.

A decrease in area covered by forest from 1987 to 1999 might be attributed to soil moisture condition. Two weather stations, Gonzales and Blanco, were used for comparing the amount of precipitation from the last 30 days prior to the image's acquisition. The record showed 96.5 and 92.6 mm for 1987 image and 4.3 and 28.2 mm in 1999. The higher the precipitation the more moisture of the soil may cause the non-forested area appear like forest area in the classified image. The urban area which increased by 75.3% (79 km^2) was expected since, I-35 a major interstate highway, crossed the San Marcos River Watershed and acts as a main source of urban activity and development. Urbanization was concentrated along I-35 and distributed to the cities of San Marcos, Kyle and Buda.

Middle Guadalupe River Watershed

The Middle Guadalupe River Watershed is the largest subwatershed covering 5,556 km^2 of the Guadalupe River Watershed. Classification of land cover is presented in Figure 7 and Table 11 summarizes the changes within this watershed. Over the period of 1987 to 2002, the area changed contributed less than 1% of total area for each class. Area covered by water, irrigated land and urban increased while forest and grassland decreased. Urbanization increased by 13.3% (20 km^2) which was the largest percent increase in area. This increase took place within the cities of New Braunfels and Seguin and along I-35. Irrigated lands, the largest increase by magnitude (29 km^2) mainly occupied the center part of watershed. In general, the Middle Guadalupe River Watershed experienced the least change in land cover during period 1987-2002 with overall changed area less than 2%.

The results showed that irrigated land decreased from 1987 to 1999 and then increased in 2002. The trend changes of irrigated land are opposite of trend founds in water area. The increase in water area was mainly caused by an increase in the number of small ponds found within this area. Dryer conditions found in the 1999 image, resulting from lower precipitation produced a clear distinction between water and other areas that improved the ability to separate water from other land covers. This condition may have increased the misclassification of irrigated land to other land cover types such as urban, grassland or forest.

Lower Guadalupe River Watershed

The Lower Guadalupe River Watershed is approximately 2,703 km^2 and drains parts of Goliad, De Witt and Victoria Countries. Unlike the other watersheds within the Guadalupe River Watershed, the Lower Guadalupe River Watershed included significant wetland area and was classified into six classes (Figure 8). Table 12 summarizes the changes in land cover during the period 1987 to 2002. The main water bodies in this area are Coleto Creek Reservoir, Saxet Lake and Linn Lake. Water area increased 9.1% (5 km^2) from 1987 to 2002. The increase in water was contributed by the presence of new water bodies below Linn Lake which were undetected in the 1987 and 1999 images. Forest increased by 39.7% (197 km^2) which was the highest by magnitude and percentage. Area covered by grassland decreased by 17.1% (302 km^2) which was mainly converted to forest and irrigated land. Irrigated lands, increased by 16.20% (19 km^2), were distributed over the watershed and were mainly concentrated on the upper part of Yorktown and the lower part of Coleto Creek Reservoir and Victoria City. Increase in

urban area by 9.8% (5 km^2) was mainly contributed by increase in the density of urban area surrounding Victoria. Wetland area is concentrated in the southern part of the City of Victoria and below the Coleto Creek Reservoir. Wetland area is most often categorized as freshwater forested/shrub wetland. This area increased by 27.9% (20 km^2) from 1987-2002.

Guadalupe River Watershed

The final results of classification process of the approximately 15,528 km^2 of the Guadalupe River Watershed divided into six land cover types are illustrated in Figures 9 through 11 and summarized in Table 13. Water areas are distributed over the entire watershed with more than 70% located on the Upper and Lower Guadalupe River Watersheds. The percentage represents the areas of the Canyon and Coleto Creek Reservoir. However, the increase in water area by 20.7% (25 km^2) from 1987-2002 was primarily contributed by the presence of new ponds or water bodies. Those new water bodies were most likely private artificial ponds (or tanks) and mostly found within the San Marcos and Middle Guadalupe River Watersheds.

Table 11. Classification results for the Middle Guadalupe River Watershed from 1987 to 2002

Land Cover Classification	1987 Area (km^2)	1999 Area (km^2)	2002 Area (km^2)	1987-2002 change (km^2)	1987-2002 change (%)
Water	22	29	24	2	7.4
Forest	1,419	1,484	1,392	-27	-1.9
Grassland	3,631	3,603	3,608	-24	-0.7
Irrigated Land	336	283	366	29	8.7
Urban	147	157	167	20	13.3

Table 12. Classification results for the Lower Guadalupe River Watershed from 1987 to 2002

Land Cover Classification	1987 Area (km^2)	1999 Area (km^2)	2002 Area (km^2)	1987-2002 change (km^2)	1987-2002 change (%)
Water	53	43	58	5	9.1
Forest	639	836	892	253	39.7
Grassland	1,772	1,616	1,470	-302	-17.1
Irrigated Land	117	77	136	19	16.2
Urban	50	49	55	5	9.8
Wetland	72	82	92	20	27.9

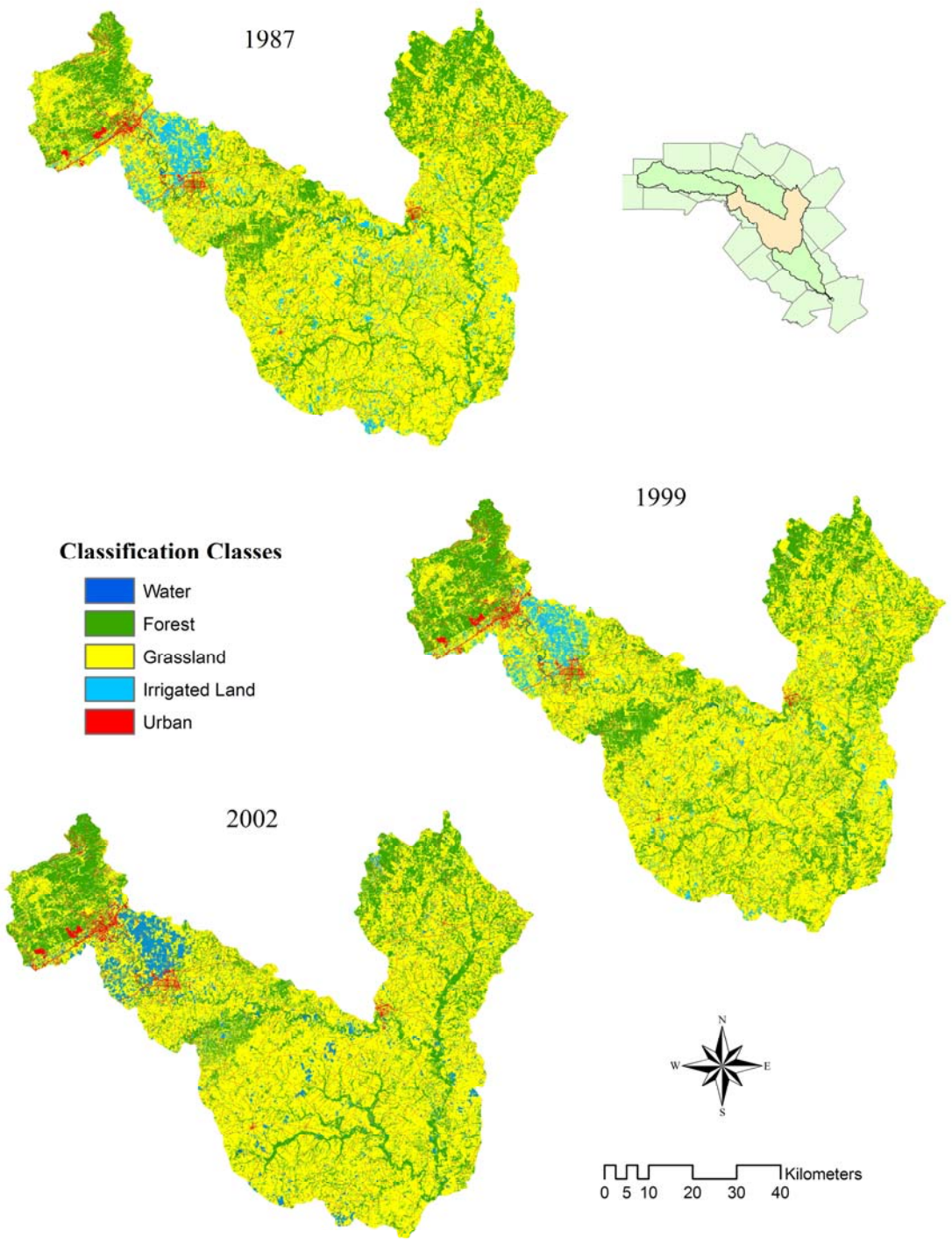

Figure 7. Land cover classification of the Middle Guadalupe River Watershed for 1987, 1999 and 2002.

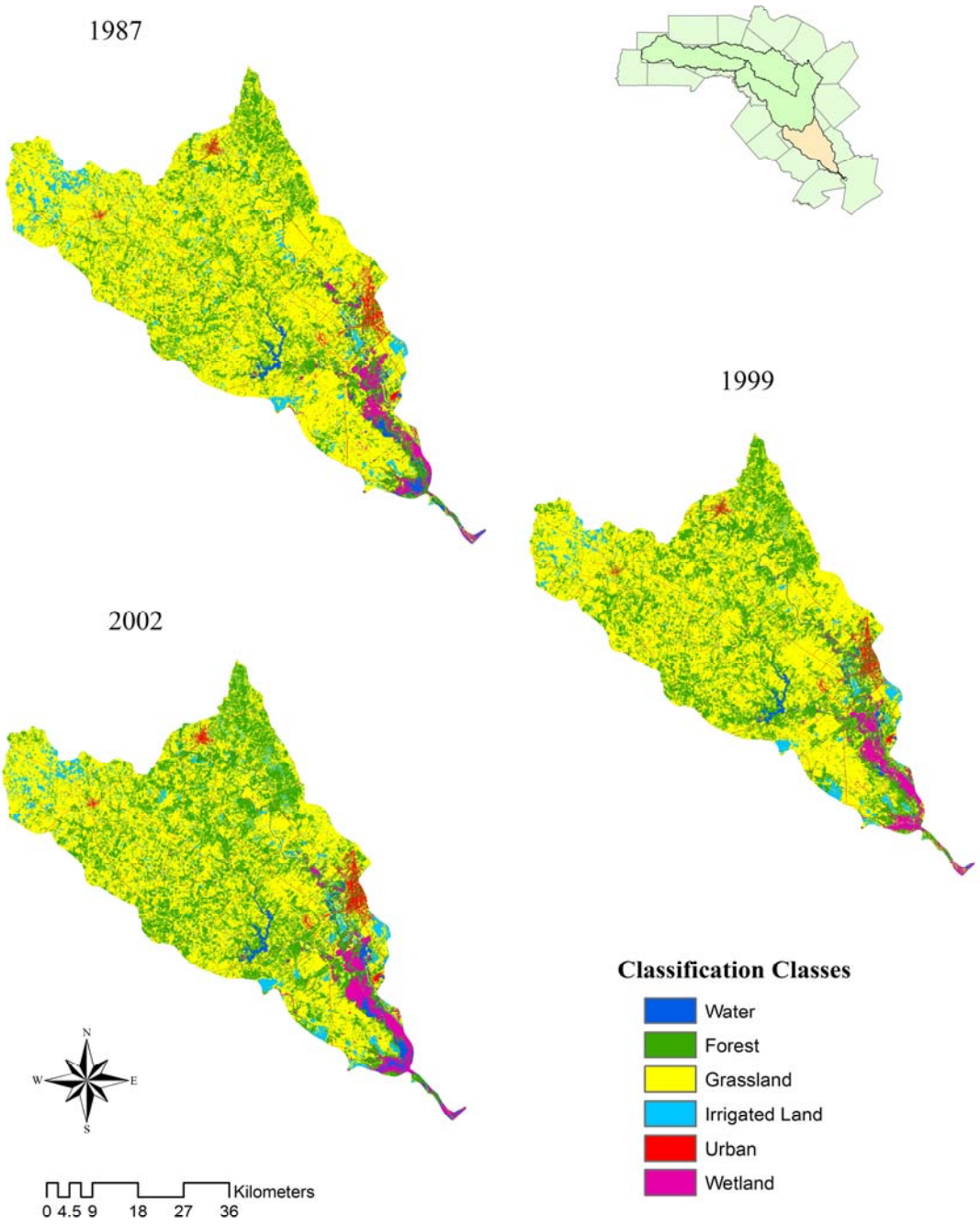

Figure 8. Land cover classification of the Lower Guadalupe River Watershed for 1987, 1999 and 2002.

Table 13. Classification results for the Guadalupe River Watershed from 1987 to 2002

Land Cover Classification	1987 Area (km^2)	1999 Area (km^2)	2002 Area (km^2)	1987-2002 change (km^2)	1987-2002 change (%)	Contributed change to total area (%)
Water	121	126	146	25	20.4	0.2
Forest	4,677	4,965	5,288	611	13.1	3.9
Grassland	9,521	9,230	8,643	-878	-9.2	-5.7
Irrigated Land	729	626	780	52	7.1	0.3
Urban	409	499	579	170	41.5	1.1
Wetland	72	82	92	20	27.9	0.1
Total	15,528	15,528	15,528			

Forest and grassland areas are the dominant land covers in the Guadalupe River Watershed covering more than 90% of the total area. The total forest area increased by 13.1% (611 km^2) mainly occurring in the San Marcos and Lower Guadalupe River Watersheds. The Middle Guadalupe River Watershed was the only watershed that experienced a decrease in forest area. Grassland decreased by 9.2% (878 km^2) which was the highest change in magnitude. Though more grassland areas were found in the Middle Guadalupe River Watershed, this watershed had the lowest decrease in grassland area.

More than 80% of the irrigated lands are distributed over the San Marcos and Middle Guadalupe River Watersheds. Because 1999 was the driest year of the three classified, the classification process failed to distinguish irrigated land in this year and resulted in a decrease in irrigated area of 14% from 1987-1999. Generally irrigated lands were misclassified into grassland because of the difficulties in distinguishing between unirrigated and irrigated land using a single date image unless there was standing water. The result found that the decrease in irrigated land was only found on the Upper Guadalupe River Watershed. The overall 7.1% (52 km^2) increase in irrigated land was primarily located in the Middle and Lower Guadalupe River Watershed.

As mentioned earlier that urban areas present surrounding I-35 connected the cities of San Antonio and Austin. The 41.6% (170 km^2) increase in urban area was principally contributed by 39.4% (67 km^2) of increase in area on the Upper Guadalupe River Watershed. However, by assuming that increasing urban area within the San Marcos and Middle Guadalupe River Watershed were located surrounding the I-35

corridor, the total increased urban area in this part of watershed was approximately 57.7% (99 km^2). The rate of increase in urban area within period 1999-2002 was nearly four times of period 1987-1999.

Accuracy Assessment

Accuracy assessments were conducted by randomly selecting points representing actual land cover using DOQQs as reference images. The points were generated using Hawth's tool and are listed in Appendix C. Comparisons between the randomly selected points and associated points within the classified images for 1987, 1999 and 2002 are presented in the form of error matrices (Tables 14-16).

The overall accuracies were 89.6% for 1987; 90% for 1999 and 91.7% for 2002. The producer's accuracies for 1987 varied from 76.9% for wetland to 98.8% for forested area while the user's varied from 71.4% for wetland to 100% for urban area. The 1999 producer accuracies ranged from 73.6% for irrigated land to 100% for forested area and the user accuracies ranged from 82.7% for forested area to 100% for urban and wetland areas. The 2002 image has producer's accuracies that varied from 75% for wetland to 96.3% for forest and user's accuracies from 89.4% for irrigated land to 97.9% for water covered area.

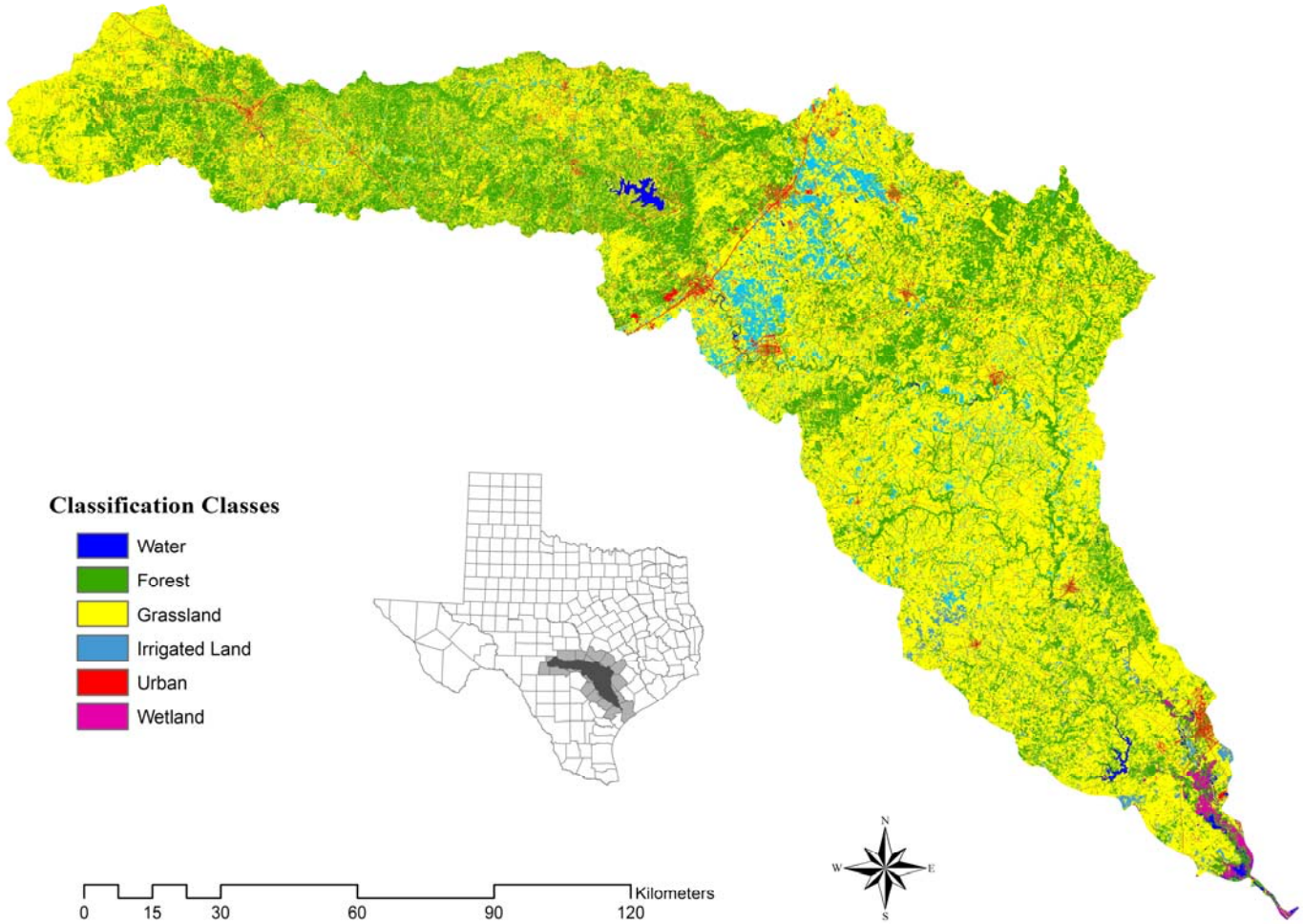

Figure 9. 1987 land cover classification of the Guadalupe River Watershed.

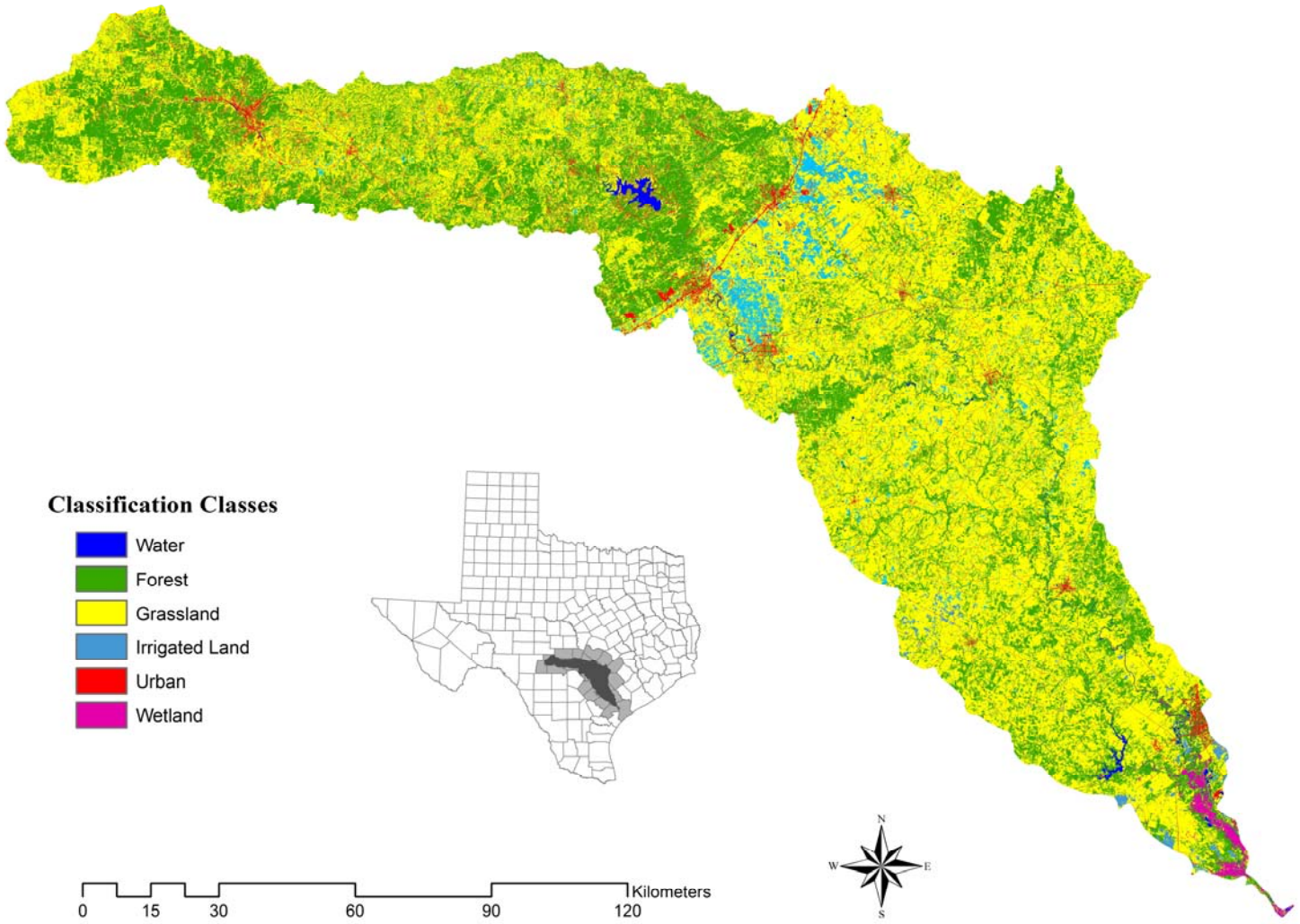

Figure 10. 1999 land cover classification of the Guadalupe River Watershed.

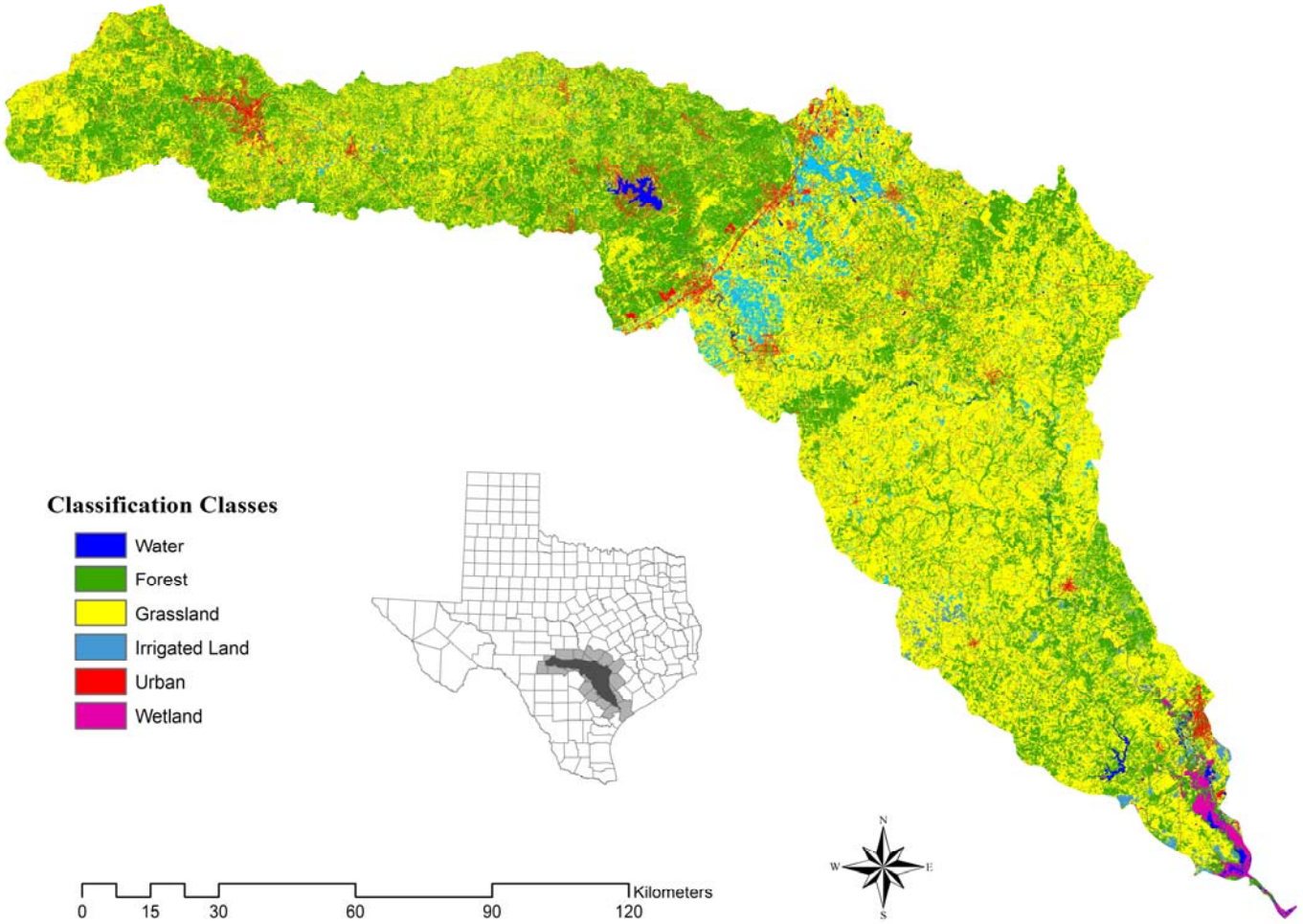

Figure 11. 2002 land cover classification of the Guadalupe River Watershed.

The results showed that the irrigated land class tended to have low producer's accuracy. The irrigated lands were commonly misclassified into the grassland class. Almost all misclassifications of ground truth points of irrigated land were found to be grassland area in the classified images. These results suggested that the classification procedure was rather unsuccessful for irrigated land. The procedure does not account for the possibility that grassland area is actually irrigated land which was not being irrigated at the time the images were captured. Application of these classification techniques to multiseasonal images would increase the ability to distinguish irrigated from non-irrigated lands.

Incorporation of the DEM dataset in the classification process increased the ability to differentiate hill shadow area and water area. It was found that in images, particularly in the Upper Guadalupe River Watershed, the hill shadow area tended to have similar spectral characteristics to the water area. In such a case, slope information increased the classification accuracies because slope values of water areas are commonly low.

Difficulties in discriminating between wetland and forested or water areas were encountered in the classification process. In some cases wetland area was misclassified into water or forest area. In contrast to other land cover classes, forest and grassland had high producer's accuracies meaning that the areas covered by these classes were much greater in the images. Misclassified forested areas were primarily either water or grassland.

Extracting and separately classifying urban areas from the whole image resulted in more consistent producer's and user's accuracies. This approach minimizes the possibility of bare land outside the urban area to be classified as urban area. However, this approach has to be carefully applied particularly in excluding the urban area from whole image. Some urban features may not be in the urban area coverage and have to be manually added.

Although this approach was also done for wetland area, the technique prevented pixels outside the area to be classified as wetland. The overall result was low accuracy for wetlands. Perhaps this is because the characteristics of wetland in this watershed are areas covered by either forest or standing water. When there is less water present, the area will be more similar to forest. When there is more water present, the area is more likely classified as water. A multiseasonal approach can be used to resolve the problems in wetland classification. Pixels that change from forest to water or visa versa during low and high rainfall seasons can be categorized into wetland area.

SUMMARY

In general, the classification process resulted in acceptable classified images, with overall accuracies of 90% or higher. The correlation approach decreased the number of bands used in classification without significantly decreasing the accuracies. This is evident in classifications of images from 1987 and 1999 which have a smaller number of bands but produce comparable accuracies with the 2002 image.

LULC changes in the Guadalupe River Watershed showed an overall trend of increasing urban area and irrigated land and decreasing grassland area. These trends

were consistent for the entire watershed with the exception of decreasing irrigated land in the Upper Guadalupe River Watershed. Increases in urban area were found on the Upper Guadalupe River Watershed and surrounding the I-35 corridor. The City of Kerrville and the area around Canyon Lake were the primary locations of new urban area within the Upper Guadalupe River Watershed. The magnitude of new urban area of those locations equaled the accumulation of new urban areas within the San Marcos and Middle Guadalupe River Watersheds.

The Middle Guadalupe River Watershed was the main location of the 7.1% increase in irrigated land. Irrigated land was primarily located on the south side of the I-35 corridor. High concentration of irrigated land was also found in the Lower Guadalupe River Watershed. The main locations of irrigated land were above the City of Yorktown and the below of Coleto Creek Reservoir and the City of Victoria City

Such trends potentially have strong impacts on the hydrologic cycle particularly in relation to availability of freshwater for human and environmental needs. The trend of increase in irrigated and urban land is a strong indication of an increase in human activities. This condition is believed to put more pressure on freshwater availability in this watershed. Conversion of natural land cover to urban or crops will significantly alter the rainfall-runoff relationship.

There was also evidence of increasing water, forested and wetland area but those increases were more likely temporary or misclassifications. The increase in water may be caused by increasing the water level of Canyon Reservoir and in the number of private ponds within the watershed. An increase in forested area might be attributed an

increase in forest density. The wetland areas were mostly misclassified into water, when more standing water was present or into forest area when there was less standing water. The classification method used in this study was ineffective to discriminate wetland areas from water or forested areas eventhough wetland areas were classified separately.

Table 14. Accuracy assessment for 1987

Land uses/covers		Ground Points							
		Water	Forest	Grassland	Irrigated Land	Urban	Wetland	Total	Users
Classified Points	Water	39	0	0	0	0	2	41	95.12
	Forest	2	80	1	0	0	1	84	95.24
	Grassland	1	0	94	15	7	0	117	80.34
	Irrigated Land	0	0	3	53	0	0	56	94.64
	Urban	0	0	0	0	34	0	34	100.00
	Wetland	3	1	0	0	0	10	14	71.43
	Total	45	81	98	68	41	13	310	
	Producers	86.67	98.77	95.92	77.94	82.93	76.92		

The overall accuracy was 89.60%

Table 15. Accuracy assessment for 1999

Land uses/covers		Ground Points							
		Water	Forest	Grassland	Irrigated Land	Urban	Wetland	Total	Users
Classified Points	Water	47	0	0	0	0	1	48	97.92
	Forest	4	81	5	8	0	0	98	82.65
	Grassland	1	0	91	6	4	0	102	89.22
	Irrigated Land	1	0	4	39	0	0	44	88.64
	Urban	0	0	0	0	38	0	38	100.00
	Wetland	0	0	0	0	0	11	11	100.00
	Total	53	81	100	53	42	12	307	
	Producers	88.68	100.00	91.00	73.58	90.48	91.67		

The overall accuracy was 90.03%

Table 16. Accuracy assessment for 2002

Land uses/covers		Ground Points							
		Water	Forest	Grassland	Irrigated Land	Urban	Wetland	Total	Users
Classified Points	Water	45	0	0	0	0	3	48	97.92
	Forest	1	78	2	0	0	1	82	95.12
	Grassland	2	3	95	4	2	0	106	89.62
	Irrigated Land	1	0	2	42	2	0	47	89.36
	Urban	0	0	1	3	39	0	43	90.70
	Wetland	1	0	0	0	0	12	13	92.31
	Total	50	81	100	49	43	16	339	
	Producers	90.00	96.30	95.00	85.71	90.70	75.00		

The overall accuracy was 91.74%

CHAPTER V

MODELING FRESHWATER INFLOWS USING SWAT

INTRODUCTION

Watershed responses to natural and anthropogenic impacts are indicators of overall watershed health and function. There are many factors that can be used as indicators of watershed health. Many of these factors relate to the most important need for all forms of life, water. Watershed function can be related to the movement of water from precipitation to a definite point such as an outlet or storage. Watersheds receive, store and distribute water over a period of time before releasing it back out into the overall hydrologic system. All of these processes involve the interaction between water, the environment and all living things.

In their interaction with the environment, human beings introduce changes to the environment natural conditions. It is a natural behavior in the effort to fulfill their need for food and shelter. Unfortunately, the changes can be unfavorable to the natural environment. In many cases, human have had a significant impact toward degradation of many of the World's ecosystems. The most obvious impact is change in LULC. This change has been driven by a significant increase in the human population.

Increase in human population is an inescapable natural phenomenon. Many studies have been addressed to minimize major impacts on the environment. On the watershed scale, investigation on anthropogenic impacts is crucial because it provides useful information for catchment management and development. Furthermore, because

of high spatial variation in watershed characteristics, the impacts occur in different rates through time (Miller et al., 2002).

The complexity of processes involved in the interaction between water movement and the characteristics of a specific location results in variabilities in the hydrologic response that need to be studied and managed independently. General assumptions and standardization of responses often leads to misinterpretation in formulating and applying the appropriate strategies to minimize anthropogenic impacts.

Hydrologic models are a powerful tool for studying and understanding the hydrologic process. The models provide a conceptual representation of real world hydrological processes. The main purpose of hydrologic modeling can be defined by the following statement (Black, 1996):

> … to illustrate (explain or expedite understanding of) a large or complex system in a simplified and readily comprehended manner, or (2) to permit prediction of hydrologic events (and resultant design of management control systems) once the basic relationship(s) between components of the model are established.

With increasing computational efficiency of computers, numerous hydrologic models have been developed. These models are generally classified into three categories: empirical, conceptual and physically based distributed models. Generally, a model consists of input, process, and output variables. In empirical models, the process is not explicitly explained; instead it relates input and output. This model is also known as a "black box" model. Physically based distributed models explicitly characterize the physical laws and spatial attributes involved in the process of output generation. Conceptual models are lumped models that consider the physical laws of processes as a homogenous response for an entire area. Because spatially distributed models can

directly relate the physical characteristics of an area to model parameters, these models have become an important tool for interpretation and prediction of LULC change impact (Legesse et al., 2003).

The Soil and Water Assessment Tool (SWAT) model is one of the most widely used hydrologic models, simulating watershed hydrology along with dissolved nutrients, sediments and pesticides. SWAT is a physically-based distributed model because it represents the spatial variability in watershed characteristics such as land use, slope, topography and soil. SWAT has been used for simulating a wide range of water resources problems since its introduction in 1998. In their very comprehensive review, Gassman et al. (2007) highlighted more than 250 peer reviews of SWAT applications to water resources problems. In general, the application of SWAT has been extended throughout the world and across many fields of study. Most applications were driven by the need of government agencies to evaluate anthropogenic, climate and other impacts to water resources.

SWAT has been used extensively to simulate long term anthropogenic impact because the model has shown sensitivity to soil and water management practices in a variety of locations. For example, SWAT has been used to predict the flow, sediment and nutrient load in the Upper North Bosque River Watershed in Texas. The model successfully estimated the flow, sediment and nutrient loading from a dairy waste application field, and simulated scenarios of removing a wastewater treatment plant and changing a manure waste application field to grassland (Saleh et al., 2000). VanLiew et al. (2007) did a suitability assessment of SWAT applied to five experimental watersheds:

Mahantango Creek Watershed (Pennsylvania), Reynolds Creek Watershed (Idaho), Little River Watershed (Georgia), Little Washita River Watershed (Oklahoma) and Walnut Gulch Watershed (Arizona). Although the study suggested that the model performs better when applied in more humid climates, the overall result revealed the robustness of SWAT in a wide range of topographic, land use and soil conditions.

Most past studies of the impact of LULC change on water flow using SWAT simply applied various hypothetical scenarios representing the common trend or possibility of LULC changes within the study area. Hernandez et al. (2000) used SWAT to simulate the effect of conversion of desert scrub and grassland area within an experimental watershed in southeastern Arizona to ten North American Landscape Characterization (NALC) land cover classes. Results of the SWAT simulation showed a decrease in annual runoff as vegetation cover increased. Weber et al. (2001) used SWAT as a sub-model to simulate the effect of long term land use change which focused on agricultural economics, geology and hydrology. Two land use datasets were utilized, original land use which was derived from a 1987 Landsat TM satellite scene and predicted land use change generated from the Prognosis of Land use (ProLand) model. ProLand is used to predict the impact of changes in ecological and social economic framework on agriculture and forestry. SWAT output was calibrated with streamflow data recorded from 1983 to 1987. The simulation results suggested that the land use has significant impact on water balance components. For instance, the presence of grassland increased infiltration and the rate of groundwater recharge and, forested area contributed to a higher evapotranspiration rate even during the dry period in autumn.

Miller et al. (2002) used SWAT with historical land use datasets. Four classified satellite scenes for 1973, 1985, 1991 and 1998 that covered two different watersheds were used as input to SWAT. The selected watersheds were the Cannonsville Subwatershed, New York and the Upper San Pedro Basin located within Sonora, Mexico, and Arizona. The San Pedro Basin experienced significant increase in urban area, mesquite woodlands, and agricultural area. The basin also experienced a decrease in grassland and desertscrub. Using 14 years of continuous rainfall, the simulation showed an increase in runoff volume. The land use changes from agriculture to forest in the Cannonsville Watershed did not significantly change the hydrologic response because the difference between forest and agriculture curve numbers was not significant. Another reason the results were not significantly different was that changed area was less than 5% in any land cover class.

SWAT has shown to be a robust model to predict the watershed response in various land use, topographic and soil conditions on agricultural watersheds. Therefore, this study used SWAT to predict the impact of LULC changes within the Guadalupe River Watershed on freshwater inflow to the Guadalupe Estuary. The freshwater inflows are simply the amount of water released from the watershed outlet to the estuary. This flow is contributed by surface runoff and baseflow (streamflow), which are highly influenced by upstream activities such as urbanization and agricultural development. Streamflow may also be altered from its natural condition as the result of diversions in the upper regions of watershed. This study focused on these activities as the main sources of freshwater inflow modification.

Trend analysis results from Chapter III showed no significant trend was found on streamflow recorded in the period of 1970-2005. Satellite image classification results from Chapter IV suggested increases in urban, irrigated and forested areas. Increase in irrigated land mostly takes place on the middle and lower parts of the watershed below the urbanized area surrounding the interstate highway I-35. Increase in forested area is concentrated in the upper part of the San Marcos River Watershed and distributed over the entire area of the Lower Guadalupe River Watershed. Based on those results, the following hypotheses will be tested:

1. Increase in urban and agricultural areas within the Guadalupe River Watershed from 1987 to 2002 which was concentrated in the middle of the watershed will increase both monthly and annual freshwater inflows rates to the Guadalupe Estuary.
2. The presence of reservoirs in the stream network in the Guadalupe River Watershed will modify monthly freshwater inflows by increasing freshwater inflows during low flow months and decreasing them during high flow months.

The specific objectives used to test these hypotheses were:

1. Develop the SWAT model for the Guadalupe River Watershed using 1987's land use dataset derived from Landsat satellite data classification.
2. Calibrate and validate the SWAT model by comparing the simulated flow with measured Guadalupe River flows.

3. Describe the characteristics of annual and monthly freshwater inflows to the Guadalupe Estuary in response to historical urbanization, agricultural development and upstream water diversion.

SWAT MODEL OVERVIEW

The SWAT model was selected to simulate the freshwater inflows because of its suitability to large and agricultural basins. It is also takes into account spatial variability in watershed properties such as land use and soils. SWAT was developed by the United State Department of Agriculture – Agricultural Research Service (USDA-ARS) to predict the impacts of land management practices on hydrology, sediment and agricultural chemical yields in large and ungauged basins (Arnold et al., 1998).

The model initially separates the area into subwatersheds or drainage areas. The number of drainage areas can be specified using defined watersheds, outlet subwatershed locations or a selected minimum area for subwatersheds to be generated. SWAT lumps together homogenous units, called hydrologic response units (HRU), based on land use and soil properties. Users also have the option to assign the HRUs as representative of the subbasin based on dominant land use or soil types.

SWAT simulates hydrologic processes generally divided into upland and stream components (Fohrer et al., 2005; Govender and Everson, 2005). The upland component simulates movement of water, nutrients, sediment and pesticides to the main channel in each subbasin based on a mass balance approach. The stream component simulates the water flow in channels to the watershed outlet using a variable storage coefficient and

Muskingum routing methods. The water balance in SWAT is calculated as (Neitsch et al., 2002):

$$SW_{(t)} = SW_{(0)} + \sum_{i=1}^{t}\left(R_{(t)} - Qs_{(t)} - E_{(t)} - W_{(t)} - Qg_{(t)}\right) \quad (14)$$

where *t* is the daily time step, $SW_{(0)}$ and $SW_{(t)}$ are the initial and current soil water content, $R_{(t)}$ is the total precipitation, $Qs_{(t)}$ is the surface runoff, $E_{(t)}$ is the evapotranspiration, W_t is the percolation, and $Qg_{(t)}$ is the return flow.

The model uses either the Soil Conservation Service Curve Number (SCS-CN) or the Green-Ampt infiltration method to calculate the surface runoff. The SCS-CN method uses to a daily time step while Green-Ampt can be used at a sub-daily time step. In this application, the SCS-CN approach was used. The method estimates the amount of runoff from precipitation based on the following formula:

$$Q = \frac{(P - 0.2S)^2}{P + 0.8S} \quad (15)$$

Where Q is the amount of runoff (cm) resulted from precipitation, P (cm). Runoff occurs only when the precipitation is greater than 0.2 S. The term S is the maximum soil water retention parameter and is calculated by (Haan et al., 1994):

$$S = \frac{25400}{CN} - 254 \quad (16)$$

where CN is the curve number based on soil properties and land use. SCS classified soils into 4 main classes (A, B, C and D) based on their infiltration characteristics. In general, impervious surfaces are represented by higher CN which decreases the value of S and increases runoff.

SWAT calculates runoff from urban areas by calculating the percentage of pervious and impervious area. These percentages are determined by specifying the urban density. In more dense urban areas, more runoff will be produced because there is more impervious area. The density of urban area also helps to characterize the hydraulic connection between the area and drainage system. An increase in density of urban areas consequently increases the efficiency of water flow to main channels.

SWAT provides several water management options to improve its ability to predict streamflow. Those options include irrigation, tile drainage, impounded/depressional areas, water transfer, consumptive use and loading from point sources (Neitsch et al., 2002). Irrigation can be applied automatically by the model based on water stress condition or can be specified manually by the user. The model provides five sources of water for irrigation including reaches, reservoirs, shallow and deep aquifers and sources from outside the watershed. Impounded and tile drainage are related to specific agricultural practices. Water transfer is related to the water distribution that moves the water from one place to another within the watershed. Point sources offer the user the option to bring water into the watershed, while consumptive use allows the removal of water from the watershed.

The model provides three methods to estimate the potential evapotranspiration including Priestley-Taylor, Penman-Monteith and Hargreaves. This study used the Penman-Monteith method to calculate potential evapotranspiration. The Penman-Monteith method is believed to be the most accurate but it requires more input data (Heuvelmans et al., 2005) such as solar radiation, wind speed, humidity and air

temperature. The Hargreaves method is the simplest method, requiring only air temperature and solar radiation.

Continuous downward flow or percolation occurs only if the soil's water holding capacity is exceeded. The water that flows downward below the root zone is considered lost from the watershed until it appears again as return flow (Arnold et al., 1998). The model integrates reservoirs by simulating the water released from the reservoirs or accepting the recorded flow as an input. If the latter option is selected then not all water flow on the upstream side of the reservoir will affect flow on the downstream side because the model will only use the released flow as input. To simulate the former option, the model needs information about reservoir characteristics and management including normal and emergency volume, area and initial year of operation.

METHODOLOGY

SWAT Inputs

SWAT is a data intensive model. Elevation, land use/cover, and soils are the minimum input for the model. Weather can be generated by SWAT or provided by the user. If the latter option is chosen, the user needs to provide at least precipitation and temperature (minimum and maximum) data. Better Assessment in Science Integrating Point and Non-point Sources (BASINS) available from United States Environmental Protection Agency (www.epa.gov) was used to extract important datasets including the Digital Elevation Model (DEM), National Hydrographic Dataset (NHD), and STATSGO

soil dataset. ArcSWAT 2005 which is compatible with ArcGIS 9.1 was obtained from the SWAT website (www.bcs.tamus.edu).

DEM data having a resolution of 83 m x 83 m were used in the watershed delineation process. The elevation ranged from 0 to 731 m with most of the hilly area located on the Upper Guadalupe Subwatershed and on the upper part of the San Marcos Subwatershed (Figure 12). The NHD was used to assist the model in generating reaches that fit with existing ones.

The Landsat image from 1987 classified in Chapter IV was used as the input for land use. The resolution of the images was decreased to 83 x 83 m to agree with the DEM resolution. The six land use categories generated previously were assigned to six SWAT land use classifications as described in Table 17.

Table 17. Classified and SWAT land use names

Classified Land Use Name	SWAT Land Use	
	Name	Definition
Water	WATR	Water
Forest	FRST	Forest-Mixed
Grassland	PAST	Pasture
Irrigated Land	AGRR	Agricultural Land-Row Crops
Urban	URBN	Residential
Wetland	WETL	Wetland-Mixed

The STATSGO soil database revealed that the watershed area is dominated by hydrologic soil group D (Figure 12). On the lower part of watershed the soil hydrologic groups are approximately evenly distributed between groups B, C and D. Only a small

part of the watershed is underlain by soil group A. The soil shape file was converted into a grid file. A table was created to assign soil properties using the state map unit identifier (stmuid) option.

The weather data were collected from several meteorological stations in and surrounding the watershed. Recorded precipitation, and minimum and maximum temperatures were obtained from the National Climatic Data Center (NCDC) covering the period from January 1, 1950 to December 31, 2006. Relative humidity, solar radiation and wind speed were simulated by SWAT. As many as eleven rain gauges and nine weather stations were added to the model. Seven rain gauges and six weather stations ultimately were accepted by the model as input (Table 18).

A total of 13 reservoirs were identified in the Guadalupe River Watershed (Table 19). Most of the reservoirs are located in the middle of the watershed along the highly urbanized area surrounding the I-35 corridor. In general, the reservoirs are purposed for water supply, hydroelectricity, recreation and flood control. Two main reservoirs, Canyon and Coleto Creek Reservoirs, are used primarily for flood control. Canyon Reservoir is located on the Guadalupe River at the outlet of the Upper Guadalupe River Subwatershed, Coleto Creek Reservoir is situated on Coleto Creek in the lower part of the Lower Guadalupe River Subwatershed. All information about the reservoirs was obtained from the National Atlas of The United States website (www.nationalatlas.gov).

Table 18. List of weather stations used for SWAT input

COOP ID	Name	Elevation (m)
410428[1*]	Austin Mueller Municipal Airport	201
413622[3*]	Gonzales 1N	116
417945[3*]	San Antonio International Airport	247
410639[3]	Beeville 5 NE	73
410832[3*]	Blanco	418
419364[3*]	Victoria Regional Airport	35
415650[2*]	Mason	472
413201[1*]	Floresville	440
414254[2*]	Hondo	267
414780[1*]	Kerrville	543
417186[3]	Port O'Connor	1.5

Note: 1. Used for precipitation only
2. Used for air temperature only
3. Used for precipitation and temperature
* Accepted by model (for spatial information refer to Figure 13)

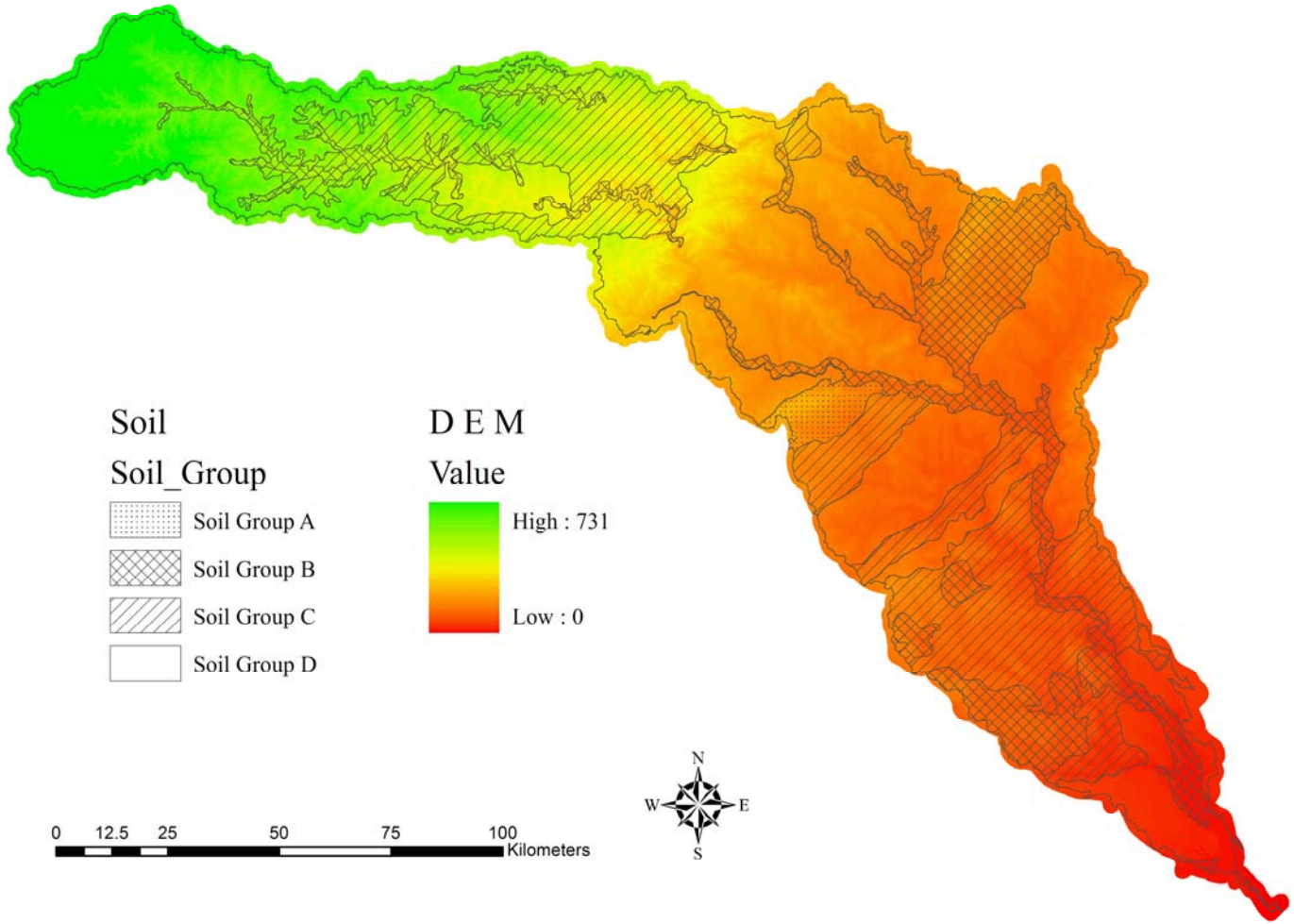

Figure 12. Soil group and elevation distribution over the Guadalupe River Watershed.

Table 19. List of reservoirs located within the Guadalupe River Watershed

Name	Year completed	Purposes	Area (Ha)	Max Storage ($10^4 m^3$)	Min Storage ($10^4 m^3$)
Canyon Lake Reservoir *	1964	SRCH	3334.62	139299.16	47637.77
York Cr WS SCS Site 1 Dam	1967	CS	7.49	563.71	16.65
Lake Gonzales Dam	1931	HR	281.66	2901.19	925.13
Comal R WS SCS Site 1 Dam*	1978	CS	7.28	834.22	9.74
Lake Dunlap Dam*	1928	HR	165.92	727.77	727.77
Comal R WS SCS Site 2 Dam	1981	CS	12.95	2346.61	21.83
Lake McQueeney Dam*	1928	HR	160.26	622.92	622.92
Upper San Marcos R WS SCS Site 4	1985	R	8.50	736.65	26.52
Upper San Marcos R WS SCS Site 1	1983	C	10.12	2269.52	13.20
Coleto Cr Dam *	1980	C	1254.53	20846.15	4327.61
Comal R WS SCS Site 4 Dam*	1965	CS	11.45	652.89	24.67
Upper San Marcos R WS SCS Site 2	1985	R	6.88	374.24	12.09
Upper San Marcos R WS SCS Site 3*	1991	C	8.09	533.24	15.67
Comal R WS SCS Site 3 Dam	1974	CS	7.69	852.47	13.69

Note : S = Water supply
R = Recreation
C = Flood control
H = Hydropower
* = Used in model (for spatial information refer to Figure 13)

Model Calibration and Validation

The main purpose of model calibration is to optimize the agreement between observed data and model output by adjusting the model parameters (Tolson and Shoemaker, 2007). This study compared the measured streamflow recorded by USGS gauging station 08176500 located near the outlet of the Guadalupe River Watershed and the simulated data. This station is the closet station to the watershed outlet with a streamflow record of more than 50 years. The USGS gauging station at the outlet of the watershed (USGS 08188800) is not appropriate for analysis because it is located below the junction between the Guadalupe and San Antonio Rivers and records the combined flow from those rivers.

In SWAT, parameters related to soil properties are the most sensitive. Based on previous studies (Arnold et al., 2000; Mulungu and Munishi, 2007; Spruill et al., 2000), calibration was performed by adjusting the curve number (CN2), soil water capacity (SOL_AWC) and soil evaporation compensation coefficient (ESCO) variables. In addition, the baseflow related parameter, baseflow recession constant (ALPHA_BF) was also adjusted in this study with consideration that on a large watershed the runoff behavior is dominated by the groundwater component (Black, 1996).

The relationship between rainfall and runoff is controlled by the ability of soil to hold water termed SOL_AWC. The greater the SOL_AWC of the soil, the less runoff will be produced. When there is less water in the soil, more water can be stored before it becomes runoff. The amount of groundwater recharge is also affected by SOL_AWC in that maximum capacity needs to be filled first before the water flows downward as

groundwater recharge. The suggested variation in SOL_AWC is ±0.04 (Neitsch et al., 2002).

ESCO is another soil-related parameter within SWAT that explains the depth distribution of soil water to compensate for the water deficit in upper layers (Arnold et al., 2000). Decreasing this coefficient will result in more evaporation and a decrease in the amount of runoff. The default value given by the model is 0.95 and SWAT allows it to vary from 0 to 1.

ALPHA_BF defines the baseflow recession parameter. This parameter determines the rate of groundwater contribution to streamflow. Adjustment of this parameter impacts the shape of hydrograph. Increasing ALPHA_BF increases the amount of groundwater contribution to streamflow over time. This action will result in a slow falling limb and high baseflow in the hydrograph.

The 1987 land use was selected as the base model. The model was run for 28 years that includes a 20 year warm-up period, 4 years for calibration and another 4 years for validation. The calibration was done manually for monthly flow using guidelines provided in the 2002 SWAT user manual. For this purpose, Microsoft Excel macros were created to process the output from the model and calculate the model goodness-of-fit parameters. The goodness-of-fit was evaluated using three commonly used criteria, coefficient of determination (R^2), Nash-Sutcliffe coefficient (E_{NS}), and percent bias (P_{BIAS}) (Gosain et al., 2005) calculated from equations 17, 18 and 19, respectively.

$$R^2 = \left[\frac{\sum_{i=1}^{n} \left(O_i - \overline{O}\right)\left(P_i - \overline{P}\right)}{\sqrt{\sum_{i=1}^{n} \left(O_i - \overline{O}\right)^2} \sqrt{\sum_{i=1}^{n} \left(P_i - \overline{P}\right)^2}} \right]^2 \quad (17)$$

$$E_{NS} = 1 - \frac{\sum_{i=1}^{n} \left(O_i - P_i\right)^2}{\sum_{i=1}^{n} \left(O_i - \overline{O}\right)^2} \quad (18)$$

$$P_{BIAS} = \frac{\sum_{i=1}^{n} \left(O_i - P_i\right)}{\sum_{i=1}^{n} Oi} \times 100 \quad (19)$$

where P_i is the *i*th simulated value; O_i is the *i*th observed value; $\overline{P}$ is the average of the simulated values; $\overline{O}$ is the average of the observed values and n is the number of observations in the data set.

Coefficient of determination (R^2) describes the fraction of the variance in observed data that can be explained by the simulated data. The higher this value the better the model fit. The optimum value is +1 and the range is from -1 to +1. E_{NS} describes how well the model output can explain the variations in the observed data compared to the average observed data. When the model has better prediction, the errors between observed and predicted values will be close to zero and the E_{NS} will be close to 1. The model is considered satisfactory when E_{NS} value falls between 0.36 and 0.75 and good if it is higher than 0.75 (Larose et al., 2007). P_{BIAS} determines the percentage

difference between observed and predicted values. A positive value indicates that that model is under-predicting while a negative value indicates over-prediction. The best prediction will result in a P_{BIAS} value close to zero.

Scenarios

Three scenarios were simulated using the calibrated model for 50 years with a seven years warm up period. The simulations were started on January 1, 1950 and ended on December 31, 2006. Two scenarios represented regulated and unregulated flows from the land cover dataset in 1987. Regulated flows were simulated flow which included reservoirs; unregulated flows were those without reservoirs. To remove the reservoirs from the simulation, the initial year of operation for each reservoir was set to 2008. To incorporate land use changes, the 1987 land use in the calibrated model was replaced by land use from 2002 derived in chapter IV with all other parameters kept constant, hereafter referred to as the 2002 model. The predicted seasonal and annual mean flows were used for analyses. Data were analyzed over the period of 1957-2006.

RESULTS AND DISCUSSION

Watershed Delineation

A total of 96 subbasins were generated by SWAT using a 15,000 ha threshold value and manually-added points for USGS 08176500 and reservoirs (Figure 13). The subbasin areas varied from 4 km^2 to 530 km^2. The total generated watershed area was 15,574 km^2. Only one-half of the reservoirs identified were added to the model, the remaining one-half were outside of the stream network.

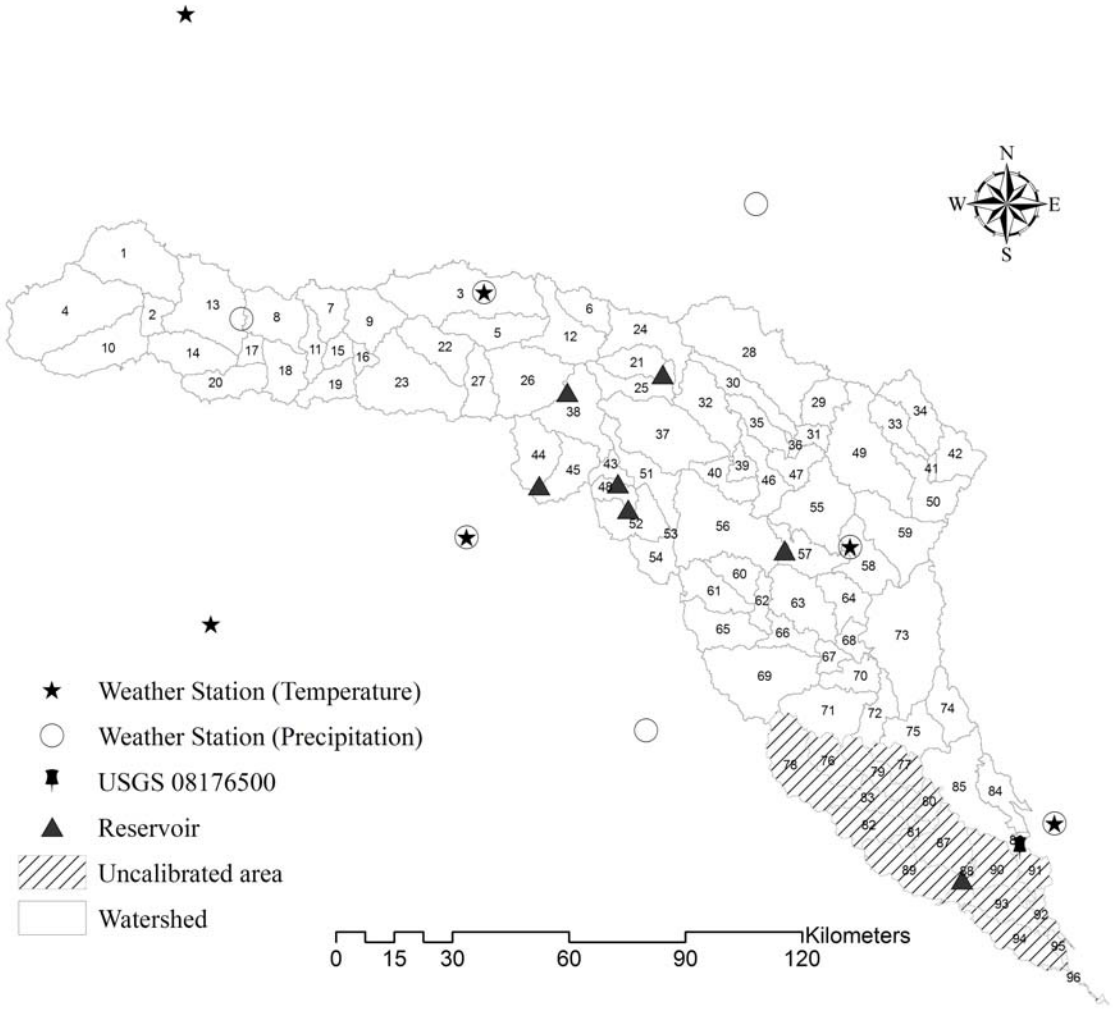

Figure 13. Spatial characteristics of SWAT model for the Guadalupe River Watershed.

Three slope classes, < 2%, 2-10% and >10%, were used for a better representation of the topography of the Guadalupe River Watershed. The combination allowed the hilly areas in the Upper Guadalupe River Watershed to be well described and reduced the slope of flatter areas mostly located in the Middle and Lower Guadalupe River Watersheds. Threshold values of 5, 10 and 10% were used for land use, soil and slope, respectively in the definition step. The thresholds resulted in a watershed dominated by forest (FRST) and pasture (PAST). At least 65% of the subbasins were dominated by forest and pasture. Agricultural land-row crops (AGRR) appeared in 24 subbasins while urban areas were distributed over eight subbasins. Wetland (WETL) and water (WATR) areas were found in seven and eight subbasins, respectively, which were mostly located in the lower part of watershed.

Calibration and Validation of the 1987 Model

Calibrated parameters for the 1987 land use data set are shown in Table 20. Using SWAT selected default values resulted in over prediction of flow. The calibrated model changed the default CN2 by -7. The ESCO, which is allowed to vary between 0.75-1 (Arnold et al., 2000), resulted in a value of 0.75. The groundwater recession parameter, ALPHA_BF was adjusted to 0.03.

Based on E_{NS}, the performance of the model ranged from “good” in the calibration process to “satisfactory” in validation (Table 21). The values also reflect the common phenomena in hydrologic modeling that the validation is usually worse than calibration (Tolson and Shoemaker, 2007). The linear agreement between predicted and observed data decreased in the validation process. This means the model was able to

preserve the flow trend much better during the calibration period. Figure 14 presents simulated and observed data during both periods of calibration and validation. The model preserved peak flows with tendency of overestimating them. A general tendency for SWAT to underestimate flow was shown by the positive value of P_{BIAS} which increased from calibration to validation.

No calibration was done for the watershed areas located upstream of Coleto Creek Reservoir and downstream of USGS 08176500. These areas cover 1,958 km^2 or approximately 12% of the watershed area (Figure 13). Most of the land covered by water bodies and wetland areas are located in this area. No specific information was given to the model to simulate the wetland areas and water bodies. This restriction might increase the bias of the freshwater simulation result. However, since more than 85% of the contributing watershed was calibrated, it is assumed that the characteristic of freshwater inflows will be well preserved.

Table 20. Initial and final values of selected parameters for calibration

Parameter	Initial value	Range	Calibrated/final value
ESCO	0.95	0.75 - 1	0.75
CN2	default	+/- 7	-7
SOL_AWC	default	+/- 0.04	default
ALPHA_BF	0.048	0 - 0.3	0.03

Table 21. Model performance during calibration and validation periods

Model	Calibration (1984-1987)			Validation (1988-1991)		
	E_{NS}	R^2	P_{BIAS} (%)	E_{NS}	R^2	P_{BIAS} (%)
1987	0.83	0.96	3.81	0.68	0.75	29.38

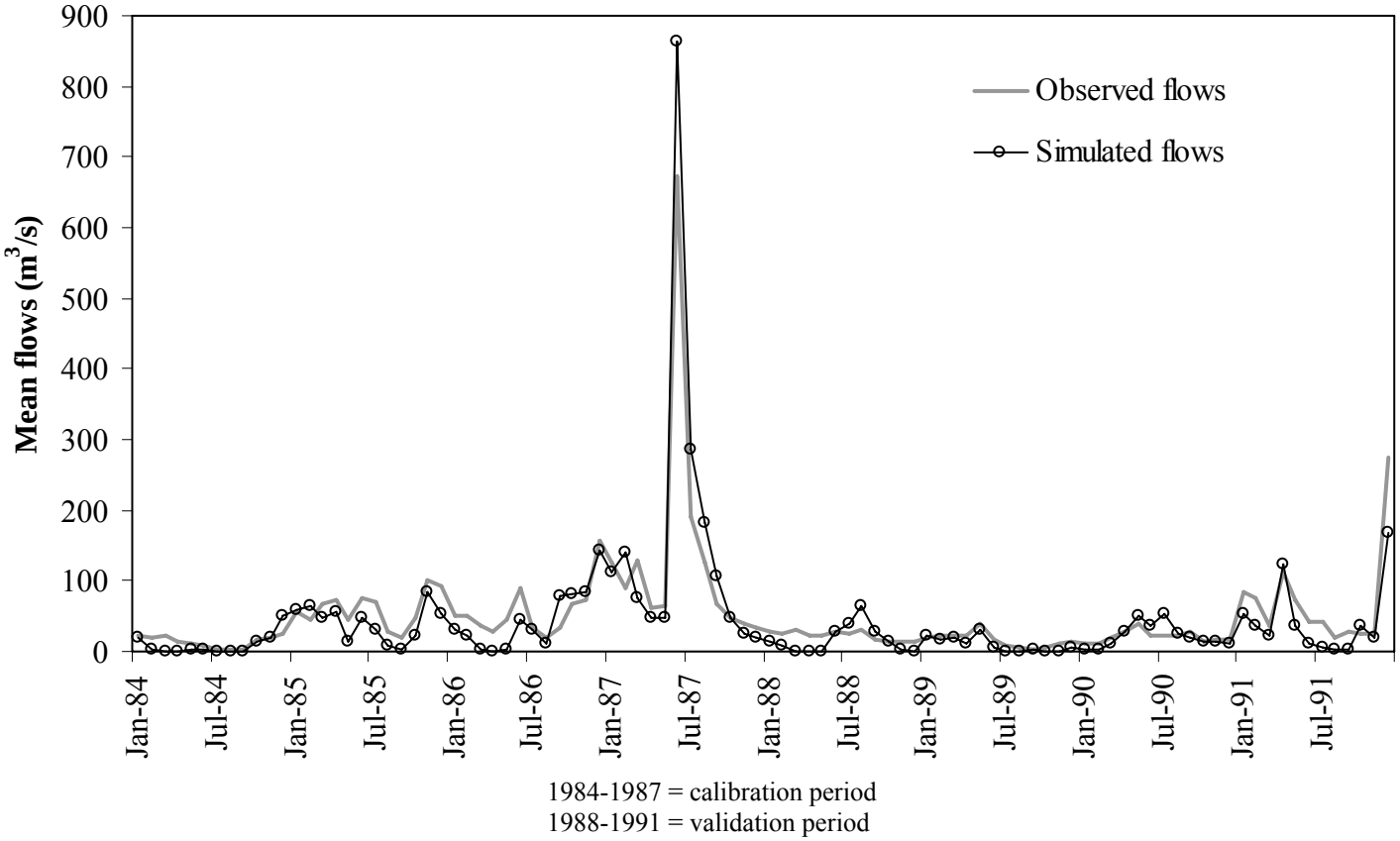

Figure 14. Simulated vs observed monthly streamflow at station USGS 08176500.

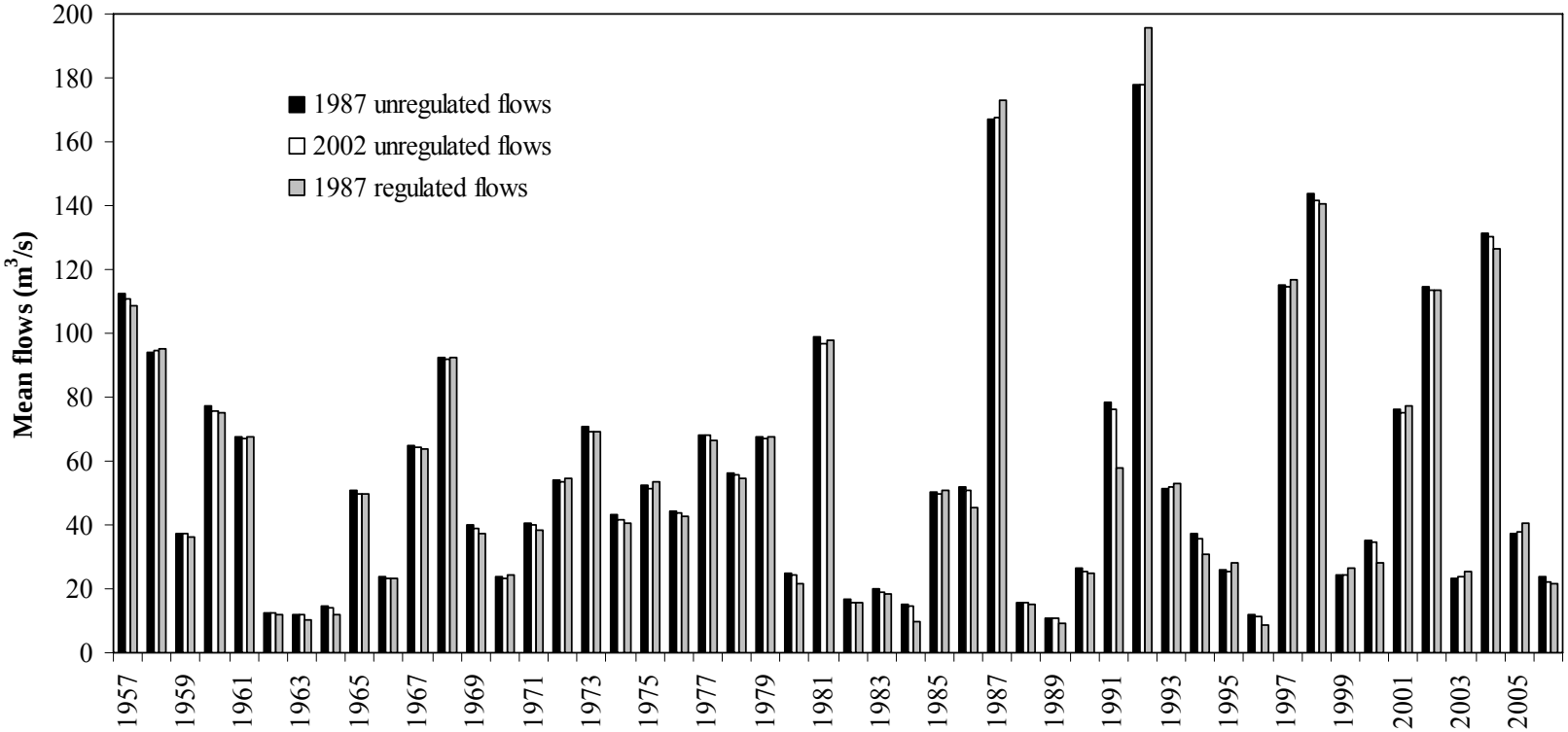

Figure 15. SWAT prediction of annual mean freshwater inflows contributed by the Guadalupe River Watershed.

Modeling Results

Predicted annual mean flows for the period 1957-2006 for all three scenarios are presented in Figure 15. The highest annual mean flow was detected in 1992 followed by the flow in 1987 for all scenarios. The lowest mean flow was found in 1996 (8.67 m^3/s) and two years with flow lower than 10 m^3/s occurred in 1984 (9.25 m^3/s) and 1989 (9.57 m^3/s) for 1987 regulated flows scenario. The lowest mean flow resulted from 1987 and 2002 unregulated flows scenarios were found in 1989.

Visually, there was a significant change in annual mean flow starting from 1987 for all scenarios. High and low flows were more drastic with significant differences between the adjacent years from 1987-2006. Both of the highest and lowest annual mean flows occurred during the period of 1987-2006. From 1987 to 2002 there is a cycle of high flow every five years. If this trend continues, we would expect that 2007 should

Figure 16. Statistical characteristic of precipitation during the simulation period.

also have a high median monthly mean flow. At the time this research was completed, the recorded median monthly mean flow at station USGS 08176500 was 136.6 m^3/s for 2007 which can be classified as high flow.

Precipitation Variability

As streamflow is highly influenced by variability in precipitation, a changing trend detected in streamflow could be attributed to changes in precipitation characteristics. Analysis of precipitation variability is important in the issue of global climate change and also because precipitation is a primary driver of freshwater inflows. Based on visual observation of predicted freshwater inflows (Figure 15), the trend in freshwater inflows changed throughout the simulation period. Assuming that the drastic fluctuations started in 1987, analysis of precipitation variability and its impact on freshwater inflows was performed based on the periods of 1957-1986 and 1987-2006.

Figure 16 illustrates the characteristics of annual precipitation for the periods of 1957-1986 and 1987-2006. Median annual precipitation increased from 845 mm in 1957-1986 to 895 mm in 1987-2006. An increase in variability of annual precipitation was also seen. Descriptive statistics showed that the standard deviation increased from 190 to 256 mm. Comparing the upper and lower percentiles suggests higher variability (i.e. more extreme highs and lows) in precipitation in 1987-2002.

To analyze the impact of precipitation variability on freshwater inflows, the predicted median of monthly mean unregulated flows of the 1987 model were used. The simulated results presented only the impact of precipitation because the land use was constant and none of reservoirs were active. Figure 17 illustrates characteristics of

predicted seasonal freshwater inflow rates. Obviously, seasonal freshwater inflows changed from the period 1957-1986 to 1987-2006. Seasonal mean flows for the later time series increased during the winter months (January to March) and decreased during the autumn (September to November). The frequency of months with more freshwater inflow decreased in the period of 1987-2002. During the period of 1957-1986 the volume of freshwater inflows were greatest in May, June, and September. Although in the period of 1987-2002 the highest flow occurred in June 1987 (931 m^3/s), mean seasonal freshwater inflows in June was found to be much less than in 1957-1986. Precipitation variability increased freshwater inflows in May by approximately 27%, from 50.6 m^3/s in 1957-1986 to 64.2 m^3/s in 1987-2006. Although it has less impact on annual mean flow, the change in precipitation variability affected not only the rate of freshwater inflows, but also significantly modified the characteristics of seasonal freshwater inflows.

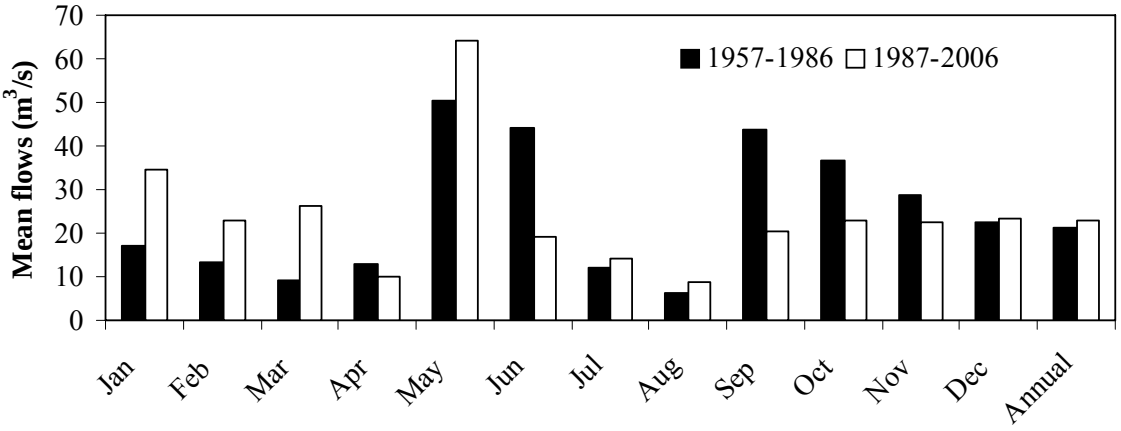

Figure 17. Characteristic of seasonal freshwater inflows for the periods 1957-1986 and 1987-2006.

Land cover change scenarios

Replacing the land use of 1987 by that from 2002 in the model yielded a different combination of LULC classes (Table 22). The model reduced pasture and agricultural land. The remaining LULC types increased, with the highest percentage increase in wetland area. The decrease in agricultural land in the 2002 model was unexpected because it was contrary to the classification results from Chapter IV. The increase by 50% of wetland covered area was also very high when compared to the classification results. However, the simulation results from this scenario need to be analyzed with respect to land use composition in SWAT rather than the classification process.

Table 22. Land use/cover characteristics for 1987 and 2002 models

Land use/cover	1987 model (km^2)	2002 model (km^2)	Change	
			(km^2)	(%)*
WATR	8	19	12	0.1
FRST	4913	5568	655	4.2
PAST	9960	9107	-853	-5.5
AGRR	553	511	-42	-0.3
URBN	85	283	199	1.3
WETL	57	85	29	0.2

* compare to total watershed area (15,574 km^2)

In general, Figure 15 illustrates annual freshwater inflows resulted from 1987 and 2002 models. Annual freshwater inflows rates in the 2002 model were consistently lower than 1987 model, with the exception of few years (1958, 1987, 1993, 2003, and 2005). Figure 18 presents monthly freshwater inflow rates for both land use scenarios. Mean annual freshwater inflows decreased by less than 2% because of change in land use/cover from 1987 to 2002. The 235% increase in urban area did not greatly influence

freshwater inflow rates to the Guadalupe Estuary. As mentioned in Chapter IV, most of the urban area is located in the middle of the watershed, while forest covers over 30% of the total area. The increase in impervious area might have significant impact on flows but the impact is probably more significant on localized streamflow rather than on freshwater inflows further downstream. The trend analysis on streamflow recorded in the period of 1950-2005 in Chapter III showed the number of significant trends decrease as analysis moves to downstream stations. A 50% increase in wetland area potentially decreased the freshwater inflows rate because most of wetland area is located in the lower part of the watershed near the watershed outlet. Wetlands essentially provide more storage. The decrease in freshwater inflows could also be introduced by an increase in forested area and a decrease in grassland and irrigated land.

With the exception of January and November flows, monthly freshwater inflow rates decreased in the 2002 model (Figure 18). The highest and the lowest rates for both scenarios were found in May and August, respectively. Both land use scenarios produced a similar monthly flow pattern throughout the year. The decrease in monthly freshwater inflow rates was more profound during months with higher flow rates. In general, the changes in land use/cover from 1987 to 2002 put more pressure on monthly freshwater availability by decreasing the flow rates.

Table 23 presents the water balance components with respect to land use/cover changes. The model predicted surface runoff contribution to the freshwater inflows decreased by 5%. An increase in water balance components other than surface runoff seemed to be mainly influenced by the increase in forest and wetland areas. An increase in forested area results in more water lost by evaporation. The increase in forested area

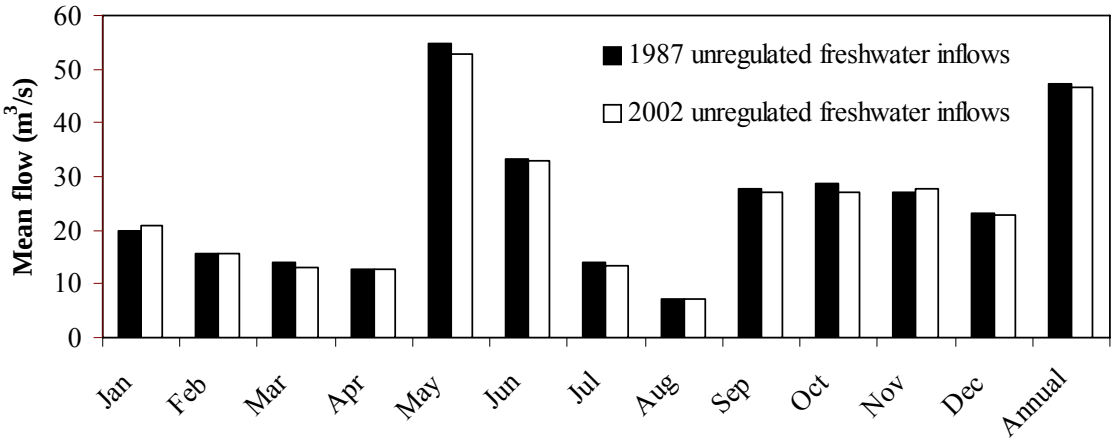

Figure 18. Predicted mean unregulated freshwater inflows contributed from the Guadalupe River Watershed for 1987 and 2002 land use scenarios.

also increased pervious area that has the potential to increase soil water capacity and to absorb and store water. These results are in agreement with a previous study conducted by Miller et al. (2002) in the Cannonsville Watershed, New York. They found that a small change in LULC (<5%) over the entire watershed did not affect the simulated watershed responses. Although this study also found less than 5% change in all LULC categories, changes in watershed responses were detected. This may be caused by the

combination of changes in forest, pasture and wetland areas which contribute almost 10% of the total change. The changes tended to decrease runoff and increase baseflow.

Table 23. Water balance component changes for 1987 and 2002 land cover scenarios

Water balance components	Total amount (mm)		Changes	
	1987	2002	mm	(%)
Precipitation	44288.32	44288.32		
Evapotranspiration	36792.22	36836.51	44.3	0.12
Surface Runoff	4544.67	4333.64	-211.0	-4.64
Lateral Flow	191.28	192.85	1.6	0.82
Baseflow	2225.16	2387.56	162.4	7.30
Soil Storage	534.99	537.76	2.8	0.52

Impact of Water Regulation on Freshwater Inflows

Assuming that model simulations of freshwater inflow that exclude reservoirs represents the unregulated freshwater inflow rate, water diversion structures in the stream network have modified the freshwater inflow rate. Because most of the reservoirs were intended as flood control, it was expected that during high flow conditions, the unregulated rates would always be higher than the regulated rate. However, in some cases during high flow years (Figure 15), for example, 1987, 1992 and 1997, unregulated freshwater inflows were lower than regulated ones. This would be the expected result of the effects of very large storms that could not be fully controlled by reservoirs.

SWAT, using 1987's model, predicted a 6% decrease in annual freshwater inflows rate because of water regulation (Figure 19). The decreased rates were detected in May, June, September and October. The highest decrease in freshwater inflows was in May which was the month with the highest amount of precipitation. During this month, reservoirs played an important role in flood control. During low flow months, regulated freshwater inflows tended to have higher rates than unregulated flows. In general, the reservoir function of storage during periods of high flow and release during low flow was demonstrated well by the model.

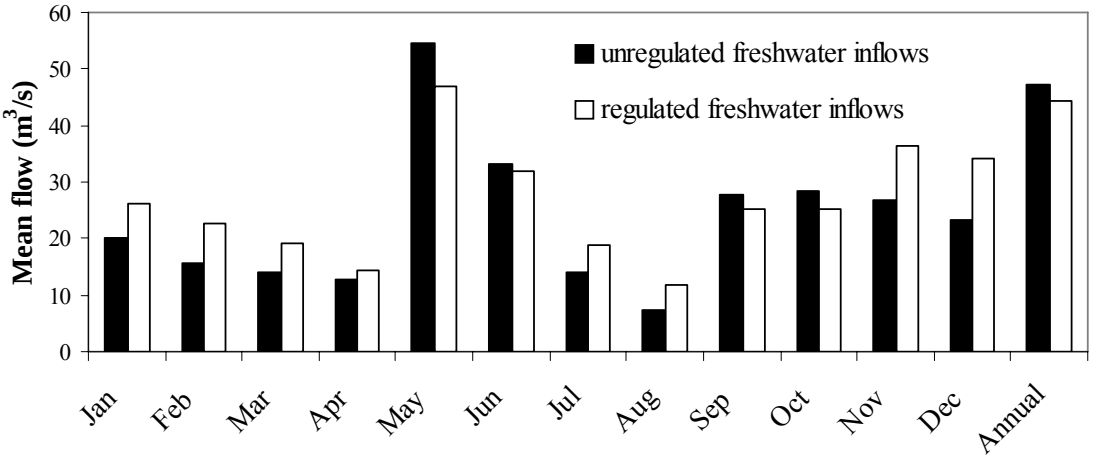

Figure 19. Predicted monthly mean freshwater inflows contributed from the Guadalupe River Watershed for scenarios with and without reservoirs.

This study relied only on reservoir characteristics such as reservoir volume, area and initial operation date. No specific information about reservoir management was available for the model. Because the model was calibrated for regulated flow, lack of information on reservoir management such as the amount of water used for municipal and industrial purposes might lead to underestimating unregulated freshwater inflows. Water uses for any purposes tend to decrease the amount of water in the system. This reduction was not accounted for in simulating unregulated flow.

CONCLUSIONS

The impact of LULC changes and water diversion structures on freshwater inflows was simulated using SWAT. The first objective was to examine the impact of two LULC scenarios on freshwater inflows. In this study, the two LULC data sets were obtained from satellite image classifications from 1987 and 2002. The results suggested that LULC change from 1987 to 2002 which was dominated by an increase in forest and urban areas decreased the rate of freshwater inflows by decreasing surface runoff contribution by 5%. The mean annual freshwater inflow rate decreased by less than 2%. The monthly freshwater inflow rate decreased throughout the year, with the exception of January and November. Simulation results suggested that increased urban area within the Guadalupe River Watershed did not significantly contribute to freshwater inflows. Total runoff generated by the increase in impervious area seemed to be diminished by an increase in pervious area resulting from forest expansion. This result rejected the first hypothesis that increase in urban area and irrigated land will increase the freshwater rates. However, the spatial variability in runoff and baseflow response to the LULC

changes were not considered in this study. This information may help to determine which subbasins generated more runoff or baseflow.

The second objective was to analyze the impact of reservoirs on freshwater inflows. The model, in general, showed its ability to predict freshwater inflows when including reservoirs. The model demonstrated that LULC change had less impact on freshwater inflow than the presence of reservoirs. Reservoirs modified the freshwater inflows in terms of reducing peaks and a maintaining minimum flow level. The overall result showed that reservoirs decreased unregulated annual freshwater inflows rate by 6%. This reduction was more profound during high flow periods. The model also demonstrated that during low flow periods, reservoirs tended to increase freshwater inflow rates. These finding resulted in accepting the second hypothesis of this study. Regardless of human influences, SWAT has shown an ability to represent reservoir functions properly although no specific information about reservoir management was given to the model.

The hydrologic modeling revealed effects of variability in precipitation on freshwater inflow. In this study, using visual inspection, the trend of median annual freshwater inflows significantly altered. Analysis of precipitation variability suggested that precipitation events in the period of 1987-2002 were more extreme than those in the period of 1957-1986. As a result, more extreme flows occurred during the period of 1987-2002. It was also evident that change in precipitation characteristics altered monthly freshwater inflows. The rate of freshwater inflows increased during the winter

months and decreased during the autumn. The frequency of the months with high freshwater inflows decreased during 1987-2002.

The overall results suggested that the integration of land cover changes, impact of upstream water diversion and precipitation variability significantly changed the characteristics of freshwater inflows to the Guadalupe Estuary. Future work needs to address water quality and water rights policy which were not part of this study. It is also important to address the issue of upstream and downstream watershed management to obtain the best watershed management plan that fulfills both human and environmental needs. SWAT which provides a wide range of watershed management options could be the proper tool to answer those questions.

CHAPTER VI

GENERAL CONCLUSIONS AND RECOMMENDATIONS

CONCLUSIONS

Previous studies have shown that the majority of freshwater inflows (approximately 70%) to the Guadalupe Estuary are contributed by the Guadalupe River Watershed. Hence this study focused on analyzing factors that have a strong relationship with streamflow in the watershed and which potentially influence the freshwater inflow rate. Those factors were land use/cover change, water regulation by reservoirs and precipitation variability.

Trend tests were performed on the recorded streamflow at USGS stations over the period 1930-2005, divided into three study periods, 1930-2005, 1950-2005 and 1970-2005. The results showed that during 1930-2005 and 1950-2005 streamflow exhibited significant increasing trends in minimum and mean flows both annually and seasonally. No significant trends were found in maximum flows, excepting winter flows at stations located upstream of Canyon Reservoir (08167000 and 08167500) and the station 08168500 during the period of 1950-2005. Additionally, significant trends were more pronounced at upstream stations and decreased as the analyses moved to downstream stations. Trends in precipitation, over the same period were found to be more significant on the lower part of the watershed. This finding suggests that factors other than precipitation contributed to the increase of streamflow.

Trend test results during the period of 1970-2005 found no significant trends in streamflow although the number of stations included in the analysis increased by 86% (from 7 to 13) from the 1950-2005 period. This indicates a change in the characteristics of streamflow within the last 35 years (1970-2005) that resulted in the failure of trend analysis to detect significant trends. Results of the trend analysis led to further investigation of factors that could directly influence freshwater inflows such as LULC change, water regulation, and the precipitation variability.

Analyses of Landsat satellite images using an unsupervised classification approach on scenes from 1987, 1999 and 2002 showed a significant increase in urban and irrigated area from 1987 to 2002 within the watershed. Urban and irrigated areas increased by 42% and 7%, respectively. Urbanized areas were mostly found on the middle part of watershed while irrigated areas were distributed over the entire watershed. Other changes observed were a 13% increase in forest and a 9% decrease in grassland coverage. Wetland and water areas increased by 20% and 25%, respectively.

A hydrologic model, SWAT, was used to estimate the impact of changes in LULC on freshwater inflows. Simulation results predicted a 2% decrease in annual freshwater inflows because of LULC change from 1987 to 2002. The monthly freshwater inflow rates consistently decreased from 1987-2002. The highest decrease in the flows was found during months with overall higher flow, particularly in May. The main contributor to the decrease in freshwater inflow predicted by SWAT came from a decrease in surface runoff (5%).

An increase in forested area amplified infiltration processes by creating more pervious surfaces. As a result, lateral flow and baseflow increased by 1 and 7%, respectively. An increase in forest density was the main factor in the increase of forested areas, but evapotranspiration increased by less than 1%.

It hypothesized that there would be an increase in freshwater inflows because of the increase in impervious area particularly around the I-35 corridor. However, simulation results suggest that the increase in urbanized area in the Guadalupe River Watershed did not have a significant impact on freshwater inflows. Urbanization may have an impact on local streamflow but because of the large size of the watershed and the distance of urban areas from the outlet, those effects were diminished by significant increases in forested and wetland areas. The changes more likely tended to improve the overall watershed condition by creating more pervious areas and increase the water holding capacity.

Interesting results were discovered when analysis of precipitation variability within the periods of 1957-1986 and 1987-2002 was performed. This analysis found an increase in mean annual precipitation by 6%, and an increase in the variance of precipitation. Through visual analysis of annual freshwater inflows, it was concluded that more extreme rates were found in 1987-2002 than 1957-1986. Analysis of median monthly freshwater inflows also revealed that they were impacted by precipitation variability. In general, the variability found in precipitation within both of the observation periods altered seasonal freshwater inflow rates by increasing winter flow rates and decreasing autumn flow rates. Precipitation variability in 1987-2002 also

produced more extreme freshwater inflows and decreased frequency of the months with high freshwater inflows.

Simulations also predicted the impact of water regulation by reservoirs on freshwater inflows. The impact was more profound in monthly than annual flows. During low flow months, reservoirs tended to increase the flow and in high flow months decrease flows to avoid flooding in downstream areas. Reservoir regulation of streamflow had more impact on freshwater inflows when compared to the impact of LULC change.

Overall, this study showed that freshwater inflows to the Guadalupe Estuary have changed significantly over the last 50 years because of the combination of LULC changes and water regulation from reservoirs in the upper stream networks. Additionally, significant changes in freshwater inflows were seen resulting from changes in precipitation variability. Because this study did not use detailed information of water use and watershed management, simulation results have to be interpreted conservatively. However, SWAT demonstrated its ability to be used as an approach for landscape analysis. Results of this study are important for future management and allocation of water resources by showing a clear impact on freshwater inflows to the Guadalupe Estuary.

RECOMMENDATIONS

Based on the results and restrictions found in this study, the following recommendations are suggested for future research in this region:

1. It is crucial to utilize more detailed information of LULC, watershed management practices and water use in simulating freshwater inflows using SWAT.
2. It is necessary to perform more extensive analysis on precipitation characteristics and other climate factors that are related to climate change and may have a significant impact on freshwater inflows.
3. Because LULC change significantly altered the quantity of freshwater inflows, it is also necessary to consider its impact on the quality of the water delivered from this watershed.
4. Future study on effects of watershed management practices on freshwater inflows should be done using SWAT to find the best management practices in the watershed with respect to both human and ecological needs for the available water.
5. SWAT should be combined with a readily available estuarine model to predict the direct impact of watershed management on estuary health and functions.

REFERENCES

Afinowicz, J.D., C.L. Munster, B.P. Wilcox and R.E. Lacey. 2005. A process for assessing wooded plant cover by remote sensing. *Rangeland Ecol. Manage.* 58(2): 184-190.

Arnold, J.G., R.S. Muttiah, R. Srinivasan and P.M. Allen. 2000. Regional estimation of base flow and groundwater recharge in the Upper Mississippi river basin. *J. Hydrol.* 227: 21-40.

Arnold, J.G., R. Srinivasan, R.S. Muttiah and J.R. Williams. 1998. Large area hydrologic modeling and assessment part 1: Model development. *J. Am. Water Resour. Assoc.* 34(1): 73-89.

Bewket, W. and G. Sterk. 2005. Dynamics in land cover and its effect on stream flow in Chemoga Watershed, Blue Nile basin, Ethiopia. *Hydrol. Process.* 19: 445-458.

Black, P.E. 1996. *Watershed Hydrology*. 2nd ed. Boca Raton, Florida: CRC Press.

Burn, D.H., J.M. Cunderlik and A. Peitroniro. 2004. Hydrological trends and variability in the Liard river basin. *Hydrolog. Sci. J.* 49(1): 53-67.

Burn, D.H. and M.A.H. Elnur. 2002. Detection of hydrologic trends and variability. *J. Hydrol.* 255: 107-122.

Burn, D.H. and N.M. Hesch. 2007. Trends in evaporation for the Canadian Prairies. *J. Hydrol.* 336: 61-73.

Costa, M.H., A. Botta and J.A. Cardile. 2003. Effects of large-scale changes in land cover on the discharge of the Tocantins River, Southeastern Amazonia. *J. Hydrol.* 283: 206-217.

Douglas, E.M., R.M. Vogel and C.N. Kroll. 2000. Trends in floods and low flows in the United States: Impacts of spatial correlation. *J. Hydrol.* 240: 90-105.

Dow, C.L. 2007. Assessing regional land-use/cover influences on New Jersey Pinelands streamflow through hydrograph analysis. *Hydrol. Process.* 21: 185-197.

El-Magd, I.A. and T.W. Tanton. 2003. Improvements in land use mapping for irrigated agriculture from satellite sensor data using a multi-stage maximum likelihood classification. *Int. J. Remote Sens.* 24(21): 4197-4206.

Fohrer, N., S. Haverkamp and H.G. Frede. 2005. Assessment of the effects of land use patterns on hydrologic landscape functions: Development of sustainable land use concepts for low mountain range areas. *Hydrol. Process.* 19: 659-672.

Garg, G. 2004. Quantifying long term changes in streamflow characteristics in Texas. M.S. thesis. College Station, Texas: Texas A&M University.

Gassman, P.W., M.R. Reyes, C.H. Green and J.G. Arnold. 2007. The soil and water assessment tool: Historical development, applications, and future research direction. *Trans. ASABE* 50(4): 1211-1248.

GBRA. 2008. Canyon reservoir fact sheet. Guadalupe-Blanco River Authority. Available at www.gbra.org. Accessed 10 February 2008.

Gero, A.F. and A.J. Pitman. 2006. The impact of land cover change on a simulated storm event in the Sydney Basin. *Amec. Meteor. Soc.* 45(2): 283-300.

Gosain, A.K., S. Rao, R. Srinivasan and N.G. Reddy. 2005. Return-flow assessment for irrigation command in the Palleru river basin using SWAT model. *Hydrol. Process.* 19: 673-682.

Govender, M. and C.S. Everson. 2005. Modelling streamflow from two small South African experimental catchments using the SWAT model. *Hydrol. Process.* 19: 683-692.

Granskog, M.A., H. Kaartokallio, D.N. Thomas and H. Kuosa. 2005. Influence of freshwater inflow on the inorganic nutrient and dissolved organic matter within coastal sea ice and underlying waters in the Gulf of Finland (Baltic Sea). *Estuar. Coast. Shelf S.* 65(1-2): 109-122.

Haan, C.T., B.J. Barfield and J.C. Hayes. 1994. *Design Hydrology and Sedimentology for Small Catchments*. San Diego, CA: Academic Press.

Hamlin, L. 2005. The abundance and spatial distribution of blue crabs (*Callinectes Sapidus*) in the Guadalupe estuary related to low flow freshwater inflow conditions. M.S. thesis. San Marcos: Texas State University.

Hernandez, M., S.N. Miller, D.C. Goodrich, B.F. Goff, W.G. Kepner, C.M. Edmonds and K.B. Jones. 2000. Modeling runoff response to land cover and rainfall spatial variability in semi-arid watersheds. *Environ. Monit. Assess.* 64(1): 285-298.

Heuvelmans, G., J.F. Garcia-Qujano, B. Muys, J. Feyen and P. Coppin. 2005. Modeling the water balance with SWAT as part of the land use impact evaluation in a life cycle study of CO_2 emission reduction scenarios. *Hydrol. Process.* 19: 729-748.

Hirsch, R.M., R.B. Alexander and R.A. Smith. 1991. Selection of methods for the detection and estimation of trends in water quality. *Water Resour. Res.* 27(5): 803-813.

Hirsch, R.M., J.R. Slack and R.A. Smith. 1982. Techniques of trend analysis for monthly water quality data. *Water Resour. Res.* 18(1): 107-121.

Iroume, A., A. Huber and K. Schulz. 2005. Summer flows in experimental catchments with different forest covers, Chile. *J. Hydrol.* 300: 300-313.

Jensen, J.R. 2005. *Introductory Digital Image Processing: A Remote Sensing Perspective*. 3rd ed. Upper Saddle River, New Jersey: Pearson Prentice Hall.

Jiang, H., J.R. Strittholt, P.A. Frost and N.C. Slosser. 2004. The classification of late seral forests in the Pacific Northwest, USA using Landsat ETM+ imagery. *Remote Sens. Environ.* 91(3-4): 320-331.

Joy, S.M., R.M. Reich and R.T. Reynolds. 2003. A non-parametric, supervised classification of vegetation types on the Kaibab National Forest using decission trees. *Int. J. Remote Sens.* 24(9): 1835-1852.

Konrad, C.P., D.B. Booth and S.J. Burges. 2005. Effects of urban development in the Puget Lowland, Washington, on interannual streamflow patterns: Consequences for channel form and streambed disturbance. *Water Resour. Res.* 41. W07009, doi:10.1029/2005WR004097.

Larose, M., G.C. Heathman, L.D. Norton and B. Engel. 2007. Hydrologic and Atrazine simulation of the Cedar Creek Watershed using SWAT model. *J. Environ. Qual.* 36(2): 521-531.

Legesse, D., C. Vallet-Coulomb and F. Gasse. 2003. Hydrological response of a cathment to climate and land use change in Tropical Africa: case study South Central Ethiopia. *J. Hydrol.* 275: 67-85.

Lillesand, T.M. and R.W. Kiefer. 1994. *Remote Sensing and Image Interpretation*. 3rd New York: John Wiley & Sons.

Lindstrom, G. and S. Bergstrom. 2004. Runoff trends in Sweden 1807-2002. *Hydrolog. Sci. J.* 49(1): 69-83.

Longley, W.L. 1994. *Freshwater Inflows to Texas Bays and Estuaries: Ecological Relationships and Methods for Determination of Needs*. Austin, TX: Texas Water Development Board and Texas Parks and Wildlife Department.

Mann, H.B. 1945. Nonparametric tests against trend. *Econometrica* 13(3): 245-259.

McKinney, L., D. Bowles and A. Bright. 2003. *Regional Habitat Conservation Plan*. Austin: Conservation Committee. Texas Parks and Wildlife.

Miller, S.N., W.G. Kepner, M.H. Mehaffey, M. Hernandez, R.C. Miller, D.C. Goodrich, K.K. Devonald, D.T. Heggem and W.P. Miller. 2002. Integrating landscape assessment and hydrologic modeling for land cover change analysis. *J. Am. Water Resour. Assoc.* 38(4): 915-929.

Mulungu, D.M.M. and S.E. Munishi. 2007. Simiyu River catchment parameterization using SWAT model. *Phys. Chem. Earth* 32(15-18): 1032-1039.

Musaoglu, N., A. Tanik and V. Kocabas. 2005. Identification of land-cover changes through image processing and associated impacts on water reservoir conditions. *Environ. Manage.* 35(2): 220-230.

Neitsch, S.L., J.G. Arnold, J.R. Kiniry, J.R. Williams and K.W. King. 2002. *Soil and Water Assessment Tools Theoretical Documentation: Version 2000*. College Station: Texas Water Resources Institute.

Notaro, M., Z. Liu, R. Gallimore, S.J. Vavrus, J.E. Kutzbach, I.C. Prentice and R.L. Jacob. 2005. Simulated and observed preindustrial to modern vegetation and climate changes. *Amec. Meteor. Soc.* 18(17): 3650-3671.

Novotny, E.V. and H.G. Stefan. 2007. Stream flow in Minnesota: Indicator of climate change. *J. Hydrol.* 334: 319-333.

Oetter, D.R., W.B. Cohen, M. Berterretche and T.K. Maiersperger. 2000. Land cover mapping in an agricultural setting using multiseasonal Thematic Mapper data. *Remote Sens. Environ.* 76(2): 139-155.

Paquini, A.I. and P.J. Depetris. 2007. Discharge trends and flow dynamics of South American rivers draining the southern Atlantic seaboard: An Overview. *J. Hydrol.* 333: 385-399.

Peschel, J.M. 2004. Quantifying land cover in a semi-arid region of Texas. M.S. thesis. College Station: Texas A&M University.

Phillips, J. and N. Melcher, 2006. The U.S. Geological Survey water-resources data program present and future challenges: Dealing with data. *Southwest Hydrology* 5(3): 18-31.

Pizarro, R., S. Araya, C. Jordan, C. Farias, J.p. Flores and P.B. Bro. 2006. The effects of changes in vegetative cover on river flows in the Purapel river basin of central Chile. *J. Hydrol.* 327: 249-257.

Pontee, N.I., P.A. Whitehead and C.M. Hayes. 2004. The effects of freshwater flow on siltation in the Humber estuary, north east UK. *Estuar. Coast. Shelf S.* 60(2): 241-249.

Porter-Bolland, L., E.A. Ellis and H.L. Gholz. 2007. Land use dynamics and landscape history in La Montana, Campeche, Mexico. *Landscape Urban Plan.* 82(4): 198-207.

Potter, K.W. 1991. Hydrological impacts of changing land management practices in a moderate-sized agricultural catchment. *Water Resour. Res.* 27(5): 845-855.

Rodriguez, C.A., K.W. Flessa and D.L. Dettman. 2001. Effects of upstream diversion of Colorado River water on the estuarine Bivalve Mollusc *Mulinia Coloradoensis*. *Conserv. Biol.* 15(1): 249-258.

Rose, S. and N.E. Peters. 2001. Effects of urbanization on streamflow in the Atlanta area (Georgia, USA): A comparative hydrological approach. *Hydrol. Process.* 15: 1441-1457.

Rozas, L.P., T.J. Minello, I. Munuera-Fernandez, B. Fry and B. Wissel. 2005. Macrofaunal distributions and habitat change following winter-spring releases of freshwater into the Breton Sound estuary, Lousiana (USA). *Estuar. Coast. Shelf S.* 65(1-2): 319-336.

Russell, M.J., P.A. Montagna and R.D. Kalke. 2006. The effect of freshwater inflow on net ecosystem metabolism in Lavaca Bay, Texas. *Estuar. Coast. Shelf S.* 68(1-2): 231-244.

Sahoo, D. 2008. Modeling the effect of land cover land use change on estuarine environmental flows. Ph.D. dissertation. College Station: Texas A&M University.

Saleh, A., J.G. Arnold, P.W. Gassman, L.M. Hauck, W.D. Rosenthal, J.R. Williams and A.M.S. McFarland. 2000. Application of SWAT for the Upper North Bosque River Watershed. *Trans. ASAE* 43(5): 1077-1087.

Schone, B.R., K.W. Flessa, D.L. Dettman and D.H. Goodwin. 2003. Upstream dams and downstream clams: Growth rates of bivalve mollusk unveil impact of river management on estuarine ecosystem (Colorado River Delta, Mexico). *Estuar. Coast. Shelf S.* 58(4): 715-726.

Song, C., C.E. Woodcock, K.C. Seto, M.P. Lenney and S.A. Macomber. 2001. Classification and change detection using Landsat TM data: When and how to correct atmosphere effects? *Remote Sens. Environ.* 75(2): 230-244.

Spruill, C.A., S.R. Workman and J.L. Taraba. 2000. Simulation of daily and monthly stream discharge from small watershed using the SWAT model. *Trans. ASAE* 43(6): 1431-1439.

Stehn, T. 2001. Relationship between inflows, crabs, salinities, and whooping cranes. Journey North: Whooping Crane. Available at: http://www.learner.org/jnorth/tm/crane/Stehn_CrabDocument.html. Accessed November 3, 2007.

Taylor, C.M., E.F. Lambin, N. Stephenne, R.J. Harding and R.L.H. Essery. 2002. The influence of land use change on climate in the Sahel. *Amec. Meteor. Soc.* 15(24): 3615-3629.

Thanapakpawin, P., J. Richey, D. Thomas, S. Rodda, B. Campbell and M. Logsdon. 2007. Effects of landuse change on the hydrologic regime of the Mae Chaem River Basin, NW Thailand. *J. Hydrol.* 334: 215-230.

Tolson, B.A. and C.A. Shoemaker. 2007. Cannonsville reservoir watershed SWAT2000 model development, calibration and validation. *J. Hydrol.* 337(1-2): 68-86.

TPWD. 2007. Freshwater inflow recommendation for the Guadalupe estuary of Texas. Texas Parks and Wildlife. Available at: http://www.tpwd.state.tx.us/landwater/water/conservation/freshwater_inflow/guadalupe/index.phtml. Accessed December 17, 2007.

TPWD. 2008. Texas Gems - Guadalupe Delta Wildlife management area. Texas Parks and Wildlife. Available at: http://www.tpwd.state.tx.us/landwater/water/conservation/txgems/guadalup/index.phtml. Accessed February 21, 2008.

TWDB. 2007. Bays and estuaries - hydrology. Texas Water Development Board. Available at: http://hyper20.twdb.state.tx.us/data/bays_estuaries/hydrologypage.html. Accessed November 10, 2007.

TWDB. 2008. The regional water plans: South central Texas region (L). Texas Water Development Board. Available at www.twdb.state.tx.us. Accessed 11 March 2008.

UNEP, 2006. *Challenges to International Waters - Regional Assessments in a Global Perspective*, United Nations environment programme, Nairobi, Kenya.

USACE. 2008. Historical reservoir reports. Fort Worth District Daily Reservoir Reports. US Army Corps of Engineering. Available at: www.swf-wc.usace.army.mil. Accessed 25 January 2008.

USDA. 2007. 2002 Census of Agriculture, Volume 1 Chapter 1: Texas state level data. National Agricultural Statistic Service. available at: www.nass.usda.gov. Accessed 5 June 2007.

VanLiew, M.W., T.L. Veith, D.D. Bosch and J.G. Arnold. 2007. Suitability of SWAT for the conservation effects assessment project: Comparison on USDA Agricultural Research Service Watersheds. *J. Hydraul. Eng-ASCE* 12(2): 173-189.

Ward, A.D. and S.W. Trimble. 2004. *Environmental Hydrology*. 2nd ed. Boca Raton, FL: CRC press.

Warner, R.M. 1998. *Spectral Analysis of Time-Series Data*. New York: The Guilford Press.

Weber, A., N. Fohrer and D. Moller. 2001. Long-term land use changes in a mesoscale watershed due to socio-economic factors - effects on landscape structures and functions. *Ecol. Model.* 140(1-2): 125-140.

Wickham, J.D., S.V. Stehman, J.H. Smith and L.Yang. 2004. Thematic accuracy of the 1992 National Land-Cover Data for the western United States. *Remote Sens. Environ.* 91(3-4): 452-468.

Xu, Y.J. and K. Wu. 2006. Seasonality and interannual variability of freshwater inflow to large oligohaline estuary in the Northern Gulf of Mexico. *Estuar. Coast. Shelf S.* 68(3-4): 619-626.

Yue, S., P. Pilon and G. Cavadias. 2002. Power of the Mann-Kendall and Spearman's rho tests for detecting monotonic trends in hydrological series. *J. Hydrol.* 259: 254-271.

Yue, S., P. Pilon and B. Phinney. 2003. Canadian streamflow trend detection: Impacts of serial and cross-correlation. *Hydrol. Process.* 48(1): 51-63.

Zhang, Q., C. Liu, C.-y. Xu, Y. Xu and T. Jiang. 2006. Observed trends of annual maximum water level and streamflow during past 130 years in the Yangtze river basin, China. *J. Hydrol.* 324: 255-265.

Zhang, X., K.D. Harvey, W.D. Hogg and T.R. Yuzyk. 2001a. Trend in Canadian streamflow. *Water Resour. Res.* 37(4): 987-998.

Zhang, X., W.D. Hogg and E. Mekis. 2001b. Spatial and temporal characteristics of heavy precipitation over Canada. *J. Climate* 14: 1923-1936.

Zhang, X., L.A. Vincent, W.D. Hogg and A. Niitsoo. 2000. Temperature and precipitation trends in Canada during 20th century. *Atmos. Ocean* 38(3): 395-429.

Zhang, Y.K. and K.E. Schilling. 2005. Increasing streamflow and baseflow in Mississippi River since the 1940 s: Effect of land use change. *J. Hydrol.* 324: 412-422.

APPENDIX A

TREND ANALYSIS ON HYDROLOGIC VARIABLES

A.1. Period 1930-2005

1. a. Mann-Kendall Trend Test for Minimum Annual Flow (1930-2005)

Gage	Original		Slope	Serial Correlation			Re-trended		Trend/No-
Number	MK test	P-Value		Lag-1	P-Value	S/NS*	MK test	P-value	Trend **
08167500	2.989	0.003	0.641	0.245	0.029	S	2.905	0.004	trend
08168500	3.858	0.000	1.282	0.248	0.012	S	4.048	0.000	trend
08169000	-1.601	0.109	-0.823	0.636	0	S	-1.615	0.106	no-trend
08171000	3.652	0.000	0.266	0.403	0	S	3.783	0.000	trend

* - Compare to 5% level of significance

** - Based on re-trended p-value if serial correlation is positive and significant (S) otherwise based on original p-value
- Compare to 10% level of significance

b. Bootstrap Empirical Cumulative Distribution

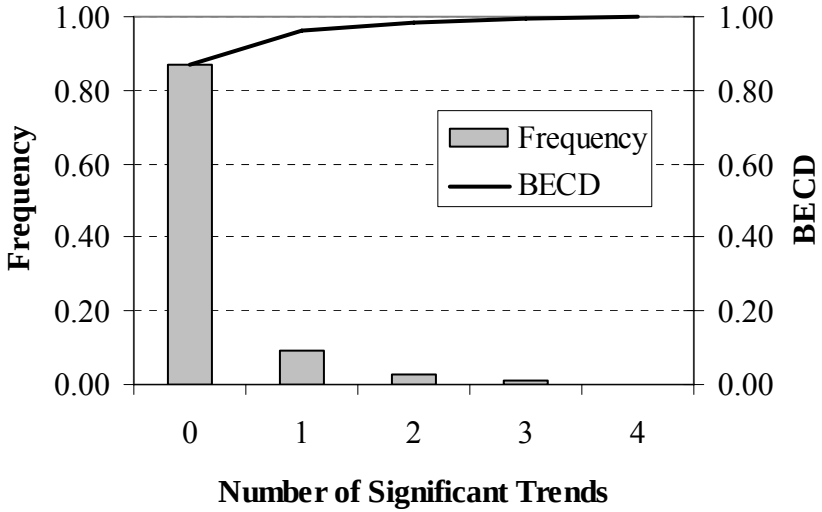

A.1. (Continued)

2. Mann-Kendall Trend Test for Maximum Annual Flow (1930-2005)

Gage	Original		Slope	Serial Correlation			Re-trended		Trend/No-
Number	MK test	P-Value		Lag-1	P-Value	S/NS*	MK test	P-value	Trend **
08167500	1.615	0.106	65.902	-0.029	0.8	S	1.660	0.097	no-trend
08168500	-1.579	0.114	-22.264	0.056	0.618	S	-1.258	0.208	no-trend
08169000	1.350	0.177	5.702	-0.08	0.478	S	1.615	0.106	no-trend
08171000	1.444	0.149	19.738	-0.137	0.222	S	1.926	0.054	no-trend

* - Compare to 5% level of significance

** - Based on re-trended p-value if serial correlation is positive and significant (S) otherwise based on original p-value
- Compare to 10% level of significance

A.1. (Continued)

3. a. Mann-Kendall Trend Test for Mean Annual Flow (1930-2005)

Gage	Original		Slope	Serial Correlation			Re-trended		Trend/No-
Number	MK test	P-Value		Lag-1	P-Value	S/NS*	MK test	P-value	Trend **
08167500	2.547	0.011	3.302	0.016	0.885	S	2.356	0.018	trend
08168500	2.485	0.013	4.242	0.054	0.631	S	2.411	0.016	trend
08169000	0.789	0.430	0.304	0.608	0.000	S	0.892	0.372	no-trend
08171000	2.673	0.008	1.322	-0.608	0.547	S	2.218	0.027	trend

* - Compare to 5% level of significance

** - Based on re-trended p-value if serial correlation is positive and significant (S) otherwise based on original p-value
- Compare to 10% level of significance

b. Bootstrap Empirical Cumulative Distribution

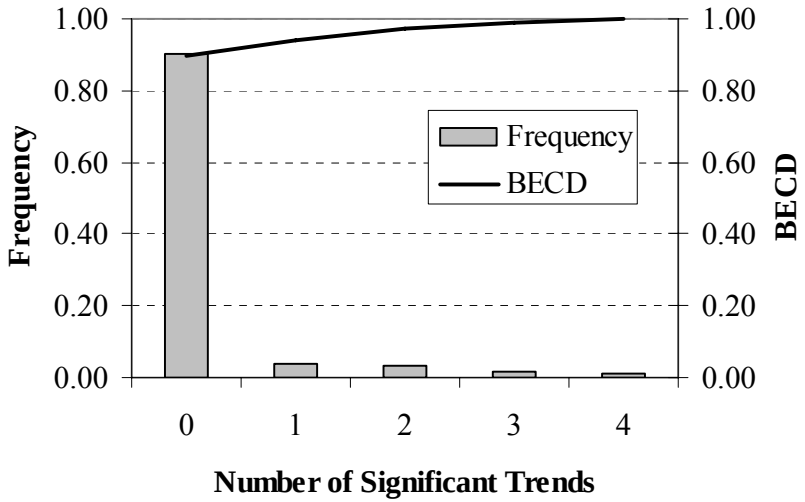

A.1. (Continued)

4. a. Mann-Kendall Trend Test for Minimum Seasonal Dec-Mar Flow (1930-2005)

Gage	Original		Slope	Serial Correlation			Re-trended		Trend/No-
Number	MK test	P-Value		Lag-1	P-Value	S/NS*	MK test	P-value	Trend **
08167500	3.525	0.000	1.510	0.031	0.785	S	3.426	0.001	trend
08168500	2.969	0.003	1.667	-0.021	0.853	S	2.786	0.005	trend
08169000	1.032	0.302	0.395	0.627	0.000	S	1.011	0.312	no-trend
08171000	3.405	0.001	0.509	0.070	0.535	S	3.399	0.001	trend

* - Compare to 5% level of significance

** - Based on re-trended p-value if serial correlation is positive and significant (S) otherwise based on original p-value
- Compare to 10% level of significance

b. Bootstrap Empirical Cumulative Distribution

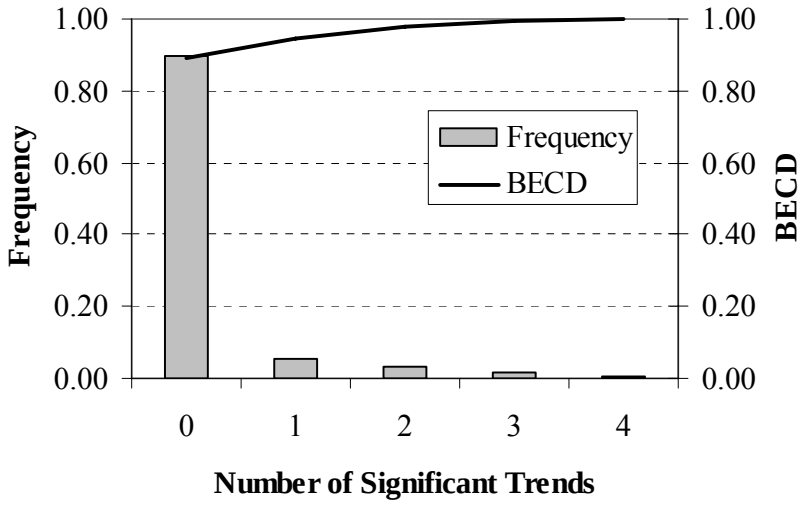

A.1. (Continued)

5. Mann-Kendall Trend Test for Maximum Seasonal Dec-Mar Flow (1930-2005)

Gage	Original		Slope	Serial Correlation			Re-trended		Trend/No-
Number	MK test	P-Value		Lag-1	P-Value	S/NS*	MK test	P-value	Trend **
08167500	1.130	0.258	4.844	-0.065	0.562	S	1.075	0.282	no-trend
08168500	0.099	0.921	0.344	-0.114	0.310	S	-0.096	0.923	no-trend
08169000	0.583	0.560	0.550	-0.049	0.662	S	0.343	0.732	no-trend
08171000	0.861	0.389	1.312	-0.122	0.279	S	0.508	0.612	no-trend

* - Compare to 5% level of significance

** - Based on re-trended p-value if serial correlation is positive and significant (S) otherwise based on original p-value
- Compare to 10% level of significance

A.1. (Continued)

6. a. Mann-Kendall Trend Test for Mean Seasonal Dec-Mar Flow (1930-2005)

Gage	Original		Slope	Serial Correlation			Re-trended		Trend/No-
Number	MK test	P-Value		Lag-1	P-Value	S/NS*	MK test	P-value	Trend **
08167500	2.790	0.005	3.542	-0.071	0.526	S	2.511	0.012	trend
08168500	2.736	0.006	4.559	-0.060	0.593	S	2.292	0.022	trend
08169000	1.597	0.110	0.730	0.563	0.000	S	1.304	0.192	no-trend
08171000	2.242	0.025	1.174	-0.071	0.531	S	1.953	0.051	trend

* - Compare to 5% level of significance

** - Based on re-trended p-value if serial correlation is positive and significant (S) otherwise based on original p-value
- Compare to 10% level of significance

b. Bootstrap Empirical Cumulative Distribution

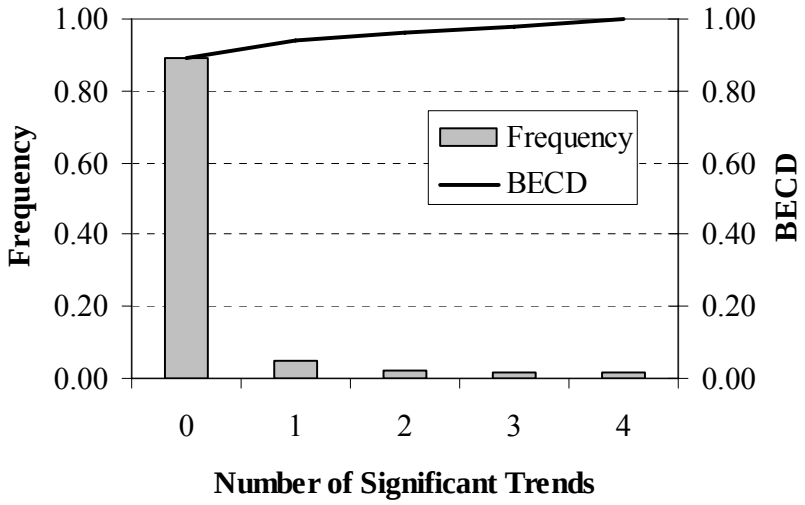

A.1. (Continued)

7. a. Mann-Kendall Trend Test for Minimum Seasonal Apr-Jul Flow (1930-2005)

Gage	Original		Slope	Serial Correlation			Re-trended		Trend/No-
Number	MK test	P-Value		Lag-1	P-Value	S/NS*	MK test	P-value	Trend **
08167500	2.660	0.008	1.021	-0.098	0.383	S	2.758	0.006	trend
08168500	3.593	0.000	2.000	-0.172	0.126	S	3.444	0.001	trend
08169000	-1.126	0.260	-0.560	0.492	0.000	S	-1.084	0.278	no-trend
08171000	3.728	0.000	0.500	-0.042	0.711	S	3.605	0.000	trend

* - Compare to 5% level of significance

** - Based on re-trended p-value if serial correlation is positive and significant (S) otherwise based on original p-value
- Compare to 10% level of significance

b. Bootstrap Empirical Cumulative Distribution

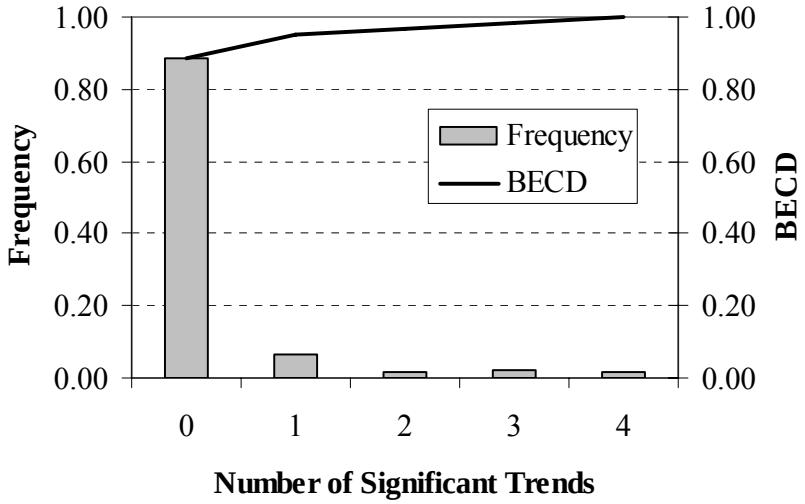

A.1. (Continued)

8. a. Mann-Kendall Trend Test for Maximum Seasonal Apr-Jul Flow (1930-2005)

Gage	Original		Slope	Serial Correlation			Re-trended		Trend/No-
Number	MK test	P-Value		Lag-1	P-Value	S/NS*	MK test	P-value	Trend **
08167500	-0.704	0.481	-10.721	-0.087	0.440	S	0.059	0.953	no-trend
08168500	-2.709	0.007	-26.795	0.075	0.507	S	-2.676	0.007	trend
08169000	0.444	0.657	1.083	-0.044	0.695	S	0.508	0.612	no-trend
08171000	0.166	0.868	0.814	-0.111	0.325	S	0.791	0.429	no-trend

* - Compare to 5% level of significance

** - Based on re-trended p-value if serial correlation is positive and significant (S) otherwise based on original p-value
- Compare to 10% level of significance

b. Bootstrap Empirical Cumulative Distribution

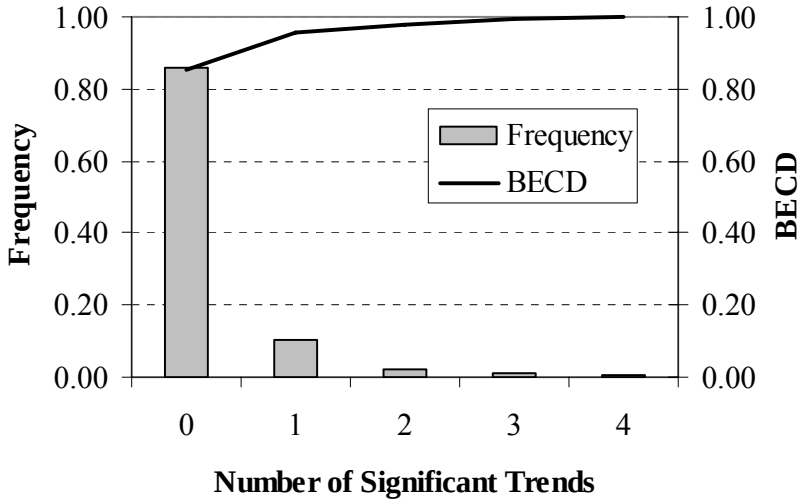

A.1. (Continued)

9. a. Mann-Kendall Trend Test for Mean Seasonal Apr-Jul Flow (1930-2005)

Gage	Original		Slope	Serial Correlation			Re-trended		Trend/No-
Number	MK test	P-Value		Lag-1	P-Value	S/NS*	MK test	P-value	Trend **
08167500	1.345	0.178	2.560	-0.129	0.252	S	1.670	0.095	no-trend
08168500	1.408	0.159	3.102	-0.098	0.383	S	1.606	0.108	no-trend
08169000	0.197	0.844	0.122	0.459	0.000	S	0.252	0.801	no-trend
08171000	1.668	0.095	1.381	-0.161	0.152	S	1.990	0.047	no-trend

* - Compare to 5% level of significance

** - Based on re-trended p-value if serial correlation is positive and significant (S) otherwise based on original p-value
- Compare to 10% level of significance

A.1. (Continued)

10. a. Mann-Kendall Trend Test for Minimum Seasonal Aug-Nov Flow (1930-2005)

Gage	Original		Slope	Serial Correlation			Re-trended		Trend/No-
Number	MK test	P-Value		Lag-1	P-Value	S/NS*	MK test	P-value	Trend **
08167500	2.858	0.004	0.857	0.131	0.243	S	2.575	0.010	trend
08168500	4.450	0.000	1.442	0.272	0.015	S	4.387	0.000	trend
08169000	-0.691	0.490	-0.367	0.550	0.000	S	-0.782	0.434	no-trend
08171000	3.809	0.000	0.355	0.208	0.064	S	3.710	0.000	trend

* - Compare to 5% level of significance

** - Based on re-trended p-value if serial correlation is positive and significant (S) otherwise based on original p-value
- Compare to 10% level of significance

b. Bootstrap Empirical Cumulative Distribution

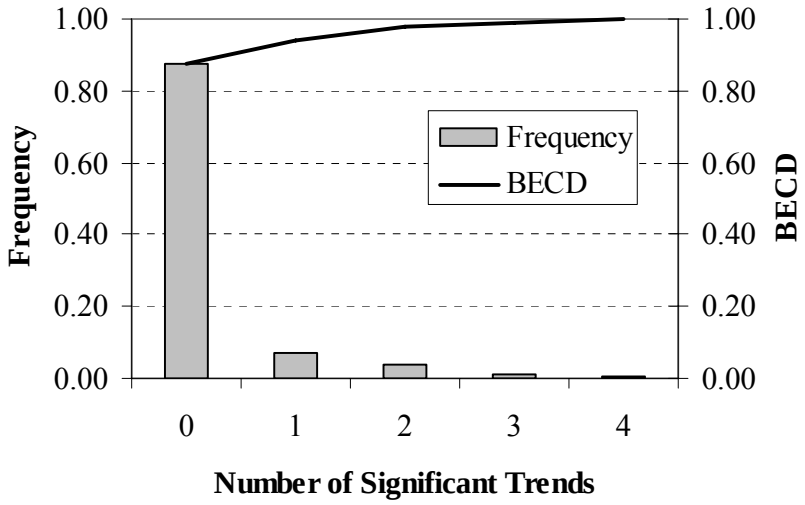

A.1. (Continued)

11. a. Mann-Kendall Trend Test for Maximum Seasonal Aug-Nov Flow (1930-2005)

Gage Number	Original MK test	Original P-Value	Slope	Serial Correlation Lag-1	Serial Correlation P-Value	Serial Correlation S/NS*	Re-trended MK test	Re-trended P-value	Trend/No-Trend **
08167500	2.005	0.045	18.912	-0.131	0.244	S	2.045	0.041	trend
08168500	0.058	0.954	0.225	0.054	0.632	S	0.956	0.339	no-trend
08169000	0.866	0.387	1.150	-0.060	0.591	S	0.874	0.382	no-trend
08171000	0.507	0.612	0.919	-0.030	0.793	S	1.048	0.295	no-trend

* - Compare to 5% level of significance

** - Based on re-trended p-value if serial correlation is positive and significant (S) otherwise based on original p-value
- Compare to 10% level of significance

b. Bootstrap Empirical Cumulative Distribution

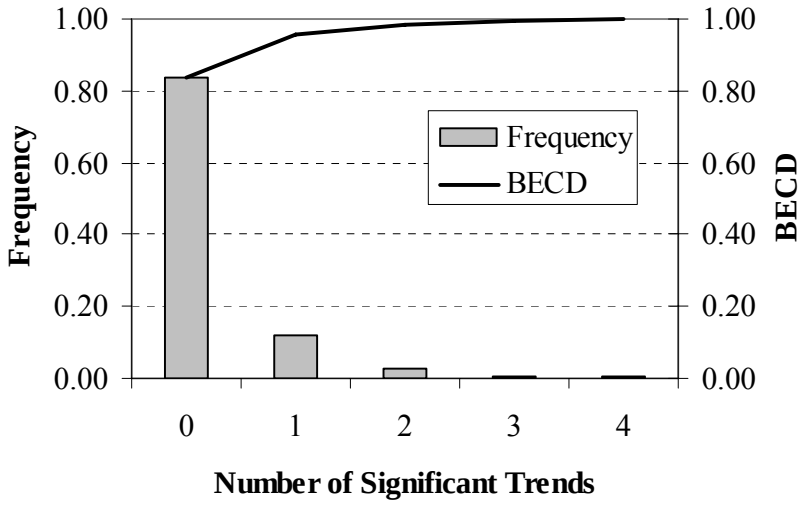

A.1. (Continued)

12. a. Mann-Kendall Trend Test for Mean Seasonal Aug-Nov Flow (1930-2005)

Gage	Original		Slope	Serial Correlation			Re-trended		Trend/No-
Number	MK test	P-Value		Lag-1	P-Value	S/NS*	MK test	P-value	Trend **
08167500	2.682	0.007	3.513	-0.033	0.767	S	2.850	0.004	trend
08168500	2.754	0.006	5.091	0.229	0.042	S	2.658	0.008	trend
08169000	0.206	0.837	0.138	0.505	0.000	S	-0.233	0.816	no-trend
08171000	2.601	0.009	0.871	-0.026	0.818	S	2.639	0.008	trend

* - Compare to 5% level of significance

** - Based on re-trended p-value if serial correlation is positive and significant (S) otherwise based on original p-value
- Compare to 10% level of significance

b. Bootstrap Empirical Cumulative Distribution

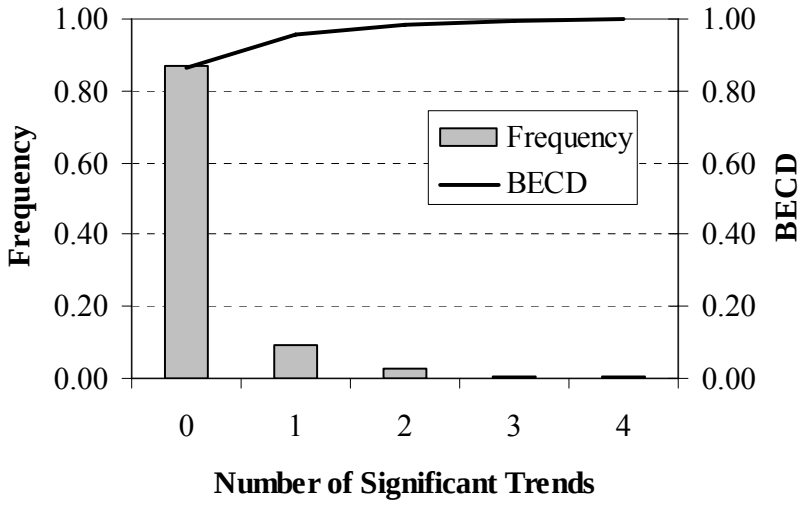

A.2. Period 1950-2005

1.a. Mann-Kendall Trend Test for Minimum Annual Flow (1950-2005)

Gage	Original		Slope	Serial Correlation			Re-trended		Trend/No-
Number	MK test	P-Value		Lag-1	P-Value	S/NS*	MK test	P-value	Trend **
08167500	2.818	0.005	1.000	0.221	0.090	S	2.490	0.013	trend
08169000	2.220	0.026	1.753	0.531	0.000	S	2.374	0.018	trend
08167000	3.583	0.000	0.866	0.189	0.147	S	3.521	0.000	trend
08171000	1.732	0.083	0.228	0.329	0.011	S	1.372	0.170	no-trend
08172000	2.036	0.042	0.772	0.372	0.004	S	1.662	0.096	no-trend
08176500	1.611	0.107	3.958	0.439	0.001	S	1.561	0.119	no-trend
08168500	2.997	0.003	1.687	0.242	0.063	S	2.998	0.003	trend

* - Compare to 5% level of significance

** - Based on re-trended p-value if serial correlation is positive and significant (S) otherwise based on original p-value
- Compare to 10% level of significance

b. Bootstrap Empirical Cumulative Distribution

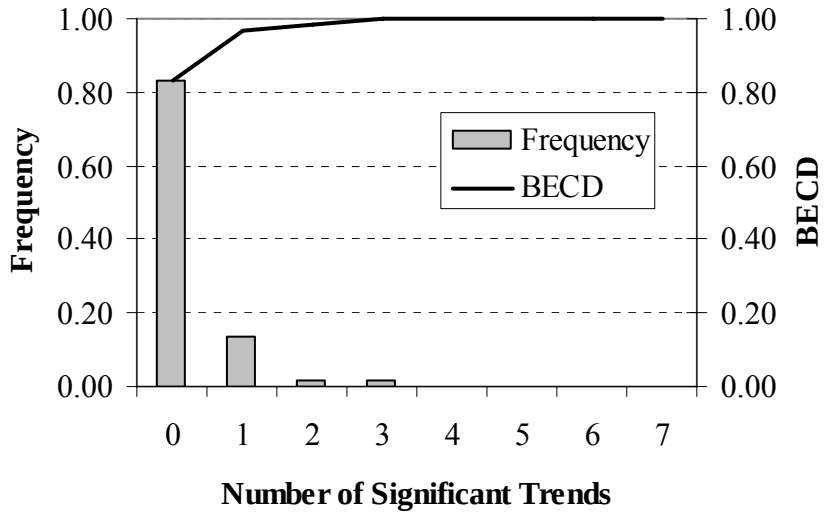

A.2. (Continued)

2. Mann-Kendall Trend Test for Maximum Annual Flow (1950-2005)

Gage	Original		Slope	Serial Correlation			Re-trended		Trend/No-
Number	MK test	P-Value		Lag-1	P-Value	S/NS*	MK test	P-value	Trend **
08167500	1.103	0.270	63.224	-0.106	0.414	S	1.241	0.214	no-trend
08169000	0.841	0.400	4.272	-0.112	0.388	S	0.777	0.437	no-trend
08167000	0.714	0.475	27.381	0.072	0.583	S	0.327	0.744	no-trend
08171000	0.806	0.420	19.526	-0.187	0.151	S	1.082	0.279	no-trend
08172000	0.170	0.865	16.792	-0.197	0.130	S	0.748	0.455	no-trend
08176500	1.117	0.264	131.825	-0.124	0.339	S	1.691	0.091	no-trend
08168500	-0.276	0.783	-4.104	0.034	0.796	S	-0.501	0.616	no-trend

* - Compare to 5% level of significance

** - Based on re-trended p-value if serial correlation is positive and significant (S) otherwise based on original p-value
- Compare to 10% level of significance

A.2. (Continued)

3. a. Mann-Kendall Trend Test for Mean Annual Flow (1950-2005)

Gage	Original		Slope	Serial Correlation			Re-trended		Trend/No-
Number	MK test	P-Value		Lag-1	P-Value	S/NS*	MK test	P-value	Trend **
08167500	2.714	0.007	6.113	-0.074	0.571	S	2.635	0.008	trend
08169000	3.053	0.002	2.581	0.491	0.000	S	3.289	0.001	trend
08167000	3.237	0.001	3.710	0.043	0.742	S	2.940	0.003	trend
08171000	1.922	0.055	1.650	-0.114	0.381	S	1.764	0.078	no-trend
08172000	2.007	0.045	3.928	-0.057	0.663	S	1.721	0.085	trend
08176500	2.544	0.011	23.638	-0.043	0.738	S	2.156	0.031	trend
08168500	2.728	0.006	7.648	-0.033	0.801	S	2.476	0.013	trend

* - Compare to 5% level of significance

** - Based on re-trended p-value if serial correlation is positive and significant (S) otherwise based on original p-value
- Compare to 10% level of significance

b. Bootstrap Empirical Cumulative Distribution

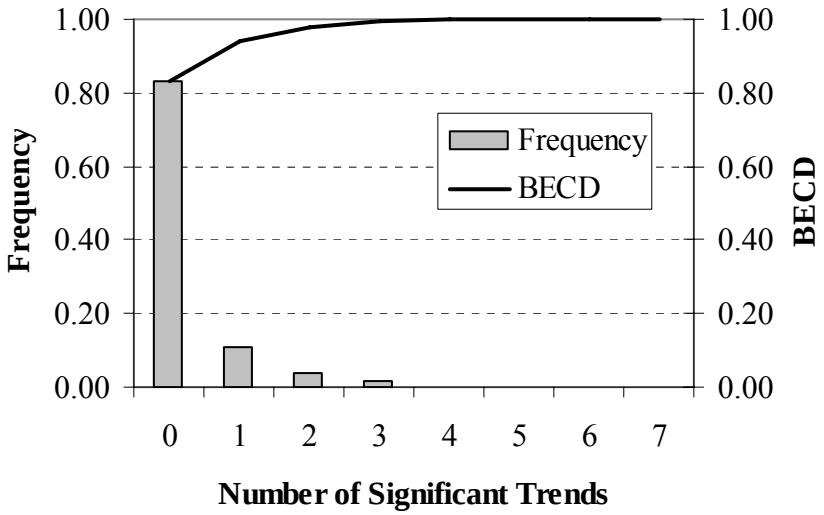

A.2. (Continued)

4. a. Mann-Kendall Trend Test for Minimum Seasonal Dec-Mar Flow (1950-2005)

Gage	Original		Slope	Serial Correlation			Re-trended		Trend/No-
Number	MK test	P-Value		Lag-1	P-Value	S/NS*	MK test	P-value	Trend **
08167500	3.612	0.000	2.696	-0.010	0.938	S	3.419	0.001	trend
08169000	3.104	0.002	2.464	0.561	0	S	3.913	0.000	trend
08167000	4.100	0.000	2.132	-0.041	0.755	S	4.044	0.000	trend
08171000	2.199	0.028	0.615	0.096	0.459	S	2.214	0.027	trend
08172000	2.064	0.039	1.563	0.115	0.376	S	1.996	0.046	trend
08176500	2.382	0.017	9.568	0.182	0.162	S	2.868	0.004	trend
08168500	3.159	0.002	2.804	-0.040	0.758	S	2.998	0.003	trend

* - Compare to 5% level of significance

** - Based on re-trended p-value if serial correlation is positive and significant (S) otherwise based on original p-value
- Compare to 10% level of significance

b. Bootstrap Empirical Cumulative Distribution

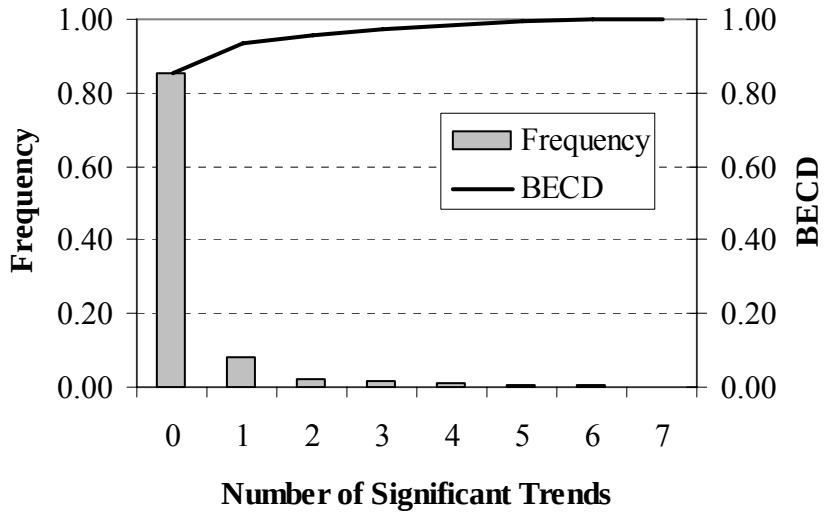

A.2. (Continued)

5. a. Mann-Kendall Trend Test for Maximum Seasonal Dec-Mar Flow (1950-2005)

Gage	Original		Slope	Serial Correlation			Re-trended		Trend/No-
Number	MK test	P-Value		Lag-1	P-Value	S/NS*	MK test	P-value	Trend **
08167500	2.036	0.042	111.324	-0.090	0.491	S	0.544	0.586	trend
08169000	2.106	0.035	2.722	-0.040	0.759	S	1.764	0.078	trend
08167000	2.106	0.035	5.958	-0.076	0.557	S	1.837	0.066	trend
08171000	1.590	0.112	4.053	-0.123	0.343	S	1.198	0.231	no-trend
08172000	0.820	0.412	4.500	0.007	0.955	NS	0.704	0.481	no-trend
08176500	1.619	0.106	58.378	-0.044	0.733	S	1.401	0.161	no-trend
08168500	1.442	0.149	7.616	-0.093	0.476	S	1.387	0.166	no-trend

* - Compare to 5% level of significance

** - Based on re-trended p-value if serial correlation is positive and significant (S) otherwise based on original p-value
- Compare to 10% level of significance

b. Bootstrap Empirical Cumulative Distribution

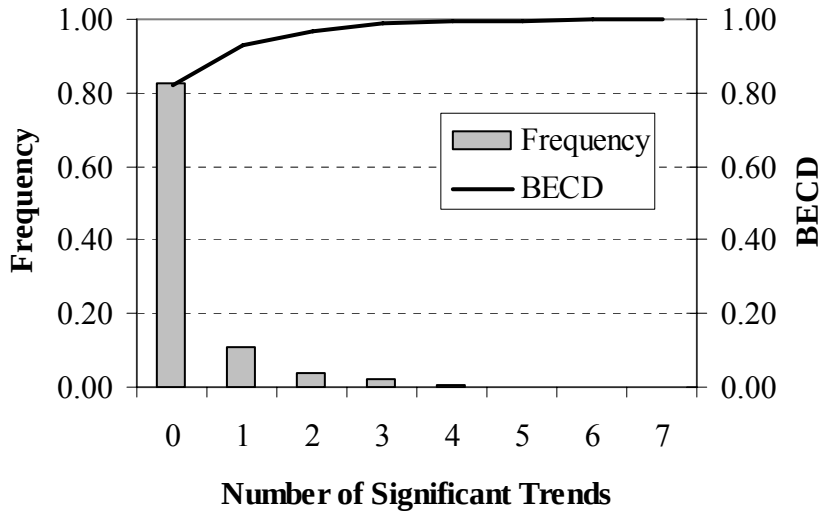

A.2. (Continued)

6. a. Mann-Kendall Trend Test for Mean Seasonal Dec-Mar Flow (1950-2005)

Gage	Original		Slope	Serial Correlation			Re-trended		Trend/No-
Number	MK test	P-Value		Lag-1	P-Value	S/NS*	MK test	P-value	Trend **
08167500	3.520	0.000	6.875	-0.090	0.489	S	3.143	0.002	trend
08169000	3.223	0.001	3.384	0.490	0.000	S	3.782	0.000	trend
08167000	4.014	0.000	4.616	-0.103	0.429	S	3.579	0.000	trend
08171000	2.375	0.018	2.052	-0.086	0.511	S	2.040	0.041	trend
08172000	2.474	0.013	5.392	-0.029	0.825	S	2.287	0.022	trend
08176500	2.884	0.004	29.141	-0.045	0.731	S	2.635	0.008	trend
08168500	3.520	0.000	10.292	-0.104	0.423	S	3.100	0.002	trend

* - Compare to 5% level of significance

** - Based on re-trended p-value if serial correlation is positive and significant (S) otherwise based on original p-value
- Compare to 10% level of significance

b. Bootstrap Empirical Cumulative Distribution

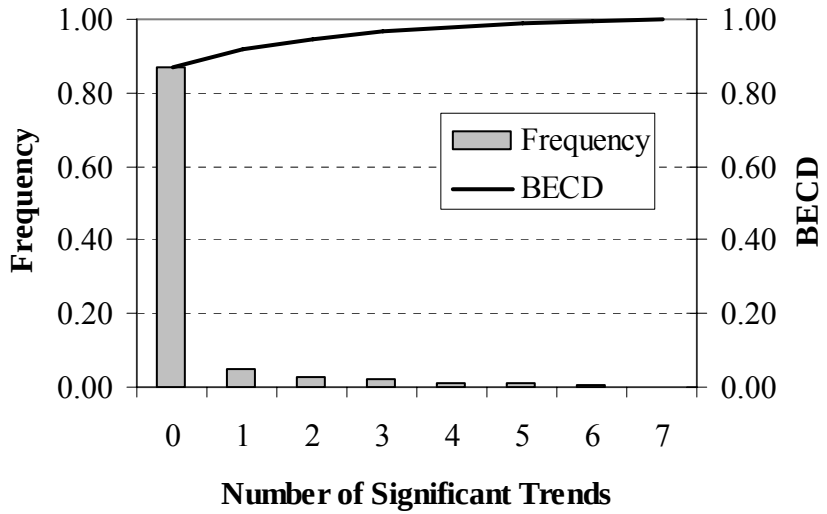

A.2. (Continued)

7. a. Mann-Kendall Trend Test for Minimum Seasonal Apr-Jul Flow (1950-2005)

Gage	Original		Slope	Serial Correlation			Re-trended		Trend/No-
Number	MK test	P-Value		Lag-1	P-Value	S/NS*	MK test	P-value	Trend **
08167500	3.400	0.001	2.154	-0.174	0.182	S	3.405	0.001	trend
08169000	2.213	0.027	2.080	0.363	0.005	S	2.838	0.005	trend
08167000	3.628	0.000	1.338	-0.160	0.218	S	3.724	0.000	trend
08171000	3.090	0.002	0.654	-0.050	0.701	S	3.027	0.002	trend
08172000	2.241	0.025	1.333	0.078	0.548	S	1.924	0.054	no-trend
08176500	2.650	0.008	9.750	0.021	0.874	S	2.650	0.008	trend
08168500	3.527	0.000	3.211	-0.215	0.098	S	3.201	0.001	trend

* - Compare to 5% level of significance

** - Based on re-trended p-value if serial correlation is positive and significant (S) otherwise based on original p-value
- Compare to 10% level of significance

b. Bootstrap Empirical Cumulative Distribution

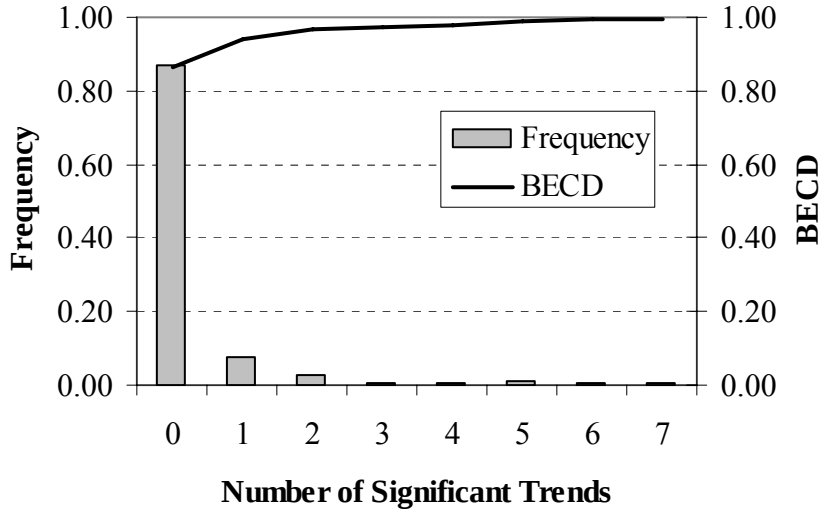

A.2. (Continued)

8. Mann-Kendall Trend Test for Maximum Seasonal Apr-Jul Flow (1950-2005)

Gage	Original		Slope	Serial Correlation			Re-trended		Trend/No-
Number	MK test	P-Value		Lag-1	P-Value	S/NS*	MK test	P-value	Trend **
08167500	0.799	0.424	15.533	-0.156	0.232	S	1.750	0.080	no-trend
08169000	1.308	0.191	4.833	-0.060	0.643	S	1.488	0.137	no-trend
08167000	0.975	0.329	7.083	-0.066	0.664	S	1.793	0.073	no-trend
08171000	0.608	0.543	3.956	-0.139	0.286	S	1.154	0.248	no-trend
08172000	-1.166	0.244	-28.472	-0.214	0.101	S	-0.719	0.472	no-trend
08176500	-0.360	0.718	-22.500	0.182	0.203	S	-0.138	0.890	no-trend
08168500	-0.064	0.949	-0.701	-0.098	0.590	S	-0.515	0.606	no-trend

* - Compare to 5% level of significance

** - Based on re-trended p-value if serial correlation is positive and significant (S) otherwise based on original p-value
- Compare to 10% level of significance

A.2. (Continued)

9. a. Mann-Kendall Trend Test for Mean Seasonal Apr-Jul Flow (1950-2005)

Gage	Original		Slope	Serial Correlation			Re-trended		Trend/No-
Number	MK test	P-Value		Lag-1	P-Value	S/NS*	MK test	P-value	Trend **
08167500	2.672	0.008	8.149	-0.216	0.096	S	2.940	0.003	trend
08169000	2.558	0.011	3.365	0.353	0.007	S	2.868	0.004	trend
08167000	2.982	0.003	4.581	-0.186	0.153	S	3.593	0.000	trend
08171000	1.979	0.048	2.386	-0.193	0.138	S	1.967	0.049	trend
08172000	1.555	0.120	5.036	-0.147	0.258	S	1.401	0.161	no-trend
08176500	1.668	0.095	24.393	-0.095	0.465	S	1.387	0.166	no-trend
08168500	2.742	0.006	10.225	-0.191	0.143	S	2.897	0.004	trend

** - Compare to 5% level of significance

** - Based on re-trended p-value if serial correlation is positive and significant (S) otherwise based on original p-value
- Compare to 10% level of significance

b. Bootstrap Empirical Cumulative Distribution

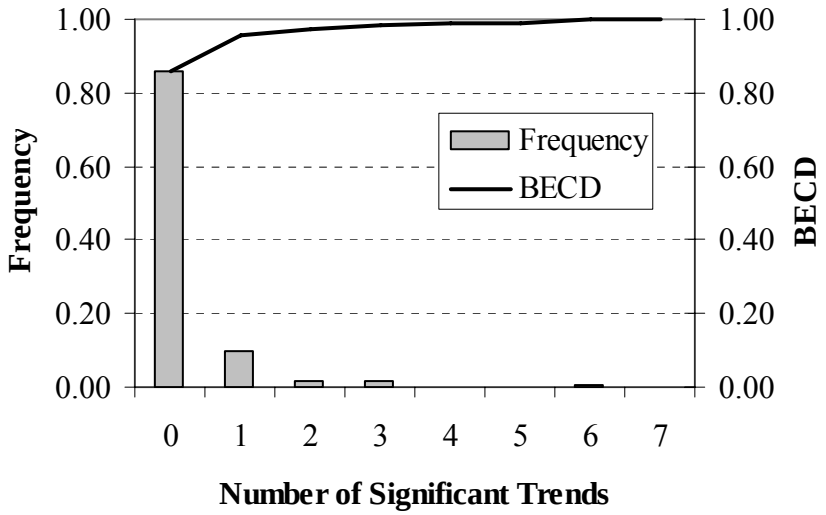

A.2. (Continued)

10. a. Mann-Kendall Trend Test for Minimum Seasonal Aug-Nov Flow (1950-2005)

Gage	Original		Slope	Serial Correlation			Re-trended		Trend/No-
Number	MK test	P-Value		Lag-1	P-Value	S/NS*	MK test	P-value	Trend **
08167500	3.784	0.000	1.786	0.046	0.725	S	3.884	0.000	trend
08169000	2.637	0.008	2.407	0.412	0.002	S	2.984	0.003	trend
08167000	4.214	0.000	1.347	0.033	0.803	S	4.276	0.000	trend
08171000	2.849	0.004	0.455	0.206	0.113	S	2.635	0.008	trend
08172000	2.714	0.007	1.436	0.105	0.419	S	2.359	0.018	trend
08176500	2.240	0.025	7.700	0.265	0.042	S	2.345	0.019	trend
08168500	4.092	0.000	2.438	0.122	0.350	S	3.927	0.000	trend

* - Compare to 5% level of significance

** - Based on re-trended p-value if serial correlation is positive and significant (S) otherwise based on original p-value
- Compare to 10% level of significance

b. Bootstrap Empirical Cumulative Distribution

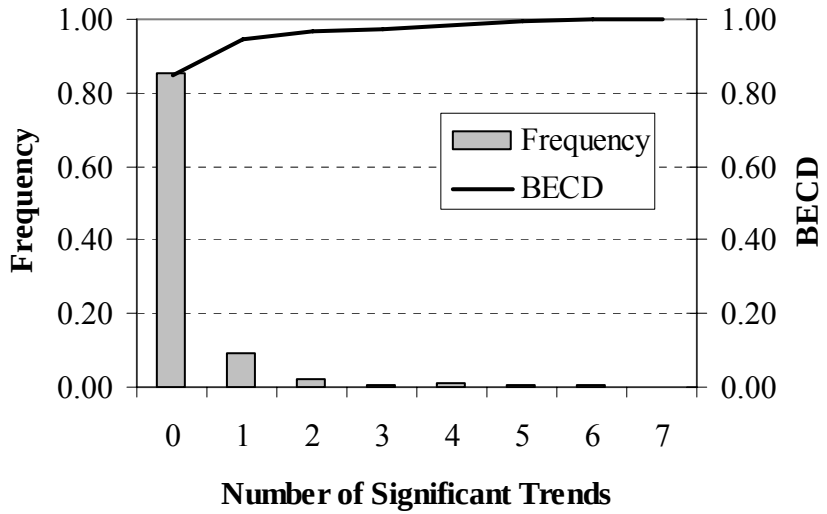

A.2. (Continued)

11. Mann-Kendall Trend Test for Maximum Seasonal Aug-Nov Flow (1950-2005)

Gage	Original		Slope	Serial Correlation			Re-trended		Trend/No-
Number	MK test	P-Value		Lag-1	P-Value	S/NS*	MK test	P-value	Trend **
08167500	1.654	0.098	25.360	-0.164	0.208	S	1.198	0.231	no-trend
08169000	1.159	0.246	2.563	-0.076	0.558	S	0.661	0.509	no-trend
08167000	0.728	0.467	3.182	-0.103	0.431	S	0.544	0.586	no-trend
08171000	0.565	0.572	0.429	-0.047	0.718	S	0.733	0.463	no-trend
08172000	0.212	0.832	-1.405	-0.066	0.611	S	0.733	0.463	no-trend
08176500	1.110	0.267	44.923	-0.071	0.586	S	1.604	0.109	no-trend
08168500	0.799	0.424	5.178	0.053	0.683	S	0.356	0.722	no-trend

* - Compare to 5% level of significance

** - Based on re-trended p-value if serial correlation is positive and significant (S) otherwise based on original p-value
- Compare to 10% level of significance

A.2. (Continued)

12. a. Mann-Kendall Trend Test for Mean Seasonal Aug-Nov Flow (1950-2005)

Gage	Original		Slope	Serial Correlation			Re-trended		Trend/No-
Number	MK test	P-Value		Lag-1	P-Value	S/NS*	MK test	P-value	Trend **
08167500	2.035	0.042	4.168	-0.081	0.533	S	1.880	0.060	trend
08169000	2.898	0.004	3.382	0.400	0.002	S	2.955	0.003	trend
08167000	2.785	0.005	3.526	-0.054	0.676	S	2.417	0.016	trend
08171000	1.343	0.179	0.684	-0.040	0.761	S	1.241	0.214	no-trend
08172000	1.428	0.153	1.941	-0.036	0.784	S	1.416	0.157	no-trend
08176500	1.739	0.082	16.065	-0.067	0.605	S	1.750	0.080	no-trend
08168500	1.866	0.062	5.181	0.021	0.871	S	1.648	0.099	no-trend

* - Compare to 5% level of significance

** - Based on re-trended p-value if serial correlation is positive and significant (S) otherwise based on original p-value
- Compare to 10% level of significance

b. Bootstrap Empirical Cumulative Distribution

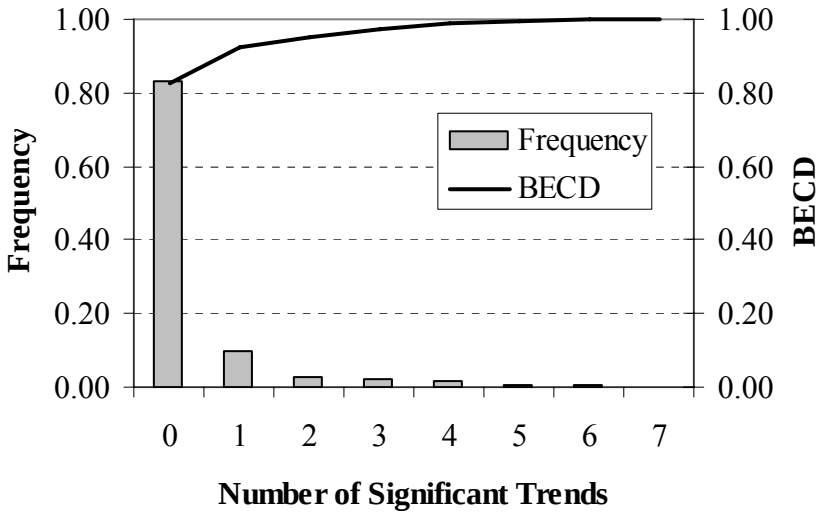

A.3. Period 1970-2005

1. Mann-Kendall Trend Test for Minimum Annual Flow (1970-2005)

Gage	Original		Slope	Serial Correlation			Re-trended		Trend/No-
Number	MK test	P-Value		Lag-1	P-Value	S/NS*	MK test	P-value	Trend **
08165300	1.451	0.147	0.100	0.066	0.681	S	1.207	0.227	no-trend
08165500	1.241	0.215	0.208	0.032	0.843	S	1.179	0.239	no-trend
08167000	-0.477	0.633	-0.254	0.006	0.968	NS	-0.725	0.469	no-trend
08167500	-0.859	0.391	-0.712	0.091	0.570	S	-1.082	0.279	no-trend
08168500	0.422	0.673	0.683	0.194	0.225	S	0.270	0.787	no-trend
08169000	-0.327	0.744	-0.341	0.489	0.002	S	0.128	0.898	no-trend
08171000	-0.123	0.902	-0.003	0.374	0.019	S	0.156	0.876	no-trend
08171300	-0.761	0.447	0.000	0.290	0.070	S	0.285	0.776	no-trend
08172000	0.000	1.000	0.000	0.366	0.022	S	0.525	0.599	no-trend
08172400	1.685	0.092	0.000	-0.001	0.996	NS	1.683	0.092	no-trend
08175000	-0.941	0.347	-0.019	-0.028	0.859	S	-1.463	0.144	no-trend
08175800	-1.008	0.313	-4.208	0.392	0.014	S	-0.696	0.487	no-trend
08176500	-1.117	0.264	-5.651	0.445	0.005	S	-0.753	0.452	no-trend

* - Compare to 5% level of significance

** - Based on re-trended p-value if serial correlation is positive and significant (S) otherwise based on original p-value
- Compare to 10% level of significance

A.3. (Continued)

2. Mann-Kendall Trend Test for Maximum Annual Flow (1970-2005)

Gage	Original		Slope	Serial Correlation			Re-trended		Trend/No-
Number	MK test	P-Value		Lag-1	P-Value	S/NS*	MK test	P-value	Trend **
08165300	-0.531	0.595	-7.200	0.293	0.067	S	-0.724	0.469	no-trend
08165500	-0.191	0.849	-2.800	0.272	0.090	S	-0.497	0.619	no-trend
08167000	-0.272	0.785	-25.655	-0.006	0.970	NS	-0.241	0.809	no-trend
08167500	-0.341	0.733	-83.927	-0.139	0.384	S	0.104	0.917	no-trend
08168500	0.450	0.653	14.722	-0.032	0.842	S	0.497	0.619	no-trend
08169000	0.313	0.754	3.295	-0.103	0.519	S	0.753	0.452	no-trend
08171000	1.062	0.288	60.000	-0.236	0.140	S	1.775	0.076	no-trend
08171300	0.545	0.586	36.796	-0.254	0.112	S	1.434	0.151	no-trend
08172000	0.381	0.703	41.667	-0.215	0.180	S	0.753	0.452	no-trend
08172400	0.422	0.673	7.217	-0.120	0.452	S	0.809	0.418	no-trend
08175000	0.136	0.892	6.125	-0.130	0.417	S	0.156	0.876	no-trend
08175800	0.736	0.462	185.191	-0.149	0.350	S	0.951	0.341	no-trend
08176500	1.022	0.307	246.667	-0.148	0.355	S	1.292	0.196	no-trend

* - Compare to 5% level of significance

** - Based on re-trended p-value if serial correlation is positive and significant (S) otherwise based on original p-value
- Compare to 10% level of significance

A.3. (Continued)

3. Mann-Kendall Trend Test for Mean Annual Flow (1970-2005)

Gage	Original		Slope	Serial Correlation			Re-trended		Trend/No-
Number	MK test	P-Value		Lag-1	P-Value	S/NS*	MK test	P-value	Trend **
08165300	-0.354	0.723	-0.074	0.113	0.479	S	-0.327	0.744	no-trend
08165500	0.027	0.978	0.013	0.096	0.548	S	-0.099	0.921	no-trend
08167000	0.163	0.870	0.587	-0.023	0.886	S	0.241	0.809	no-trend
08167500	0.245	0.806	0.772	-0.105	0.511	S	0.193	0.847	no-trend
08168500	0.518	0.605	3.052	-0.070	0.661	S	0.469	0.639	no-trend
08169000	0.327	0.744	0.585	0.438	0.006	S	0.298	0.766	no-trend
08171000	0.899	0.369	2.192	-0.125	0.436	S	0.866	0.386	no-trend
08171300	0.654	0.513	1.547	-0.135	0.399	S	0.781	0.435	no-trend
08172000	0.708	0.479	4.114	-0.057	0.723	S	0.866	0.386	no-trend
08172400	0.327	0.744	0.078	-0.033	0.839	S	0.554	0.580	no-trend
08175000	0.327	0.744	0.591	-0.064	0.688	S	0.213	0.831	no-trend
08175800	0.681	0.496	15.316	-0.098	0.539	S	0.639	0.523	no-trend
08176500	0.817	0.414	14.255	-0.072	0.655	S	0.667	0.504	no-trend

* - Compare to 5% level of significance

** - Based on re-trended p-value if serial correlation is positive and significant (S) otherwise based on original p-value
- Compare to 10% level of significance

A.3. (Continued)

4. Mann-Kendall Trend Test for Minimum Seasonal Dec-Mar Flow (1970-2005)

Gage	Original		Slope	Serial Correlation			Re-trended		Trend/No-
Number	MK test	P-Value		Lag-1	P-Value	S/NS*	MK test	P-value	Trend **
08165300	1.395	0.163	0.150	-0.011	0.947	S	1.747	0.081	no-trend
08165500	1.529	0.126	0.298	0.005	0.976	NS	1.908	0.056	no-trend
08167000	0.777	0.437	0.801	-0.203	0.204	S	1.349	0.177	no-trend
08167500	0.381	0.703	0.639	-0.095	0.553	S	0.311	0.756	no-trend
08168500	0.872	0.383	1.571	-0.206	0.197	S	0.866	0.386	no-trend
08169000	0.859	0.391	1.031	0.493	0.002	S	1.122	0.262	no-trend
08171000	0.273	0.785	0.220	0.094	0.556	S	0.469	0.639	no-trend
08171300	0.109	0.913	0.068	-0.026	0.870	S	0.355	0.723	no-trend
08172000	0.436	0.663	0.517	0.084	0.598	S	0.412	0.680	no-trend
08172400	0.886	0.376	0.000	0.026	0.873	S	1.044	0.297	no-trend
08175000	0.123	0.902	0.003	0.132	0.408	S	0.099	0.921	no-trend
08175800	0.082	0.935	0.646	0.043	0.789	S	0.270	0.787	no-trend
08176500	0.354	0.723	2.283	0.088	0.581	S	0.753	0.452	no-trend

* - Compare to 5% level of significance

** - Based on re-trended p-value if serial correlation is positive and significant (S) otherwise based on original p-value
- Compare to 10% level of significance

A.3. (Continued)

5. Mann-Kendall Trend Test for Maximum Seasonal Dec-Mar Flow (1970-2005)

Gage	Original		Slope	Serial Correlation			Re-trended		Trend/No-
Number	MK test	P-Value		Lag-1	P-Value	S/NS*	MK test	P-value	Trend **
08165300	1.431	0.152	0.396	-0.053	0.741	S	1.633	0.102	no-trend
08165500	1.390	0.164	1.060	-0.077	0.632	S	1.321	0.187	no-trend
08167000	1.362	0.173	9.046	-0.087	0.587	S	1.605	0.109	no-trend
08167500	1.335	0.182	18.389	-0.080	0.617	S	1.053	0.293	no-trend
08168500	1.444	0.149	18.996	-0.126	0.432	S	1.548	0.122	no-trend
08169000	0.844	0.398	2.096	0.018	0.909	S	0.809	0.418	no-trend
08171000	1.090	0.276	7.216	-0.106	0.509	S	1.236	0.217	no-trend
08171300	0.926	0.354	4.503	-0.095	0.551	S	1.094	0.274	no-trend
08172000	0.844	0.398	16.277	0.046	0.772	S	1.037	0.300	no-trend
08172400	0.000	1.000	0.000	-0.039	0.808	S	0.327	0.744	no-trend
08175000	1.253	0.210	10.714	-0.142	0.376	S	0.667	0.504	no-trend
08175800	0.981	0.327	48.362	-0.017	0.914	S	0.809	0.418	no-trend
08176500	0.776	0.437	55.811	-0.001	0.996	NS	0.767	0.443	no-trend

* - Compare to 5% level of significance

** - Based on re-trended p-value if serial correlation is positive and significant (S) otherwise based on original p-value

- Compare to 10% level of significance

A.3. (Continued)

6. Mann-Kendall Trend Test for Mean Seasonal Dec-Mar Flow (1970-2005)

Gage	Original		Slope	Serial Correlation			Re-trended		Trend/No-
Number	MK test	P-Value		Lag-1	P-Value	S/NS*	MK test	P-value	Trend **
08165300	1.226	0.220	0.227	-0.108	0.501	S	1.520	0.129	no-trend
08165500	1.498	0.134	0.570	-101.000	0.526	S	0.014	0.989	no-trend
08167000	1.171	0.241	2.783	-0.112	0.483	S	1.292	0.196	no-trend
08167500	0.736	0.462	4.163	-0.094	0.555	S	0.430	0.667	no-trend
08168500	1.144	0.253	6.020	-0.129	0.418	S	1.037	0.300	no-trend
08169000	0.599	0.549	0.992	0.436	0.006	S	0.696	0.487	no-trend
08171000	0.627	0.531	1.719	-0.079	0.620	S	0.781	0.435	no-trend
08171300	0.572	0.567	1.261	-0.077	0.632	S	0.866	0.386	no-trend
08172000	1.008	0.313	5.985	-0.023	0.886	S	1.122	0.262	no-trend
08172400	0.436	0.663	0.204	-0.026	0.873	S	0.809	0.418	no-trend
08175000	1.444	0.149	1.255	-0.122	0.447	S	1.520	0.129	no-trend
08175800	1.335	0.182	27.200	-0.065	0.683	S	1.236	0.217	no-trend
08176500	1.199	0.231	25.830	-0.052	0.745	S	1.207	0.227	no-trend

* - Compare to 5% level of significance

** - Based on re-trended p-value if serial correlation is positive and significant (S) otherwise based on original p-value
- Compare to 10% level of significance

A.3. (Continued)

7. Mann-Kendall Trend Test for Minimum Seasonal Apr-Jul Flow (1970-2005)

Gage	Original		Slope	Serial Correlation			Re-trended		Trend/No-
Number	MK test	P-Value		Lag-1	P-Value	S/NS*	MK test	P-value	Trend **
08165300	1.951	0.051	0.207	-0.273	0.088	S	1.804	0.071	no-trend
08165500	1.432	0.152	0.300	-0.184	0.250	S	1.434	0.151	no-trend
08167000	-0.027	0.978	0.000	-0.250	0.117	S	-0.014	0.989	no-trend
08167500	0.054	0.957	0.086	-0.244	0.128	S	-0.430	0.667	no-trend
08168500	-0.245	0.806	-0.874	-0.408	0.011	S	-0.611	0.541	no-trend
08169000	0.109	0.913	0.183	0.293	0.067	S	0.327	0.744	no-trend
08171000	0.095	0.924	0.016	-0.196	0.220	S	0.270	0.787	no-trend
08171300	-0.642	0.521	-0.226	-0.115	0.471	S	-0.667	0.504	no-trend
08172000	-0.204	0.838	-0.373	-0.022	0.891	S	0.241	0.809	no-trend
08172400	-0.038	0.970	0.000	0.076	0.633	S	-0.493	0.622	no-trend
08175000	-0.232	0.817	-0.004	-0.060	0.706	S	-0.298	0.766	no-trend
08175800	-0.463	0.643	-3.900	-0.141	0.379	S	-0.525	0.599	no-trend
08176500	-0.981	0.327	-5.540	0.148	0.355	S	-0.952	0.341	no-trend

* - Compare to 5% level of significance

** - Based on re-trended p-value if serial correlation is positive and significant (S) otherwise based on original p-value

- Compare to 10% level of significance

A.3. (Continued)

8. Mann-Kendall Trend Test for Maximum Seasonal Apr-Jul Flow (1970-2005)

Gage	Original		Slope	Serial Correlation			Re-trended		Trend/No-
Number	MK test	P-Value		Lag-1	P-Value	S/NS*	MK test	P-value	Trend **
08165300	0.21807	0.82738	0.0955	-0.18	0.259	S	-0.0142	0.98867	no-trend
08165500	0.04087	0.9674	0.0313	-0.091	0.569	S	0.12781	0.8983	no-trend
08167000	-0.3406	0.73344	-7.1667	-0.194	0.225	S	0.18462	0.85353	no-trend
08167500	-0.8037	0.42157	-44.857	-0.241	0.132	S	-0.6968	0.48596	no-trend
08168500	-0.0681	0.9457	-2.1	-0.064	0.687	S	-0.071	0.94339	no-trend
08169000	-1.2124	0.22537	-15.214	-0.094	0.559	S	-0.8947	0.37095	no-trend
08171000	-0.6538	0.51324	-21.944	-0.23	0.151	S	0.21302	0.83131	no-trend
08171300	-0.9535	0.34036	-30.031	-0.191	0.233	S	-0.4118	0.68046	no-trend
08172000	-1.7707	0.07661	-96.875	-0.331	0.038	S	-1.4628	0.14354	no-trend
08172400	-1.5255	0.12712	-31.429	0.075	0.638	S	-1.3207	0.18659	no-trend
08175000	-1.2669	0.20521	-20.967	0.225	0.159	S	-0.9515	0.34135	no-trend
08175800	-1.2259	0.22024	-211.25	-0.223	0.163	S	-1.5196	0.12862	no-trend
08176500	0.04087	0.9674	4.9708	-0.081	0.612	S	1.06511	0.28683	no-trend

* - Compare to 5% level of significance

** - Based on re-trended p-value if serial correlation is positive and significant (S) otherwise based on original p-value

- Compare to 10% level of significance

A.3. (Continued)

9. Mann-Kendall Trend Test for Mean Seasonal Apr-Jul Flow (1970-2005)

Gage	Original		Slope	Serial Correlation			Re-trended		Trend/No-
Number	MK test	P-Value		Lag-1	P-Value	S/NS*	MK test	P-value	Trend **
08165300	0.926	0.354	0.223	-0.232	0.146	S	0.525	0.599	no-trend
08165500	0.708	0.479	0.527	-0.164	0.306	S	0.611	0.541	no-trend
08167000	0.300	0.764	0.710	-0.245	0.126	S	0.611	0.541	no-trend
08167500	0.027	0.978	0.131	-0.284	0.076	S	-0.193	0.847	no-trend
08168500	-0.054	0.957	-0.602	-0.286	0.074	S	-0.043	0.966	no-trend
08169000	-0.327	0.744	-0.694	0.302	0.059	S	-0.128	0.898	no-trend
08171000	-0.054	0.957	-0.205	-0.288	0.072	S	-0.014	0.989	no-trend
08171300	-0.136	0.892	-0.519	-0.305	0.056	S	-0.412	0.680	no-trend
08172000	-0.245	0.806	-2.140	-0.258	0.107	S	-0.327	0.744	no-trend
08172400	-1.008	0.313	-1.491	-0.001	0.994	NS	-0.753	0.452	no-trend
08175000	-0.953	0.340	-1.138	0.121	0.450	S	-0.838	0.402	no-trend
08175800	-0.599	0.549	-17.998	-0.199	0.214	S	-0.554	0.580	no-trend
08176500	0.082	0.935	1.098	-0.093	0.563	S	0.128	0.898	no-trend

* - Compare to 5% level of significance

** - Based on re-trended p-value if serial correlation is positive and significant (S) otherwise based on original p-value

- Compare to 10% level of significance

A.3. (Continued)

10. Mann-Kendall Trend Test for Minimum Seasonal Aug-Nov Flow (1970-2005)

Gage	Original		Slope	Serial Correlation			Re-trended		Trend/No-
Number	MK test	P-Value		Lag-1	P-Value	S/NS*	MK test	P-value	Trend **
08165300	0.178	0.859	0.000	-0.111	0.487	S	-0.014	0.989	no-trend
08165500	0.423	0.672	0.063	-0.080	0.616	S	0.270	0.787	no-trend
08167000	-0.164	0.870	-0.125	-0.131	0.481	S	-0.241	0.809	no-trend
08167500	-0.082	0.935	-0.033	-0.025	0.876	S	-0.667	0.505	no-trend
08168500	0.954	0.340	0.883	0.166	0.300	S	0.753	0.452	no-trend
08169000	0.082	0.935	0.118	0.333	0.038	S	0.043	0.966	no-trend
08171000	0.232	0.817	0.083	0.105	0.511	S	0.185	0.854	no-trend
08171300	-0.575	0.565	-0.100	-0.076	0.634	S	-0.525	0.599	no-trend
08172000	0.123	0.902	0.155	0.039	0.809	S	0.213	0.831	no-trend
08172400	1.588	0.112	0.000	-0.029	0.854	S	2.308	0.021	no-trend
08175000	-1.622	0.105	-0.029	-0.074	0.645	S	-2.286	0.022	no-trend
08175800	-1.185	0.236	-4.241	0.196	0.220	S	-0.923	0.356	no-trend
08176500	-0.341	0.733	-3.074	-0.107	0.503	S	-0.241	0.809	no-trend

* - Compare to 5% level of significance

** - Based on re-trended p-value if serial correlation is positive and significant (S) otherwise based on original p-value
- Compare to 10% level of significance

A.3. (Continued)

11. Mann-Kendall Trend Test for Maximum Seasonal Aug-Nov Flow (1970-2005)

Gage	Original		Slope	Serial Correlation			Re-trended		Trend/No-
Number	MK test	P-Value		Lag-1	P-Value	S/NS*	MK test	P-value	Trend **
08165300	0.055	0.957	0.023	0.020	0.901	S	-0.241	0.809	no-trend
08165500	-0.095	0.924	-0.462	-0.028	0.859	S	-0.639	0.523	no-trend
08167000	0.082	0.935	1.701	-0.139	0.385	S	-0.696	0.487	no-trend
08167500	0.790	0.430	27.898	-0.183	0.253	S	0.637	0.524	no-trend
08168500	-0.245	0.806	-6.167	0.126	0.430	S	-0.355	0.723	no-trend
08169000	0.191	0.849	1.317	-0.071	0.655	S	0.497	0.619	no-trend
08171000	0.000	1.000	0.013	-0.068	0.670	S	0.753	0.452	no-trend
08171300	-0.627	0.531	-4.771	-0.063	0.694	S	0.099	0.921	no-trend
08172000	0.000	1.000	0.643	-0.087	0.588	S	1.037	0.300	no-trend
08172400	0.192	0.848	0.000	-0.087	0.588	S	0.809	0.418	no-trend
08175000	0.395	0.693	3.304	-0.049	0.761	S	0.270	0.787	no-trend
08175800	0.123	0.902	12.765	-0.086	0.592	S	1.236	0.217	no-trend
08176500	-1.335	0.182	-205.794	-0.234	0.144	S	-1.406	0.160	no-trend

* - Compare to 5% level of significance

** - Based on re-trended p-value if serial correlation is positive and significant (S) otherwise based on original p-value
- Compare to 10% level of significance

A.3. (Continued)

12. Mann-Kendall Trend Test for Mean Seasonal Aug-Nov Flow (1970-2005)

Gage	Original		Slope	Serial Correlation			Re-trended		Trend/No-
Number	MK test	P-Value		Lag-1	P-Value	S/NS*	MK test	P-value	Trend **
08165300	-0.245	0.806	-0.123	-0.035	0.826	S	-0.866	0.386	no-trend
08165500	0.027	0.978	0.020	-0.023	0.866	S	-0.497	0.619	no-trend
08167000	0.082	0.935	0.266	-0.164	0.305	S	-0.639	0.523	no-trend
08167500	-0.272	0.785	-1.311	-0.172	0.282	S	-0.252	0.801	no-trend
08168500	-0.272	0.785	-1.953	0.197	0.217	S	-0.582	0.560	no-trend
08169000	0.300	0.764	0.567	0.330	0.039	S	0.128	0.898	no-trend
08171000	0.381	0.703	0.459	-0.080	0.618	S	0.781	0.435	no-trend
08171300	-0.082	0.935	-0.114	-0.090	0.575	S	0.582	0.560	no-trend
08172000	0.272	0.785	0.774	-0.078	0.624	S	0.809	0.418	no-trend
08172400	0.384	0.701	0.000	-0.068	0.669	S	0.923	0.356	no-trend
08175000	0.136	0.892	0.146	-0.086	0.592	S	0.298	0.766	no-trend
08175800	0.027	0.978	0.079	-0.096	0.549	S	0.071	0.943	no-trend
08176500	-0.463	0.643	-20.938	-0.196	0.221	S	-0.582	0.560	no-trend

* - Compare to 5% level of significance

** - Based on re-trended p-value if serial correlation is positive and significant (S) otherwise based on original p-value

- Compare to 10% level of significance

APPENDIX B

TREND ANALYSIS ON METEOROLOGIC VARIABLES

1.a. Mann-Kendall Trend Test for Maximum Annual Precipitation (1950-2005)

Station Name	Original MK test	Original P-Value	Slope	Serial Correlation Lag-1	Serial Correlation P-Value	S/NS*	Re-trended MK test	Re-trended P-value	Trend/No-Trend **
Mason	0.530	0.596	0.005	-0.190	0.143	S	0.530	0.596	no-trend
Hondo	0.756	0.450	0.008	0.099	0.447	S	0.756	0.450	no-trend
Beeville	2.474	0.013	0.025	-0.119	0.362	S	2.474	0.013	trend
San Antonio	0.912	0.362	0.011	-0.062	0.631	S	0.912	0.362	no-trend
Austin	1.039	0.299	0.013	-0.041	0.755	S	1.039	0.299	no-trend
Gonzales	0.488	0.626	0.004	-0.176	0.177	S	0.488	0.626	no-trend
Victoria	1.145	0.252	0.014	0.145	0.265	S	1.145	0.252	no-trend
Blanco	0.792	0.429	0.010	0.020	0.878	S	0.792	0.429	no-trend

* - Compare to 5% level of significance

** - Based on re-trended p-value if serial correlation is positive and significant (S) otherwise based on original p-value
- Compare to 10% level of significance

b. Bootstrap Empirical Cumulative Distribution

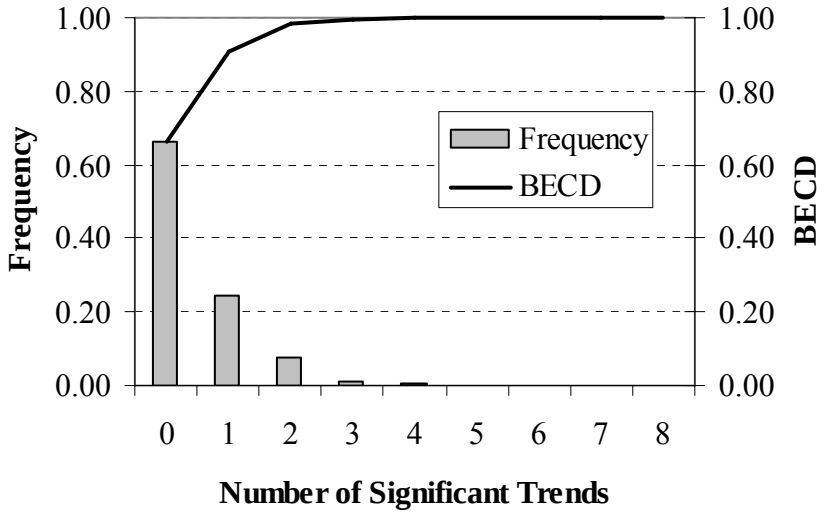

2. a. Mann-Kendall Trend Test for Mean Annual Precipitation (1950-2005)

Station Name	Original MK test	Original P-Value	Slope	Serial Correlation Lag-1	Serial Correlation P-Value	Serial Correlation S/NS*	Re-trended MK test	Re-trended P-value	Trend/No-Trend **
Mason	3.053	0.002	0.001	-0.182	0.163	S	3.053	0.002	trend
Hondo	1.329	0.184	0.000	0.165	0.204	S	1.329	0.184	no-trend
Beeville	2.841	0.004	0.001	0.027	0.835	S	2.841	0.004	trend
San Antonio	2.558	0.011	0.001	0.100	0.443	S	2.558	0.011	trend
Austin	1.887	0.059	0.000	-0.099	0.448	S	1.887	0.059	no-trend
Gonzales	1.597	0.110	0.000	-0.106	0.413	S	1.597	0.110	no-trend
Victoria	3.336	0.001	0.001	0.002	0.991	NS	3.336	0.001	trend
Blanco	0.777	0.437	0.000	-0.013	0.918	S	0.777	0.437	no-trend

* - Compare to 5% level of significance

** - Based on re-trended p-value if serial correlation is positive and significant (S) otherwise based on original p-value
- Compare to 10% level of significance

b. Bootstrap Empirical Cumulative Distribution

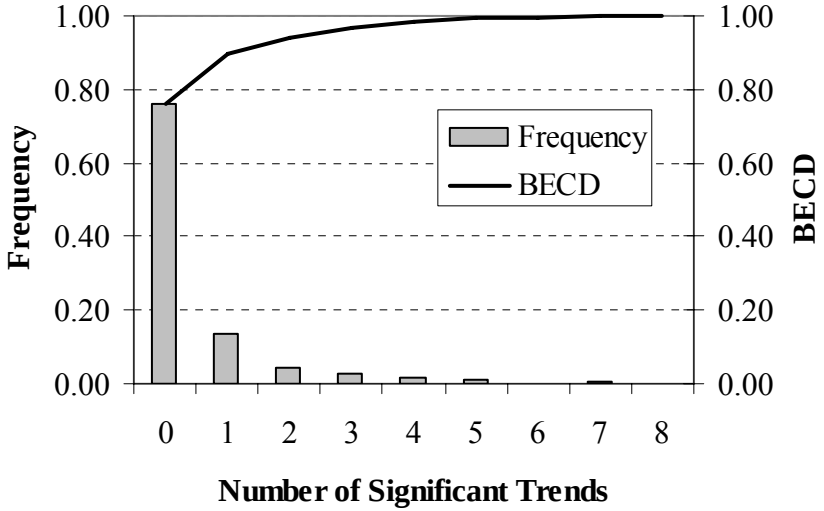

3. a. Mann-Kendall Trend Test for Maximum Seasonal Dec-Mar Precipitation (1950-2005)

Station Name	Original MK test	Original P-Value	Slope	Serial Correlation Lag-1	Serial Correlation P-Value	Serial Correlation S/NS*	Re-trended MK test	Re-trended P-value	Trend/No-Trend **
Mason	1.195	0.232	0.005	-0.001	0.994	NS	1.195	0.232	no-trend
Hondo	1.032	0.302	0.006	-0.009	0.944	S	1.032	0.302	no-trend
Beeville	1.682	0.093	0.011	0.181	0.164	S	1.682	0.093	no-trend
San Antonio	0.799	0.424	0.004	0.170	0.191	S	0.799	0.424	no-trend
Austin	0.071	0.944	0.000	0.068	0.602	S	0.071	0.944	no-trend
Gonzales	1.569	0.117	0.007	-0.056	0.667	S	1.569	0.117	no-trend
Victoria	2.036	0.042	0.013	-0.042	0.748	S	2.036	0.042	trend
Blanco	0.502	0.616	0.003	0.041	0.753	S	0.502	0.616	no-trend

* - Compare to 5% level of significance

** - Based on re-trended p-value if serial correlation is positive and significant (S) otherwise based on original p-value
- Compare to 10% level of significance

b. Bootstrap Empirical Cumulative Distribution

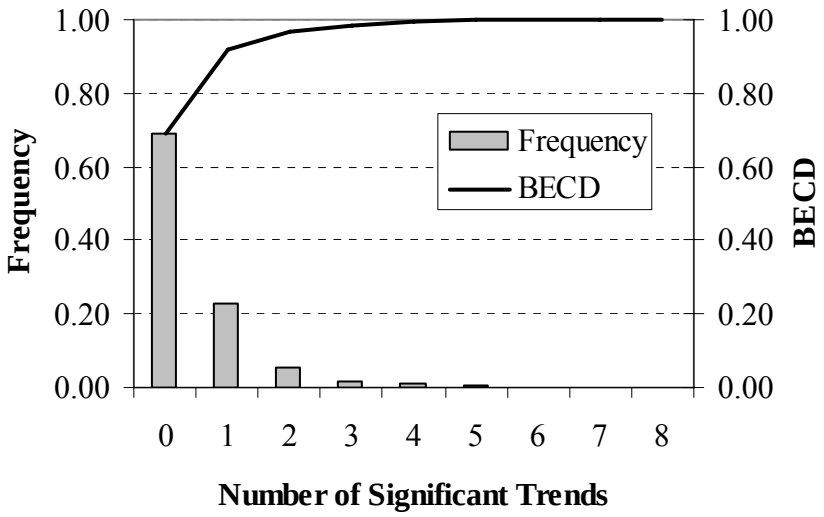

4. a. Mann-Kendall Trend Test for Mean Seasonal Dec-Mar Precipitation (1950-2005)

Station Name	Original		Slope	Serial Correlation			Re-trended		Trend/No-Trend **
	MK test	P-Value		Lag-1	P-Value	S/NS*	MK test	P-value	
Mason	2.558	0.011	0.001	-0.304	0.020	S	2.558	0.011	trend
Hondo	1.180	0.238	0.000	-0.235	0.071	S	1.180	0.238	no-trend
Beeville	2.134	0.033	0.000	0.057	0.664	S	2.134	0.033	trend
San Antonio	1.371	0.170	0.000	0.005	0.972	NS	1.371	0.170	no-trend
Austin	1.216	0.224	0.000	-0.002	0.985	NS	1.216	0.224	no-trend
Gonzales	1.611	0.107	0.000	-0.016	0.904	S	1.611	0.107	no-trend
Victoria	2.580	0.010	0.001	0.080	0.541	S	2.580	0.010	trend
Blanco	0.777	0.437	0.000	-0.066	0.615	S	0.777	0.437	no-trend

* - Compare to 5% level of significance

** - Based on re-trended p-value if serial correlation is positive and significant (S) otherwise based on original p-value
- Compare to 10% level of significance

b. Bootstrap Empirical Cumulative Distribution

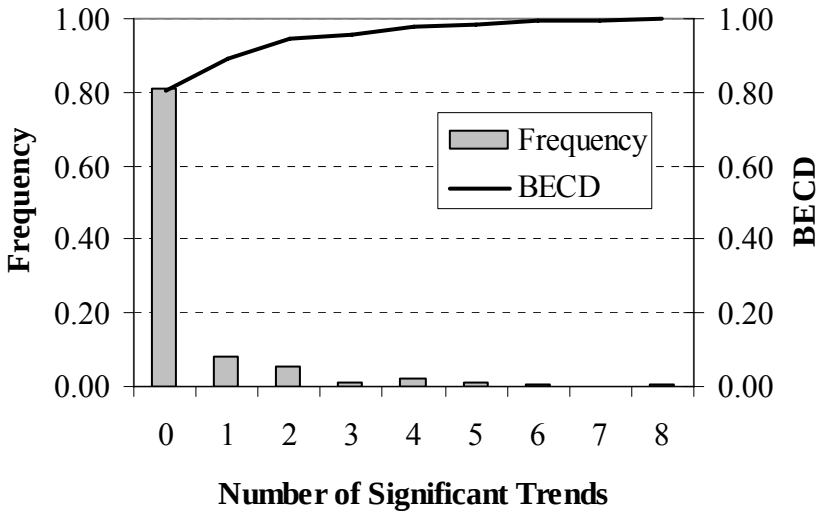

5. a. Mann-Kendall Trend Test for Maximum Seasonal Apr-Jul Precipitation (1950-2005)

Station Name	Original MK test	Original P-Value	Slope	Serial Correlation Lag-1	Serial Correlation P-Value	S/NS*	Re-trended MK test	Re-trended P-value	Trend/No-Trend **
Mason	-0.742	0.458	-0.004	-0.131	0.315	S	-0.742	0.458	no-trend
Hondo	1.513	0.130	0.012	-0.178	0.170	S	1.513	0.130	no-trend
Beeville	2.135	0.033	0.019	-0.150	0.250	S	2.135	0.033	trend
San Antonio	0.226	0.821	0.002	-0.049	0.706	S	0.226	0.821	no-trend
Austin	-0.184	0.854	-0.002	-0.113	0.386	S	-0.184	0.854	no-trend
Gonzales	0.254	0.799	0.002	-0.150	0.248	S	0.254	0.799	no-trend
Victoria	0.869	0.385	0.010	0.085	0.512	S	0.869	0.385	no-trend
Blanco	-0.346	0.729	-0.004	0.186	0.154	S	-0.346	0.729	no-trend

* - Compare to 5% level of significance

** - Based on re-trended p-value if serial correlation is positive and significant (S) otherwise based on original p-value
- Compare to 10% level of significance

b. Bootstrap Empirical Cumulative Distribution

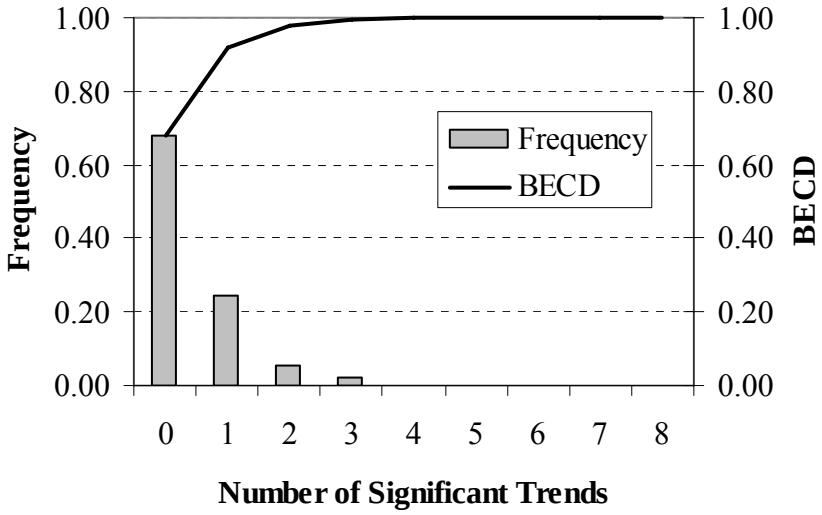

6. Mann-Kendall Trend Test for Mean Seasonal Apr-Jul Precipitation (1950-2005)

Station Name	Original MK test	Original P-Value	Slope	Serial Correlation Lag-1	Serial Correlation P-Value	Serial Correlation S/NS*	Re-trended MK test	Re-trended P-value	Trend/No-Trend **
Mason	1.520	0.129	0.000	-0.088	0.497	S	1.520	0.129	no-trend
Hondo	1.265	0.206	0.000	-0.105	0.419	S	1.265	0.206	no-trend
Beeville	1.470	0.142	0.001	-0.269	0.039	S	1.470	0.142	no-trend
San Antonio	1.555	0.120	0.001	0.025	0.851	S	1.555	0.120	no-trend
Austin	0.205	0.838	0.000	-0.274	0.035	S	0.205	0.838	no-trend
Gonzales	0.587	0.557	0.000	-0.160	0.219	S	0.587	0.557	no-trend
Victoria	1.922	0.055	0.001	-0.148	0.257	S	1.922	0.055	no-trend
Blanco	-0.205	0.838	0.000	-0.188	0.149	S	-0.205	0.838	no-trend

* - Compare to 5% level of significance

** - Based on re-trended p-value if serial correlation is positive and significant (S) otherwise based on original p-value
- Compare to 10% level of significance

7. Mann-Kendall Trend Test for Maximum Seasonal Aug-Nov Precipitation (1950-2005)

Station Name	Original MK test	Original P-Value	Slope	Serial Correlation Lag-1	Serial Correlation P-Value	Serial Correlation S/NS*	Re-trended MK test	Re-trended P-value	Trend/No-Trend **
Mason	1.258	0.208	0.010	-0.186	0.152	S	1.258	0.208	no-trend
Hondo	-0.233	0.816	-0.002	-0.079	0.543	S	-0.233	0.816	no-trend
Beeville	0.558	0.577	0.006	-0.040	0.761	S	0.558	0.577	no-trend
San Antonio	-0.523	0.601	-0.005	-0.021	0.874	S	-0.523	0.601	no-trend
Austin	0.269	0.788	0.004	0.004	0.973	NS	0.269	0.788	no-trend
Gonzales	-0.940	0.347	-0.008	-0.138	0.288	S	-0.940	0.347	no-trend
Victoria	-0.671	0.502	-0.009	-0.002	0.987	NS	-0.671	0.502	no-trend
Blanco	0.403	0.687	0.003	-0.013	0.919	S	0.403	0.687	no-trend

* - Compare to 5% level of significance

** - Based on re-trended p-value if serial correlation is positive and significant (S) otherwise based on original p-value
- Compare to 10% level of significance

8. a. Mann-Kendall Trend Test for Mean Seasonal Aug-Nov Precipitation (1950-2005)

Station Name	Original MK test	Original P-Value	Slope	Serial Correlation Lag-1	Serial Correlation P-Value	S/NS*	Re-trended MK test	Re-trended P-value	Trend/No-Trend **
Mason	2.106	0.035	0.001	-0.231	0.076	S	2.106	0.035	trend
Hondo	-0.177	0.860	0.000	0.116	0.373	S	-0.177	0.860	no-trend
Beeville	0.756	0.450	0.000	-0.133	0.305	S	0.756	0.450	no-trend
San Antonio	1.018	0.309	0.000	-0.037	0.774	S	1.018	0.309	no-trend
Austin	1.329	0.184	0.001	0.188	0.364	S	1.329	0.184	no-trend
Gonzales	0.481	0.631	0.000	-0.027	0.837	S	0.481	0.631	no-trend
Victoria	0.608	0.543	0.000	-0.001	0.993	NS	0.608	0.543	no-trend
Blanco	0.014	0.989	0.000	0.016	0.904	S	0.014	0.989	no-trend

* - Compare to 5% level of significance

** - Based on re-trended p-value if serial correlation is positive and significant (S) otherwise based on original p-value
- Compare to 10% level of significance

b. Bootstrap Empirical Cumulative Distribution

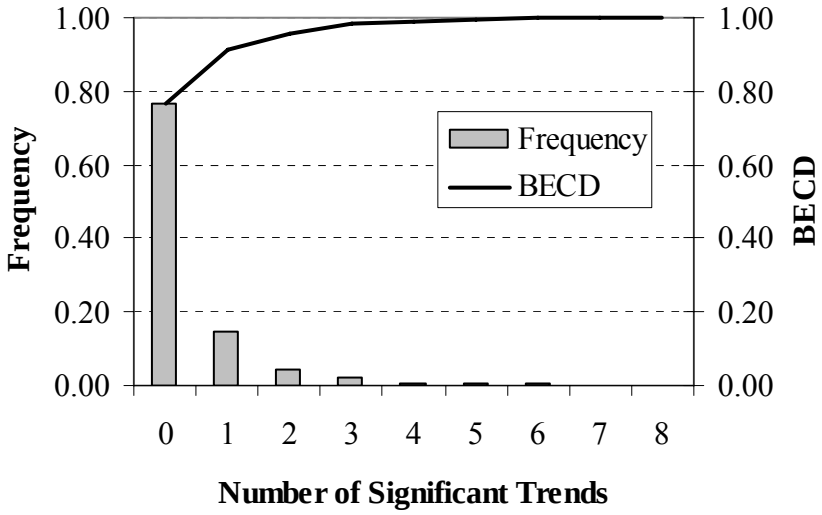

APPENDIX C

ACCURACY ASSESSMENT FOR IMAGE 1987, 1999 AND 2002

Table C.1. Accuracy assessment for the 1987's classified image of the Guadalupe River Watershed

X-Coordinate (m)	Y-Coordinate (m)	Classified Land Cover	Actual Land Cover
666165	3216255	Water	Water
670905	3200115	Water	Water
682005	3196965	Water	Water
676725	3189615	Water	Water
676605	3188985	Water	Water
678945	3186315	Water	Water
679125	3186255	Water	Water
678555	3185775	Water	Water
679695	3185625	Water	Water
679185	3185475	Water	Water
675525	3183765	Water	Water
676485	3183345	Water	Water
679035	3183045	Water	Water
697305	3177795	Water	Water
698685	3177165	Water	Water
694065	3176145	Water	Water
697785	3176145	Water	Water
698085	3175485	Water	Water
698145	3174645	Water	Water
700335	3173655	Water	Water
697305	3173505	Water	Water
699105	3170505	Water	Water
701295	3168405	Water	Water
697425	3168195	Water	Water
697785	3167715	Water	Water
698295	3166755	Water	Water
698865	3166515	Water	Water
703935	3165255	Water	Water
705735	3159435	Water	Water
610605	3282705	Water	Water
600915	3270375	Water	Water
602505	3267735	Water	Water
612315	3267705	Water	Water
619665	3304635	Water	Water
489015	3319575	Water	Water

Table C.1. (Continued)

X-Coordinate (m)	Y-Coordinate (m)	Classified Land Cover	Actual Land Cover
489675	3318585	Water	Water
568065	3309765	Water	Water
575235	3308655	Water	Water
567555	3306405	Water	Water
672525	3216465	Forest	Water
649305	3264255	Forest	Water
673575	3183225	Grassland	Water
699405	3167685	Wetland	Water
701925	3164775	Wetland	Water
705285	3157065	Wetland	Water
659985	3210015	Forest	Forest
647535	3208035	Forest	Forest
680235	3206055	Forest	Forest
670125	3200625	Forest	Forest
669975	3199785	Forest	Forest
650475	3199365	Forest	Forest
670695	3198825	Forest	Forest
678555	3198015	Forest	Forest
676035	3197055	Forest	Forest
679485	3196335	Forest	Forest
655485	3196065	Forest	Forest
657885	3196065	Forest	Forest
678915	3195555	Forest	Forest
675675	3195495	Forest	Forest
671475	3194175	Forest	Forest
673545	3190365	Forest	Forest
675675	3189735	Forest	Forest
669375	3188535	Forest	Forest
674805	3187365	Forest	Forest
701655	3177765	Forest	Forest
697125	3167295	Forest	Forest
697485	3167205	Forest	Forest
696135	3160305	Forest	Forest
580365	3298485	Forest	Forest
569895	3297945	Forest	Forest

Table C.1. (Continued)

X-Coordinate (m)	Y-Coordinate (m)	Classified Land Cover	Actual Land Cover
581745	3297105	Forest	Forest
577845	3296475	Forest	Forest
580185	3296145	Forest	Forest
573045	3296025	Forest	Forest
660825	3292905	Forest	Forest
572415	3292395	Forest	Forest
659445	3288225	Forest	Forest
666375	3287745	Forest	Forest
666825	3286665	Forest	Forest
610665	3282195	Forest	Forest
667665	3281445	Forest	Forest
659115	3279915	Forest	Forest
667335	3279135	Forest	Forest
652035	3278895	Forest	Forest
663735	3278145	Forest	Forest
651585	3275745	Forest	Forest
669525	3274815	Forest	Forest
612885	3272055	Forest	Forest
602325	3268515	Forest	Forest
609375	3268395	Forest	Forest
654585	3264345	Forest	Forest
615825	3264105	Forest	Forest
648885	3261165	Forest	Forest
636915	3251085	Forest	Forest
640365	3244815	Forest	Forest
637515	3239025	Forest	Forest
639585	3238935	Forest	Forest
637035	3235335	Forest	Forest
640575	3232065	Forest	Forest
558735	3321045	Forest	Forest
594915	3316335	Forest	Forest
585765	3311655	Forest	Forest
604425	3310065	Forest	Forest
627195	3298245	Forest	Forest
630045	3297345	Forest	Forest

Table C.1. (Continued)

X-Coordinate (m)	Y-Coordinate (m)	Classified Land Cover	Actual Land Cover
628815	3295785	Forest	Forest
616965	3279885	Forest	Forest
645735	3276735	Forest	Forest
649125	3275505	Forest	Forest
483345	3333615	Forest	Forest
487125	3333405	Forest	Forest
488145	3328665	Forest	Forest
471555	3327765	Forest	Forest
494895	3320505	Forest	Forest
442455	3319005	Forest	Forest
522375	3316515	Forest	Forest
563565	3314145	Forest	Forest
539505	3312135	Forest	Forest
523125	3311865	Forest	Forest
549045	3310665	Forest	Forest
561525	3310635	Forest	Forest
539325	3307185	Forest	Forest
535845	3305835	Forest	Forest
482835	3305415	Forest	Forest
483495	3304665	Forest	Forest
696135	3168345	Wetland	Forest
443175	3316335	Forest	Grassland
647025	3208515	Grassland	Grassland
646635	3208185	Grassland	Grassland
654795	3204855	Grassland	Grassland
670305	3199485	Grassland	Grassland
657315	3199065	Grassland	Grassland
678435	3198435	Grassland	Grassland
676155	3197265	Grassland	Grassland
681645	3196905	Grassland	Grassland
658215	3196755	Grassland	Grassland
654855	3196575	Grassland	Grassland
657705	3196485	Grassland	Grassland
654735	3196305	Grassland	Grassland
676215	3196185	Grassland	Grassland

Table C.1. (Continued)

X-Coordinate (m)	Y-Coordinate (m)	Classified Land Cover	Actual Land Cover
676365	3195735	Grassland	Grassland
658065	3195555	Grassland	Grassland
680175	3195165	Grassland	Grassland
679095	3195135	Grassland	Grassland
672615	3191085	Grassland	Grassland
680715	3190935	Grassland	Grassland
680685	3190845	Grassland	Grassland
676455	3189555	Grassland	Grassland
683115	3188115	Grassland	Grassland
681975	3187125	Grassland	Grassland
676785	3186855	Grassland	Grassland
679725	3185295	Grassland	Grassland
672435	3183855	Grassland	Grassland
697905	3181935	Grassland	Grassland
680145	3181485	Grassland	Grassland
694785	3179835	Grassland	Grassland
694785	3179145	Grassland	Grassland
698715	3174975	Grassland	Grassland
701535	3168405	Grassland	Grassland
696675	3167055	Grassland	Grassland
696375	3165975	Grassland	Grassland
696135	3162855	Grassland	Grassland
695205	3161685	Grassland	Grassland
697365	3161475	Grassland	Grassland
697095	3160755	Grassland	Grassland
570165	3295935	Grassland	Grassland
566895	3293415	Grassland	Grassland
660855	3283245	Grassland	Grassland
659115	3280425	Grassland	Grassland
666615	3279525	Grassland	Grassland
655365	3279345	Grassland	Grassland
615165	3269295	Grassland	Grassland
615075	3268455	Grassland	Grassland
619875	3266205	Grassland	Grassland
620415	3265455	Grassland	Grassland

Table C.1. (Continued)

X-Coordinate (m)	Y-Coordinate (m)	Classified Land Cover	Actual Land Cover
620265	3265395	Grassland	Grassland
639045	3242625	Grassland	Grassland
639075	3241815	Grassland	Grassland
642675	3241815	Grassland	Grassland
642885	3241065	Grassland	Grassland
644235	3239685	Grassland	Grassland
643695	3238815	Grassland	Grassland
637245	3238035	Grassland	Grassland
639615	3237195	Grassland	Grassland
642045	3237015	Grassland	Grassland
639735	3236535	Grassland	Grassland
635985	3234255	Grassland	Grassland
639525	3233355	Grassland	Grassland
575715	3327075	Grassland	Grassland
537315	3323415	Grassland	Grassland
570375	3322935	Grassland	Grassland
568725	3322575	Grassland	Grassland
589095	3322185	Grassland	Grassland
589635	3315855	Grassland	Grassland
585585	3314865	Grassland	Grassland
591975	3313125	Grassland	Grassland
592335	3311655	Grassland	Grassland
627825	3310605	Grassland	Grassland
594105	3308685	Grassland	Grassland
617445	3299325	Grassland	Grassland
649935	3272985	Grassland	Grassland
642285	3271755	Grassland	Grassland
646395	3266325	Grassland	Grassland
467595	3334425	Grassland	Grassland
472005	3331065	Grassland	Grassland
462765	3320085	Grassland	Grassland
461745	3318915	Grassland	Grassland
489195	3318585	Grassland	Grassland
490755	3318585	Grassland	Grassland
506595	3317265	Grassland	Grassland

Table C.1. (Continued)

X-Coordinate (m)	Y-Coordinate (m)	Classified Land Cover	Actual Land Cover
518385	3316665	Grassland	Grassland
507135	3316365	Grassland	Grassland
531675	3309735	Grassland	Grassland
494925	3309075	Grassland	Grassland
494235	3308985	Grassland	Grassland
485385	3308925	Grassland	Grassland
550965	3308805	Grassland	Grassland
492015	3308085	Grassland	Grassland
489435	3306585	Grassland	Grassland
489555	3305745	Grassland	Grassland
535425	3304875	Grassland	Grassland
677865	3205125	Irrigated Land	Grassland
657165	3199605	Irrigated Land	Grassland
643245	3241695	Irrigated Land	Grassland
679095	3201405	Grassland	Irrigated Land
596385	3278805	Grassland	Irrigated Land
599625	3277365	Grassland	Irrigated Land
639255	3256035	Grassland	Irrigated Land
516285	3324165	Grassland	Irrigated Land
515805	3321555	Grassland	Irrigated Land
528105	3317565	Grassland	Irrigated Land
490245	3317355	Grassland	Irrigated Land
514545	3316665	Grassland	Irrigated Land
487575	3315075	Grassland	Irrigated Land
508245	3314445	Grassland	Irrigated Land
507885	3314265	Grassland	Irrigated Land
496875	3313665	Grassland	Irrigated Land
493965	3313605	Grassland	Irrigated Land
495135	3312405	Grassland	Irrigated Land
679815	3199365	Irrigated Land	Irrigated Land
681225	3198975	Irrigated Land	Irrigated Land
681285	3198585	Irrigated Land	Irrigated Land
682665	3197595	Irrigated Land	Irrigated Land
681555	3197145	Irrigated Land	Irrigated Land
653955	3196725	Irrigated Land	Irrigated Land

Table C.1. (Continued)

X-Coordinate (m)	Y-Coordinate (m)	Classified Land Cover	Actual Land Cover
699555	3183345	Irrigated Land	Irrigated Land
699645	3183015	Irrigated Land	Irrigated Land
700035	3182745	Irrigated Land	Irrigated Land
701025	3182475	Irrigated Land	Irrigated Land
700245	3181455	Irrigated Land	Irrigated Land
701595	3177165	Irrigated Land	Irrigated Land
701325	3176805	Irrigated Land	Irrigated Land
597105	3278685	Irrigated Land	Irrigated Land
596685	3278265	Irrigated Land	Irrigated Land
599325	3277755	Irrigated Land	Irrigated Land
598725	3277725	Irrigated Land	Irrigated Land
599265	3277035	Irrigated Land	Irrigated Land
598635	3276915	Irrigated Land	Irrigated Land
653655	3276915	Irrigated Land	Irrigated Land
601365	3276765	Irrigated Land	Irrigated Land
601575	3276375	Irrigated Land	Irrigated Land
600765	3276285	Irrigated Land	Irrigated Land
596715	3275955	Irrigated Land	Irrigated Land
596055	3275925	Irrigated Land	Irrigated Land
598035	3275895	Irrigated Land	Irrigated Land
598455	3275685	Irrigated Land	Irrigated Land
597885	3275385	Irrigated Land	Irrigated Land
596715	3275325	Irrigated Land	Irrigated Land
598395	3274935	Irrigated Land	Irrigated Land
638655	3256095	Irrigated Land	Irrigated Land
639555	3256065	Irrigated Land	Irrigated Land
638895	3255345	Irrigated Land	Irrigated Land
636945	3254985	Irrigated Land	Irrigated Land
633225	3250455	Irrigated Land	Irrigated Land
633435	3250185	Irrigated Land	Irrigated Land
632775	3249795	Irrigated Land	Irrigated Land
633255	3249405	Irrigated Land	Irrigated Land
630225	3301935	Irrigated Land	Irrigated Land
630285	3301455	Irrigated Land	Irrigated Land
630435	3300915	Irrigated Land	Irrigated Land

Table C.1. (Continued)

X-Coordinate (m)	Y-Coordinate (m)	Classified Land Cover	Actual Land Cover
640545	3274125	Irrigated Land	Irrigated Land
467805	3334815	Irrigated Land	Irrigated Land
515835	3320565	Irrigated Land	Irrigated Land
528855	3320025	Irrigated Land	Irrigated Land
528765	3319485	Irrigated Land	Irrigated Land
527415	3318045	Irrigated Land	Irrigated Land
540375	3317985	Irrigated Land	Irrigated Land
514215	3316185	Irrigated Land	Irrigated Land
514245	3315795	Irrigated Land	Irrigated Land
507435	3314715	Irrigated Land	Irrigated Land
507465	3313995	Irrigated Land	Irrigated Land
495795	3310995	Irrigated Land	Irrigated Land
665505	3283695	Grassland	Urban
605445	3271215	Grassland	Urban
651495	3265065	Grassland	Urban
604095	3306585	Grassland	Urban
604365	3306195	Grassland	Urban
572175	3309345	Grassland	Urban
573135	3304125	Grassland	Urban
645975	3206805	Urban	Urban
645165	3206685	Urban	Urban
645375	3206565	Urban	Urban
699375	3173505	Urban	Urban
699705	3173085	Urban	Urban
587355	3286305	Urban	Urban
664545	3286005	Urban	Urban
587655	3285975	Urban	Urban
584385	3284475	Urban	Urban
584955	3284385	Urban	Urban
600165	3272925	Urban	Urban
600015	3272895	Urban	Urban
600105	3272505	Urban	Urban
600255	3271605	Urban	Urban
602415	3271515	Urban	Urban
600465	3271485	Urban	Urban

Table C.1. (Continued)

X-Coordinate (m)	Y-Coordinate (m)	Classified Land Cover	Actual Land Cover
600165	3271425	Urban	Urban
602295	3271425	Urban	Urban
606015	3271305	Urban	Urban
600405	3271215	Urban	Urban
651525	3265395	Urban	Urban
650025	3265005	Urban	Urban
651285	3265005	Urban	Urban
649935	3264735	Urban	Urban
649905	3264375	Urban	Urban
628275	3306885	Urban	Urban
628185	3306615	Urban	Urban
628395	3306615	Urban	Urban
628905	3304785	Urban	Urban
628695	3304365	Urban	Urban
484335	3325125	Urban	Urban
486375	3324075	Urban	Urban
485925	3323775	Urban	Urban
486915	3322725	Urban	Urban
696645	3176265	Water	Wetland
704175	3158205	Water	Wetland
696315	3177375	Forest	Wetland
698475	3174255	Wetland	Wetland
697755	3173955	Wetland	Wetland
696135	3173175	Wetland	Wetland
696195	3172965	Wetland	Wetland
697545	3170085	Wetland	Wetland
702495	3166095	Wetland	Wetland
702765	3165705	Wetland	Wetland
706305	3159705	Wetland	Wetland
702645	3157965	Wetland	Wetland
701025	3156525	Wetland	Wetland

Table C.2. Accuracy assessment for the 1999's classified image of the Guadalupe River Watershed

X-Coordinate (m)	Y-Coordinate (m)	Classified Land Cover	Actual Land Cover
665955	3216315	Water	Water
672345	3216255	Water	Water
660015	3210015	Forest	Forest
647055	3208905	Grassland	Grassland
646815	3208125	Grassland	Grassland
647655	3208065	Forest	Forest
646035	3206865	Urban	Urban
645855	3206805	Urban	Urban
644625	3206445	Grassland	Urban
645315	3206355	Grassland	Urban
680175	3206025	Forest	Forest
677925	3205065	Grassland	Grassland
654405	3204585	Grassland	Grassland
670155	3200565	Forest	Forest
670095	3200055	Irrigated Land	Water
680655	3199875	Irrigated Land	Irrigated Land
670635	3199665	Forest	Forest
657075	3199605	Grassland	Grassland
679875	3199575	Irrigated Land	Irrigated Land
671145	3199425	Forest	Forest
650655	3199305	Forest	Forest
657075	3199065	Grassland	Grassland
670755	3199035	Forest	Forest
678375	3198465	Grassland	Grassland
678555	3197955	Forest	Forest
682635	3197625	Grassland	Grassland
675825	3197385	Grassland	Grassland
681585	3197325	Grassland	Grassland
683535	3197325	Forest	Water
676035	3197085	Forest	Forest
681765	3196965	Grassland	Grassland
682065	3196815	Water	Water
654765	3196575	Grassland	Grassland
658095	3196335	Grassland	Grassland
655395	3196275	Irrigated Land	Irrigated Land

Table C.2. (Continued)

X-Coordinate (m)	Y-Coordinate (m)	Classified Land Cover	Actual Land Cover
679455	3196275	Forest	Forest
657885	3196065	Forest	Forest
676155	3196065	Grassland	Grassland
655125	3196035	Forest	Forest
676275	3195795	Grassland	Grassland
658155	3195465	Grassland	Grassland
675675	3195465	Forest	Forest
679935	3195075	Forest	Forest
679545	3194745	Grassland	Grassland
674055	3194685	Forest	Forest
671535	3194175	Forest	Forest
674865	3193965	Forest	Forest
672555	3191085	Grassland	Grassland
680655	3190935	Grassland	Grassland
676725	3190035	Water	Water
676665	3189165	Water	Water
672495	3189075	Grassland	Grassland
676125	3189015	Forest	Forest
677325	3188985	Grassland	Grassland
669375	3188535	Forest	Forest
682845	3188235	Grassland	Grassland
677265	3187635	Water	Water
677295	3187545	Water	Water
674775	3187335	Forest	Forest
682005	3187035	Grassland	Grassland
676725	3186825	Grassland	Grassland
676875	3186495	Grassland	Grassland
678915	3186405	Water	Water
679095	3186375	Water	Water
679275	3185805	Water	Water
678645	3185685	Water	Water
679335	3185535	Water	Water
679695	3185205	Forest	Forest
672495	3183765	Grassland	Grassland
676485	3183285	Forest	Water

Table C.2. (Continued)

X-Coordinate (m)	Y-Coordinate (m)	Classified Land Cover	Actual Land Cover
679035	3183015	Water	Water
673275	3182955	Grassland	Water
697605	3182385	Grassland	Grassland
697935	3181785	Grassland	Grassland
680145	3181455	Grassland	Grassland
697305	3177765	Water	Water
698715	3177135	Water	Water
696765	3177075	Wetland	Wetland
694365	3176325	Water	Water
697785	3176115	Water	Water
696345	3175965	Wetland	Wetland
698055	3175455	Water	Water
698835	3174765	Grassland	Grassland
698145	3174585	Water	Water
698355	3174465	Wetland	Wetland
697575	3174015	Wetland	Wetland
700335	3173625	Water	Water
697305	3173445	Water	Water
697335	3173415	Water	Water
696105	3173085	Wetland	Wetland
699045	3170565	Water	Water
697665	3170055	Wetland	Wetland
693585	3168465	Grassland	Grassland
701475	3168345	Forest	Grassland
701295	3168315	Water	Water
697485	3168165	Water	Water
699375	3167745	Water	Water
697845	3167715	Water	Water
696705	3167025	Forest	Grassland
698265	3166755	Water	Water
698805	3166485	Water	Water
702165	3166395	Wetland	Wetland
696495	3166155	Grassland	Grassland
702825	3165645	Wetland	Wetland
703875	3165255	Water	Water

Table C.2. (Continued)

X-Coordinate (m)	Y-Coordinate (m)	Classified Land Cover	Actual Land Cover
691995	3165075	Grassland	Grassland
701925	3164715	Water	Water
696195	3162825	Grassland	Grassland
694785	3162255	Grassland	Grassland
697065	3160845	Grassland	Grassland
706335	3159465	Wetland	Wetland
705375	3159015	Water	Water
704175	3157995	Water	Wetland
702675	3157485	Wetland	Wetland
705345	3157005	Water	Water
700785	3156885	Wetland	Wetland
580365	3298515	Forest	Forest
569925	3297945	Forest	Forest
581625	3296955	Forest	Forest
577785	3296475	Forest	Forest
580185	3296175	Forest	Forest
573015	3296025	Forest	Forest
570015	3295905	Grassland	Grassland
567045	3293475	Grassland	Grassland
660885	3292875	Forest	Forest
572445	3292365	Forest	Forest
667755	3289305	Water	Water
663195	3288555	Irrigated Land	Irrigated Land
667185	3287685	Forest	Forest
659625	3287655	Forest	Forest
666555	3287325	Forest	Forest
587355	3286395	Urban	Urban
664275	3286245	Urban	Urban
664665	3286005	Urban	Urban
584805	3284325	Urban	Urban
665355	3283635	Urban	Urban
661095	3283485	Forest	Grassland
610605	3282705	Water	Water
610905	3281835	Forest	Forest
667425	3281715	Forest	Forest

Table C.2. (Continued)

X-Coordinate (m)	Y-Coordinate (m)	Classified Land Cover	Actual Land Cover
658695	3280425	Grassland	Grassland
659085	3279945	Forest	Forest
666705	3279435	Grassland	Grassland
667365	3279105	Forest	Forest
668265	3278955	Forest	Forest
597105	3278865	Irrigated Land	Irrigated Land
652005	3278865	Forest	Forest
596745	3278835	Grassland	Irrigated Land
654735	3278835	Grassland	Grassland
663765	3278175	Forest	Forest
611865	3277875	Water	Water
596775	3277815	Irrigated Land	Irrigated Land
599145	3277725	Irrigated Land	Irrigated Land
598545	3277695	Irrigated Land	Irrigated Land
599295	3277425	Irrigated Land	Irrigated Land
598755	3277395	Irrigated Land	Irrigated Land
598965	3276765	Irrigated Land	Irrigated Land
601305	3276645	Irrigated Land	Irrigated Land
601425	3276495	Irrigated Land	Irrigated Land
596505	3276405	Grassland	Irrigated Land
600915	3276075	Grassland	Irrigated Land
596865	3275985	Irrigated Land	Irrigated Land
596895	3275985	Irrigated Land	Irrigated Land
595905	3275865	Irrigated Land	Irrigated Land
597975	3275865	Irrigated Land	Irrigated Land
596535	3275385	Irrigated Land	Irrigated Land
598305	3275325	Irrigated Land	Irrigated Land
597615	3275025	Irrigated Land	Irrigated Land
598425	3274845	Irrigated Land	Irrigated Land
669465	3274845	Forest	Forest
600105	3272955	Urban	Urban
599955	3272925	Urban	Urban
599985	3272925	Urban	Urban
600075	3272565	Urban	Urban
612765	3272055	Forest	Forest

Table C.2. (Continued)

X-Coordinate (m)	Y-Coordinate (m)	Classified Land Cover	Actual Land Cover
600255	3271845	Urban	Urban
600225	3271635	Urban	Urban
602385	3271575	Urban	Urban
600555	3271515	Urban	Urban
602115	3271485	Urban	Urban
600165	3271395	Grassland	Urban
605955	3271395	Grassland	Urban
605445	3271125	Urban	Urban
601035	3270765	Water	Water
615225	3269205	Grassland	Grassland
602235	3268575	Forest	Forest
609465	3268545	Forest	Forest
615375	3268395	Grassland	Grassland
588465	3268335	Irrigated Land	Irrigated Land
602475	3267645	Water	Water
612105	3267285	Water	Water
620205	3266175	Grassland	Grassland
619785	3265965	Grassland	Grassland
620325	3265545	Grassland	Grassland
651375	3265455	Urban	Urban
649755	3265215	Urban	Urban
651435	3265125	Urban	Urban
651285	3265065	Urban	Urban
649935	3264675	Urban	Urban
650535	3264675	Urban	Urban
649875	3264495	Urban	Urban
654345	3264495	Forest	Forest
615615	3264045	Forest	Forest
648915	3263625	Forest	Water
629865	3262815	Grassland	Grassland
648855	3261195	Forest	Forest
639075	3256065	Irrigated Land	Irrigated Land
626865	3255795	Grassland	Grassland
638595	3255405	Irrigated Land	Irrigated Land
639045	3255315	Irrigated Land	Irrigated Land

Table C.2. (Continued)

X-Coordinate (m)	Y-Coordinate (m)	Classified Land Cover	Actual Land Cover
636915	3254565	Grassland	Irrigated Land
636975	3250965	Forest	Forest
632775	3250575	Grassland	Irrigated Land
633405	3250065	Irrigated Land	Irrigated Land
632685	3249675	Grassland	Irrigated Land
640395	3244755	Forest	Forest
639225	3242685	Grassland	Grassland
643125	3242055	Grassland	Grassland
638685	3241935	Grassland	Grassland
642645	3241755	Grassland	Grassland
643215	3241485	Grassland	Grassland
637845	3239625	Forest	Forest
644415	3239505	Grassland	Grassland
651285	3239415	Grassland	Grassland
639675	3238935	Forest	Forest
637845	3238755	Water	Water
643875	3238725	Grassland	Grassland
637245	3238035	Irrigated Land	Grassland
639525	3237165	Grassland	Grassland
642075	3236955	Grassland	Grassland
639945	3236535	Grassland	Grassland
637095	3235335	Forest	Forest
635835	3234165	Forest	Grassland
639375	3233475	Irrigated Land	Grassland
640515	3231975	Forest	Forest
575655	3327015	Grassland	Grassland
537105	3323385	Grassland	Grassland
570435	3322935	Grassland	Grassland
568725	3322605	Irrigated Land	Grassland
589035	3322335	Grassland	Grassland
558735	3321045	Forest	Forest
594915	3316305	Forest	Forest
589605	3315855	Grassland	Grassland
585435	3314835	Grassland	Grassland
592245	3313065	Grassland	Grassland

Table C.2. (Continued)

X-Coordinate (m)	Y-Coordinate (m)	Classified Land Cover	Actual Land Cover
585735	3311625	Forest	Forest
592305	3311625	Grassland	Grassland
627855	3310725	Grassland	Grassland
604425	3310095	Forest	Forest
594075	3308655	Grassland	Grassland
628215	3306885	Urban	Urban
603915	3306645	Urban	Urban
628155	3306645	Urban	Urban
628455	3306645	Urban	Urban
604245	3306135	Urban	Urban
628875	3304785	Urban	Urban
619695	3304605	Forest	Water
628665	3304425	Urban	Urban
631335	3302295	Irrigated Land	Irrigated Land
631905	3302175	Irrigated Land	Irrigated Land
617355	3299475	Grassland	Grassland
627165	3298245	Forest	Forest
630015	3297375	Forest	Forest
628575	3295755	Forest	Forest
616995	3279795	Forest	Forest
645735	3277515	Forest	Forest
651315	3275805	Forest	Forest
649125	3275535	Forest	Forest
640305	3273735	Irrigated Land	Irrigated Land
649965	3273315	Grassland	Grassland
642165	3271845	Grassland	Grassland
646365	3266145	Grassland	Grassland
467955	3334755	Grassland	Grassland
467655	3334425	Grassland	Grassland
487005	3334365	Forest	Forest
483165	3333855	Forest	Forest
472035	3331065	Grassland	Grassland
471915	3328785	Forest	Forest
488145	3328545	Forest	Forest
484395	3325185	Urban	Urban

Table C.2. (Continued)

X-Coordinate (m)	Y-Coordinate (m)	Classified Land Cover	Actual Land Cover
486525	3324375	Urban	Urban
486435	3324105	Urban	Urban
524775	3324075	Irrigated Land	Irrigated Land
485895	3323745	Urban	Urban
486975	3322725	Urban	Urban
525135	3322545	Irrigated Land	Irrigated Land
462825	3320055	Grassland	Grassland
528825	3320025	Irrigated Land	Irrigated Land
485595	3319605	Forest	Forest
535875	3319575	Irrigated Land	Irrigated Land
489045	3319485	Water	Water
528735	3319425	Irrigated Land	Irrigated Land
486825	3319335	Forest	Forest
489495	3319155	Grassland	Grassland
442425	3319005	Forest	Forest
461715	3318885	Grassland	Grassland
535575	3318795	Irrigated Land	Irrigated Land
489675	3318555	Water	Water
527355	3318015	Irrigated Land	Irrigated Land
528285	3317805	Forest	Irrigated Land
506895	3317175	Grassland	Grassland
518325	3316635	Grassland	Grassland
537735	3316635	Forest	Irrigated Land
522345	3316545	Forest	Forest
538125	3316545	Forest	Irrigated Land
506685	3316455	Grassland	Grassland
443235	3316425	Forest	Grassland
507255	3316275	Grassland	Grassland
514335	3315825	Forest	Irrigated Land
539865	3315315	Forest	Irrigated Land
540225	3315045	Irrigated Land	Irrigated Land
484335	3314595	Forest	Irrigated Land
508215	3314445	Forest	Irrigated Land
563565	3314175	Forest	Forest
507495	3313995	Irrigated Land	Irrigated Land

Table C.2. (Continued)

X-Coordinate (m)	Y-Coordinate (m)	Classified Land Cover	Actual Land Cover
491295	3313605	Irrigated Land	Irrigated Land
495195	3312375	Irrigated Land	Grassland
539535	3312135	Forest	Forest
487065	3311865	Water	Water
523065	3311835	Forest	Forest
495825	3311055	Grassland	Grassland
501705	3310995	Forest	Irrigated Land
549045	3310695	Forest	Forest
561435	3310605	Forest	Forest
530745	3310545	Grassland	Grassland
568065	3309705	Water	Water
572385	3309375	Urban	Urban
550845	3308835	Grassland	Grassland
485355	3308805	Grassland	Grassland
575175	3308685	Water	Water
492165	3308115	Grassland	Grassland
485295	3307695	Water	Water
539205	3307605	Forest	Forest
489405	3306585	Grassland	Grassland
567525	3306435	Water	Water
535845	3305955	Forest	Forest
489615	3305805	Grassland	Grassland
482985	3305415	Forest	Forest
483045	3304665	Forest	Forest
534915	3304155	Grassland	Grassland
573015	3303975	Urban	Urban

Table C.3. Accuracy assessment for the 2002's classified image of the Guadalupe River Watershed

X-Coordinate (m)	Y-Coordinate (m)	Classified Land Cover	Actual Land Cover
672255	3216495	Forest	Water
666255	3216225	Water	Water
659985	3210015	Forest	Forest
677445	3209145	Water	Water
646995	3208875	Grassland	Grassland
677835	3208575	Forest	Forest
676935	3208425	Grassland	Grassland
646755	3208215	Grassland	Grassland
647595	3208065	Forest	Forest
645945	3206865	Urban	Urban
644895	3206595	Urban	Urban
645285	3206565	Urban	Urban
644685	3206535	Irrigated Land	Urban
644655	3206415	Grassland	Urban
646065	3206145	Urban	Urban
680085	3206025	Forest	Forest
677835	3205155	Irrigated Land	Irrigated Land
654375	3204645	Grassland	Grassland
670185	3200475	Forest	Forest
670155	3200025	Grassland	Water
670605	3199755	Forest	Forest
656565	3199695	Grassland	Grassland
657345	3199485	Grassland	Grassland
679785	3199455	Irrigated Land	Irrigated Land
650415	3199305	Forest	Forest
670725	3198975	Forest	Forest
671145	3198915	Forest	Forest
678315	3198435	Grassland	Grassland
678645	3197985	Forest	Forest
682605	3197595	Irrigated Land	Grassland
681465	3197355	Grassland	Grassland
683475	3197355	Water	Water
675555	3197115	Grassland	Grassland
681915	3197115	Water	Water
676035	3197085	Forest	Forest

Table C.3. (Continued)

X-Coordinate (m)	Y-Coordinate (m)	Classified Land Cover	Actual Land Cover
681765	3196665	Grassland	Grassland
657675	3196575	Grassland	Grassland
658005	3196335	Grassland	Grassland
655275	3196305	Grassland	Grassland
655635	3196305	Irrigated Land	Irrigated Land
679545	3196275	Forest	Forest
654885	3196095	Forest	Forest
657885	3196065	Forest	Forest
676155	3196035	Grassland	Grassland
676305	3195765	Grassland	Grassland
657945	3195465	Grassland	Grassland
658245	3195465	Grassland	Grassland
675705	3195465	Forest	Forest
679245	3195105	Forest	Forest
679995	3194955	Forest	Forest
674055	3194745	Forest	Forest
679785	3194535	Grassland	Grassland
674655	3194145	Forest	Forest
671475	3194085	Forest	Forest
672645	3191355	Grassland	Grassland
680775	3190875	Grassland	Grassland
676665	3189765	Water	Water
672495	3189015	Grassland	Grassland
676155	3188985	Forest	Forest
677115	3188835	Grassland	Grassland
669435	3188535	Forest	Forest
683085	3187875	Forest	Forest
677325	3187485	Water	Water
674775	3187365	Forest	Forest
681945	3187095	Grassland	Grassland
676785	3186795	Grassland	Grassland
676635	3186525	Grassland	Grassland
679155	3186255	Water	Water
679365	3185625	Water	Water
678855	3185565	Water	Water

Table C.3. (Continued)

X-Coordinate (m)	Y-Coordinate (m)	Classified Land Cover	Actual Land Cover
679695	3185145	Forest	Forest
675765	3183765	Water	Water
672435	3183645	Grassland	Grassland
676455	3183435	Water	Water
673605	3183375	Grassland	Water
679005	3182985	Water	Water
697545	3182445	Grassland	Grassland
679545	3182325	Grassland	Grassland
697845	3181995	Grassland	Grassland
697305	3177705	Water	Water
695925	3177405	Wetland	Wetland
698685	3177165	Water	Water
696675	3176325	Wetland	Wetland
694065	3176175	Water	Water
697785	3176055	Water	Water
698085	3175455	Water	Water
698655	3174975	Grassland	Grassland
698115	3174615	Water	Water
698535	3174465	Wetland	Wetland
697575	3173925	Wetland	Wetland
700365	3173625	Water	Water
697185	3173505	Water	Water
697305	3173505	Water	Water
696045	3173085	Wetland	Wetland
699105	3170715	Water	Water
697185	3170295	Water	Wetland
697815	3170025	Wetland	Wetland
693705	3168495	Grassland	Grassland
701265	3168405	Water	Water
697455	3168135	Water	Water
697815	3167775	Water	Water
699375	3167625	Water	Water
696765	3167055	Grassland	Grassland
698295	3166725	Water	Water
698805	3166515	Water	Water

Table C.3. (Continued)

X-Coordinate (m)	Y-Coordinate (m)	Classified Land Cover	Actual Land Cover
696675	3166245	Grassland	Grassland
701985	3166125	Wetland	Wetland
702765	3165945	Wetland	Wetland
703035	3165555	Wetland	Wetland
703755	3165405	Water	Water
692295	3165195	Grassland	Grassland
702045	3164475	Water	Water
696195	3162915	Grassland	Grassland
695385	3162255	Grassland	Grassland
697125	3160905	Grassland	Grassland
706485	3159555	Wetland	Wetland
705375	3159045	Water	Water
704295	3158025	Forest	Wetland
702585	3157695	Wetland	Wetland
701145	3157035	Wetland	Wetland
705435	3157035	Wetland	Water
580365	3298485	Forest	Forest
569925	3297975	Forest	Forest
581715	3296985	Forest	Forest
577755	3296475	Forest	Forest
580245	3296175	Forest	Forest
572955	3295995	Forest	Forest
570165	3295905	Grassland	Grassland
567375	3293205	Grassland	Grassland
660885	3292935	Forest	Forest
572385	3292365	Forest	Forest
667755	3289275	Water	Water
663225	3288555	Grassland	Grassland
666345	3287835	Forest	Forest
659715	3287685	Forest	Forest
666825	3286605	Forest	Forest
664365	3286065	Urban	Urban
664725	3285945	Urban	Urban
665115	3283485	Grassland	Urban
660825	3283455	Grassland	Grassland

Table C.3. (Continued)

X-Coordinate (m)	Y-Coordinate (m)	Classified Land Cover	Actual Land Cover
610605	3282705	Water	Water
610755	3282225	Forest	Forest
667515	3281655	Forest	Forest
658785	3280425	Grassland	Grassland
659055	3279945	Forest	Forest
666645	3279435	Grassland	Grassland
655335	3279405	Grassland	Grassland
667425	3279165	Forest	Forest
668295	3278925	Forest	Forest
652035	3278895	Forest	Forest
596715	3278715	Irrigated Land	Irrigated Land
597525	3278715	Irrigated Land	Irrigated Land
596895	3278295	Irrigated Land	Irrigated Land
663795	3278085	Forest	Forest
611685	3277755	Water	Water
599685	3277635	Irrigated Land	Irrigated Land
598965	3277395	Irrigated Land	Irrigated Land
599205	3276945	Irrigated Land	Irrigated Land
598935	3276765	Irrigated Land	Irrigated Land
601425	3276735	Irrigated Land	Irrigated Land
596625	3276375	Irrigated Land	Irrigated Land
601425	3276375	Irrigated Land	Irrigated Land
596025	3276105	Irrigated Land	Irrigated Land
600975	3276045	Irrigated Land	Irrigated Land
597465	3275865	Irrigated Land	Irrigated Land
596655	3275475	Irrigated Land	Irrigated Land
598515	3275325	Irrigated Land	Irrigated Land
597885	3275115	Irrigated Land	Irrigated Land
600195	3273165	Urban	Urban
600195	3272955	Urban	Urban
612945	3272835	Grassland	Forest
600135	3272805	Urban	Urban
600855	3272745	Urban	Urban
600255	3271755	Urban	Urban
600195	3271575	Urban	Urban

Table C.3. (Continued)

X-Coordinate (m)	Y-Coordinate (m)	Classified Land Cover	Actual Land Cover
602355	3271515	Urban	Urban
599595	3271455	Urban	Urban
600435	3271455	Urban	Urban
602205	3271455	Urban	Urban
600195	3271425	Urban	Urban
602295	3271125	Urban	Urban
605445	3270975	Urban	Urban
605865	3270825	Irrigated Land	Urban
601065	3270735	Water	Water
588465	3269265	Irrigated Land	Irrigated Land
615135	3269235	Grassland	Grassland
588255	3269085	Irrigated Land	Irrigated Land
615225	3268575	Grassland	Grassland
588285	3268545	Irrigated Land	Irrigated Land
602505	3268365	Grassland	Forest
609015	3268185	Grassland	Forest
602475	3267705	Water	Water
612135	3267315	Water	Water
619545	3266295	Grassland	Grassland
619725	3265455	Grassland	Grassland
620355	3265455	Grassland	Grassland
651315	3265395	Urban	Urban
651375	3265035	Urban	Urban
649905	3264825	Urban	Urban
649905	3264765	Urban	Urban
649995	3264345	Urban	Urban
654555	3264345	Forest	Forest
615705	3264075	Forest	Forest
648855	3263745	Irrigated Land	Water
629835	3262875	Grassland	Grassland
648885	3261195	Forest	Forest
627165	3257625	Forest	Forest
638685	3255945	Irrigated Land	Irrigated Land
626925	3255795	Grassland	Grassland
638985	3255495	Irrigated Land	Irrigated Land

Table C.3. (Continued)

X-Coordinate (m)	Y-Coordinate (m)	Classified Land Cover	Actual Land Cover
636915	3254745	Irrigated Land	Irrigated Land
636945	3250995	Forest	Forest
633555	3250245	Irrigated Land	Irrigated Land
632685	3250035	Irrigated Land	Irrigated Land
632655	3249615	Irrigated Land	Irrigated Land
640575	3245175	Forest	Forest
639135	3242475	Grassland	Grassland
643035	3242115	Grassland	Grassland
638775	3241815	Grassland	Grassland
642615	3241665	Grassland	Grassland
643125	3241515	Grassland	Grassland
638145	3239745	Forest	Forest
644355	3239655	Grassland	Grassland
643515	3239445	Grassland	Grassland
651255	3239385	Grassland	Grassland
639465	3238995	Forest	Forest
637845	3238695	Water	Water
637275	3238065	Grassland	Grassland
639735	3237135	Grassland	Grassland
642105	3236865	Grassland	Grassland
638925	3236655	Grassland	Grassland
637095	3235425	Forest	Forest
635955	3234285	Grassland	Grassland
639735	3233355	Grassland	Grassland
575715	3326985	Grassland	Grassland
536865	3323355	Forest	Grassland
570435	3322875	Grassland	Grassland
568755	3322635	Irrigated Land	Irrigated Land
569205	3322635	Grassland	Grassland
589035	3322305	Grassland	Grassland
558735	3321045	Forest	Forest
588195	3320175	Forest	Forest
594885	3316305	Forest	Forest
589605	3315855	Irrigated Land	Grassland
585435	3314835	Grassland	Grassland

Table C.3. (Continued)

X-Coordinate (m)	Y-Coordinate (m)	Classified Land Cover	Actual Land Cover
592245	3313095	Grassland	Grassland
585765	3311625	Forest	Forest
592335	3311625	Grassland	Grassland
627795	3310665	Grassland	Grassland
604425	3310095	Forest	Forest
594075	3308745	Grassland	Grassland
628305	3306855	Urban	Urban
628395	3306705	Urban	Urban
628185	3306675	Urban	Urban
603945	3306465	Urban	Urban
604155	3306075	Urban	Urban
628545	3305175	Urban	Urban
629025	3304845	Urban	Urban
619755	3304635	Water	Water
628545	3304335	Urban	Urban
629115	3303645	Irrigated Land	Irrigated Land
628965	3303075	Grassland	Irrigated Land
629385	3302835	Irrigated Land	Irrigated Land
630045	3302175	Irrigated Land	Irrigated Land
630105	3301845	Irrigated Land	Irrigated Land
630255	3301455	Irrigated Land	Irrigated Land
617595	3299355	Grassland	Grassland
627195	3298215	Forest	Forest
629985	3297375	Forest	Forest
628905	3296085	Forest	Forest
617115	3279435	Forest	Forest
651435	3275775	Forest	Forest
649125	3275565	Forest	Forest
640185	3273855	Grassland	Grassland
649845	3273105	Grassland	Grassland
641775	3271935	Grassland	Grassland
646305	3266205	Grassland	Grassland
467925	3334875	Grassland	Grassland
467625	3334365	Grassland	Grassland
486825	3334095	Forest	Forest

Table C.3. (Continued)

X-Coordinate (m)	Y-Coordinate (m)	Classified Land Cover	Actual Land Cover
483285	3333705	Forest	Forest
472095	3331035	Grassland	Grassland
488175	3328665	Forest	Forest
471885	3328635	Forest	Forest
484305	3325215	Urban	Urban
486615	3324285	Urban	Urban
486435	3324015	Urban	Urban
485985	3323565	Urban	Urban
516105	3323175	Irrigated Land	Irrigated Land
486945	3322785	Urban	Urban
515355	3320565	Irrigated Land	Irrigated Land
515685	3320565	Irrigated Land	Irrigated Land
494925	3320505	Forest	Forest
462735	3320085	Grassland	Grassland
489045	3319425	Water	Water
489405	3319245	Urban	Grassland
442455	3319005	Forest	Forest
461805	3318885	Grassland	Grassland
489675	3318615	Water	Water
490305	3317415	Grassland	Irrigated Land
506685	3317205	Grassland	Grassland
518505	3316635	Grassland	Grassland
506745	3316455	Grassland	Grassland
522495	3316455	Forest	Forest
507195	3316425	Grassland	Grassland
443085	3316335	Forest	Grassland
514065	3316275	Irrigated Land	Irrigated Land
514275	3315735	Irrigated Land	Irrigated Land
486855	3314895	Urban	Irrigated Land
507375	3314685	Grassland	Irrigated Land
508245	3314415	Urban	Irrigated Land
563595	3314175	Forest	Forest
496905	3313635	Irrigated Land	Irrigated Land
495165	3312375	Irrigated Land	Irrigated Land
539535	3312195	Forest	Forest

Table C.3. (Continued)

X-Coordinate (m)	Y-Coordinate (m)	Classified Land Cover	Actual Land Cover
487065	3311835	Water	Wetland
522885	3311625	Forest	Forest
495855	3310965	Grassland	Grassland
549045	3310695	Forest	Forest
530625	3310605	Grassland	Grassland
561405	3310545	Forest	Forest
568065	3309645	Water	Water
568065	3309615	Water	Water
572535	3309435	Urban	Urban
494265	3308895	Grassland	Irrigated Land
485385	3308865	Grassland	Grassland
550905	3308835	Grassland	Grassland
494655	3308745	Urban	Irrigated Land
575265	3308745	Water	Water
492045	3308085	Irrigated Land	Irrigated Land
485295	3307695	Water	Wetland
539175	3307605	Forest	Forest
489405	3306645	Grassland	Grassland
567585	3306375	Water	Water
535995	3306015	Forest	Forest
489615	3305595	Grassland	Grassland
482745	3305295	Forest	Forest
535035	3304125	Grassland	Grassland
572925	3303915	Urban	Urban

VITA

Teuku Ferijal

Address

Jl. BPD 2 No. 42, Gue Gajah
Darul Imarah, Aceh Besar
Nanggroe Aceh Darussalam - Indonesia

Education

- M.S., Biological and Agricultural Engineering (August 2008)
  Texas A & M University

- B.S., Agricultural Engineering (1995-1999)
  Brawijaya University, Malang, Indonesia

Experience

- **Syiah Kuala University**, Banda Aceh, Indonesia (2003 - Present)
  Faculty member

- **Astra Agro Lestari, ltd.**, Jakarta, Indonesia (2001 - 2003)
  Head of Support and Maintenance Department